UNIVERSITAT ROVIRA I VIRGILI

NEW CATALYTIC ADVANCED OXIDATION PROCESSES FOR WASTEWATER TREATMENT

Mohammad Sadegh Yalfani

ISBN:
Dipòsit Legal: T-1259-2011

UNIVERSITAT ROVIRA I VIRGILI
NEW CATALYTIC ADVANCED OXIDATION PROCESSES FOR WASTEWATER TREATMENT
Mohammad Sadegh Yalfani
ISBN:/DL:T.1259-2011

NEW CATALYTIC ADVANCED OXIDATION PROCESSES FOR WASTEWATER TREATMENT

Mohammad Sadegh Yalfani

Doctoral Thesis

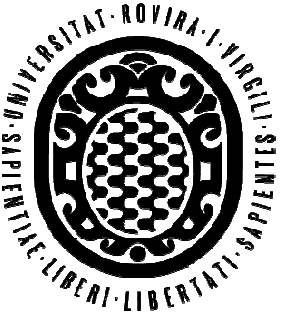

Universitat Rovira i Virgili

Tarragona

2011

UNIVERSITAT ROVIRA I VIRGILI
NEW CATALYTIC ADVANCED OXIDATION PROCESSES FOR WASTEWATER TREATMENT
Mohammad Sadegh Yalfani
ISBN:/DL:T.1259-2011

UNIVERSITAT ROVIRA I VIRGILI
NEW CATALYTIC ADVANCED OXIDATION PROCESSES FOR WASTEWATER TREATMENT
Mohammad Sadegh Yalfani
ISBN:/DL:T.1259-2011

Mohammad Sadegh Yalfani

NEW CATALYTIC ADVANCED OXIDATION PROCESSES FOR WASTEWATER TREATMENT

Doctoral Thesis

Supervised by

Prof. Dr. Francesc Medina and Dr. Sandra Contreras

Department of Chemical Engineering

Universitat Rovira i Virgili

Tarragona

2011

UNIVERSITAT ROVIRA I VIRGILI
NEW CATALYTIC ADVANCED OXIDATION PROCESSES FOR WASTEWATER TREATMENT
Mohammad Sadegh Yalfani
ISBN:/DL:T.1259-2011

Prof. Dr. Francesc Medina and Dr. Sandra Contreras

Certify:

that the present study, entitled "NEW CATALYTIC ADVANCED OXIDATION PROCESSES FOR WASTEWATER TREATMENT", presented by Mohammad Sadegh Yalfani for the award of the degree of Doctor, has been carried out under their supervision at the Department of Chemical Engineering of this university, and that it fulfils all the requirements to be eligible for the European Doctorate Award.

Tarragona 21 March 2011

Prof. Dr. Francesc Medina **Dr. Sandra Contreras**

UNIVERSITAT ROVIRA I VIRGILI
NEW CATALYTIC ADVANCED OXIDATION PROCESSES FOR WASTEWATER TREATMENT
Mohammad Sadegh Yalfani
ISBN:/DL:T.1259-2011

With them the seed of wisdom did I sow,
And with- my own hand labour´d it to grow:
And this was all the Harvest that I reap´d-
"I came like water, and like wind I go."

یک چند به کودکی به استاد شدیم

یک چند ز استادی خود شاد شدیم

پایان سخن شنو که ما را چه رسید

از خاک بر آمدیم و بر باد شدیم

Khayyam (1048-1131 AD)

UNIVERSITAT ROVIRA I VIRGILI
NEW CATALYTIC ADVANCED OXIDATION PROCESSES FOR WASTEWATER TREATMENT
Mohammad Sadegh Yalfani
ISBN:/DL:T.1259-2011

Acknowledgements

I would like to present my deep appreciation to my supervisors Dr. Francesc Medina and Dr. Sandra Contreras for their management on this thesis and beneficial and instructive discussions carried out during the last four years.

Rovira i Virgili University (URV) for the three years PhD grant and providing me a great and peaceful scientific atmosphere and also Spanish Ministry of Science and Innovation for the three months mobility grant are acknowledged. My special thanks is to "Foundation of Rovira i Virgili University" (Ms. Sandra Ramos) for all supports given during my PhD carrier in URV.

Helmholtz-Center for Environmental research in Leipzig-Germany (Dr. Anett Georgi and Prof. Frank-Dieter Kopinke) is really appreciated for my three months research stage.

Dr. Jordi Llorca (*Polytechnic University of Catalonia) is acknowledged for conclusive characterization analyses and helpful discussions.*

All personnel of "the department of chemical engineering" and "Scientific and Technical Services of URV" are sincerely acknowledged for their warm and helpful collaborations that without them the fulfillment of the thesis might not be materialized.

Deeply appreciations are dedicated to all members of the Heterogeneous Catalysis group with whom I enjoyed a fantastic social and scientific life in Tarragona.

… and finally

I would like to thank my wife (Zahra) and my parent whose spiritual supports and their patience are always the best encouragement for me.

UNIVERSITAT ROVIRA I VIRGILI
NEW CATALYTIC ADVANCED OXIDATION PROCESSES FOR WASTEWATER TREATMENT
Mohammad Sadegh Yalfani
ISBN:/DL:T.1259-2011

… to my beloved parent

UNIVERSITAT ROVIRA I VIRGILI
NEW CATALYTIC ADVANCED OXIDATION PROCESSES FOR WASTEWATER TREATMENT
Mohammad Sadegh Yalfani
ISBN:/DL:T.1259-2011

Contents

UNIVERSITAT ROVIRA I VIRGILI
NEW CATALYTIC ADVANCED OXIDATION PROCESSES FOR WASTEWATER TREATMENT
Mohammad Sadegh Yalfani
ISBN:/DL:T.1259-2011

Introduction

1. Advanced Oxidation Processes (AOPs)

Advances in chemical water and wastewater treatment have led to a range of processes termed advanced oxidation processes (AOPs) being developed [1]. The process have shown great potential in treating pollutants of low or high concentrations and have found applications as diverse as groundwater treatment, industrial wastewater treatment, municipal wastewater sludge destruction and volatile organic compounds (VOCs) treatment. General speaking, the AOPs have proceeded along one of the two routes [2]:

– Wet Air Oxidation (WAO) processes: oxidation with O_2 in temperature ranges between ambient conditions and those found in incinerators in the region of 1–20 MPa and 200–300 °C.

ISBN:/DL:T.1259-2011

– The use of high energy oxidants such as ozone and H_2O_2 and/or photons those are able to generate highly reactive intermediates - $^{\bullet}OH$ radicals.

However, specifically, AOPs have been defined as "near ambient temperature and pressure water treatment processes which involve the generation of hydroxyl radicals in sufficient quantity to effect water purification" [3].

The hydroxyl radical ($^{\bullet}OH$) is a powerful (E° = 2.80 V), non-selective chemical oxidant, which acts very rapidly with most organic compounds [4]. A free radical is not an ionic species but is formed from an equal cleavage of a two electron bond. The main source of hydroxyl radicals are hydrogen peroxide, ozone, oxygen and air.

Developments in chemical treatment have made a range of AOPs suitable for water and wastewater applications. Table 1 lists those AOPs that have been developed and could have applications in water and wastewater treatment [1].

Table 1. AOP´s evaluated for water and wastewater treatment

Electrochemical	Catalytic ozonation
Fenton´s reagent	Supercritical water oxidation
Ionizing radiation	Ultrasound
Microwave	UV
Photo Fenton´s reagent	UV/H_2O_2
Photocatalysis	$UV/H_2O_2/O_3$
Catalytic wet air oxidation	Vacuum UV

A number of these processes are commercially available and in some instances widely used. Ultraviolet (UV) radiation for instance has over 3000 applications in Europe as a disinfection processes and is used in the US for treating groundwater pollutants such as methyl tertiary-butyl ether (MTBE) and N-nitroso-dimethylamine (NDMA). Processes such as chemical combinations of H_2O_2, O_3 and UV, Fenton´s reagent, wet air oxidation, supercritical water oxidation and electron beam have all been used at full scale.

ISBN:/DL:T.1259-2011

Other processes such as photocatalysis and ultrasound have been evaluated at pilot scale but many of the processes are being developed at laboratory bench. While the list includes individual processes, much research has been undertaken using a combination of the process, such as UV, ultrasound and ozone together, which offer significant kinetics and performance benefits over each other of the processes alone [1]. Here, the Fenton process and catalytic ozonation, which are the main topics of this thesis, are introduced in more details.

1.1. Fenton processes

Fenton and related reactions involve reactions of peroxides (usually H_2O_2) with iron ion to form active oxygen species. These active oxygen species are able to oxidize organic or inorganic compounds. The process was discovered by Henry J. Fenton for the first time who reported that H_2O_2 could be activated by Fe(II) salts to oxidize tartaric acid [5]. Since then, Fenton and related reactions have become of great interest for the relevance to biological chemistry, synthesis, the chemistry of natural waters, and the treatment of hazardous wastes.

In 1934 Haber and Weiss, proposed that the active oxygen species generated by the Fenton reaction are the hydroxyl radicals ($^{\bullet}OH$) [6]. Fifteen years later, Barb et al. studied more deeply the original mechanism proposed by Haber and Weiss and reached to what is now known globally as the classical or free radical Fenton chain reactions involving $^{\bullet}OH$ production as key step [7-9]. The free radical pathway was further promoted by Walling over contemporary challenges and served to renew interest in Fenton chemistry among workers in several fields of chemistry [10].

The Fenton and related reactions are viewed as potentially convenient and economical ways to generate oxidizing species for treating chemical waste. Both Fenton´s reagents i.e. hydrogen peroxide and iron possess advantageous properties. Compared to the other bulk oxidants, hydrogen peroxide is

ISBN:/DL:T.1259-2011

relatively safe, and does not make environmental threat since it readily decomposes to water and oxygen. Likewise, iron is comparatively inexpensive, safe, and environmentally friendly and is highly abundant (and maybe naturally occurring in the system being treated).

In some cases, complete mineralization of some organic compounds can be achieved using Fenton processes which are able to convert them to CO_2, H_2O and inorganic ions. However, to do so large excess chemicals are required, often preventing the process from being cost effective; hence only partial degradation usually occurs [11]. Partial degradation can be useful reducing the toxicity of the contaminants and hence increases the biodegradability of the residue. However, it is sometimes possible for the process to generate products with the same or higher toxicity than the parent compound [12].

1.1.1. Homogeneous Fenton processes

When all the Fenton reagents are present in the dissolved phase, the process is categorized as homogeneous Fenton. This process may still lead to the precipitation of some insoluble species like metal hydroxide which are not a part of the main process. The main reagents or factors which can participate in a homogeneous Fenton reaction are H_2O_2, Fe(II), Fe(III), light (UV), and organic or inorganic ligands [1].

Reaction between dissolved Fe(II) and H_2O_2 in acidic aqueous solution leads to oxidation of Fe(II) to Fe(III) and consequently highly reactive hydroxyl radicals ($^{\bullet}OH$) are formed. The reaction is spontaneous and can occur without influence of light.

The mechanism proposed by Barb et al. [7-9] for iron-catalyzed decomposition of H_2O_2 in acidic solution in the dark and in the absence of an organic compound consists of the sequence of the reactions 1-7. This sequence will be referred to as the thermal Fenton reaction, meaning that it is driven by thermal energy from the surrounding rather than photochemical energy. In this

ISBN:/DL:T.1259-2011

sequence, Fe(II) and Fe(III) are taken to represent all species in solution in each respective oxidation state.

(1) $Fe(II) + H_2O_2 \rightarrow Fe(III) + {}^{\bullet}OH + OH^-$

(2) $Fe(III) + H_2O_2 \rightarrow Fe(II) + HO_2^{\bullet} + H^+$

(3) $HO^{\bullet} + H_2O_2 \rightarrow HO_2^{\bullet} + H_2O$

(4) $HO^{\bullet} + Fe(II) \rightarrow Fe(III) + OH^-$

(5) $Fe(III) + HO_2^{\bullet} \rightarrow Fe(II) + O_2H^+$

(6) $Fe(II) + HO_2^{\bullet} + H^+ \rightarrow Fe(III) + H_2O_2$

(7) $HO_2^{\bullet} + HO_2^{\bullet} \rightarrow H_2O_2 + O_2$

Based on the above mechanism, iron cycles between Fe(II) and Fe(III) oxidation states. The net reaction is oxidation of H_2O_2 to O_2 and water which is catalyzed by iron. In the presence of an oxidizable substance such as organic compounds, carbon-centered radical intermediates are formed as a result of the reaction with ${}^{\bullet}OH$. The hydroxyl radical - always present in vanishingly small concentrations – reacts in well-known ways with organic compounds, principally by abstracting H from C-H, N-H, or O-H bonds, adding to C=C bonds, or adding to aromatic rings [13,14].

(8) $HO^{\bullet} + R{-}H \rightarrow H_2O + R^{\bullet}$

(9) $HO^{\bullet} + C{=}C \rightarrow HO{-}C{-}C^{\bullet}$

In the presence of O_2, the carbon-centered radicals may react with O_2 to form $HO_2^{\bullet}$, peroxyl radicals $R\text{-}OO^{\bullet}$, or oxyl radicals $R\text{-}O^{\bullet}$. The carbon-centered, peroxyl and oxyl radicals can be converted to stable organic intermediates as a result of coupling or reaction with iron ions. Such organic intermediates formed in the first stage of the oxidation may react further with $OH^{\bullet}$ and oxygen arriving eventually in mineralization to CO_2, H_2O and inorganic acids [18].

Oxidative degradation of organic contaminants by Fenton reaction is efficient only in the pH range 2-4 and is usually most efficient at around pH 2.8

ISBN:/DL:T.1259-2011

[15]. This is particularly due to the tendency for ferric oxyhydroxide precipitation (which has a low catalytic activity) to occur at pH > 3-4 (depending on the iron concentration). It is worth to note that the rate of the reaction (1) for Fe(II) increases at pH above 3 until it reaches a plateau at about pH 4. This has been attributed to the formation of $Fe(OH)_2$ which is about 10 times more reactive than Fe^{2+} [16]. Hence, the process is inefficient in the pH range of most natural waters (pH 5-9). Therefore, the addition of large amount of acid to achieve the optimum process efficiency, followed by base addition to neutralize the water after the oxidation is completed, makes the process unsuitable for many applications.

As an alternative for the above drawback, it has been found that addition of certain organic ligands that can complex Fe(III), enables the process to be carried out at higher pH [17]. This occurs because complexation limits the loss of the Fe(III) by oxyhydroxide precipitation. The higher the concentration of the organic complexant, the greater the extent of Fe(III) available. However, since most organic compounds also react with radicals and other oxidants, increasing the concentration of these organic-complexing agents can also lead to a decrease in the rate of oxidation of the contaminant. Nevertheless, the use of ligands does not solve the problem of iron remaining in solution after treatment. Moreover, in the presence of ligands, Fe precipitation by alkali or coagulant addition at the end of the treatment may be prevented. Significant reduction in dissolved Fe can be achieved by the use of heterogeneous Fenton processes, where the iron remains substantially in the solid phase, either as a mineral or as an adsorbed ion. Most of these heterogeneous processes have the added advantage that they can be operated in close to neutral pH range.

If the homogeneous Fenton reaction is initiated by $Fe(III)/H_2O_2$, the reaction rate would be slower than for $Fe(II)/H_2O_2$, because, in the former case, Fe(III) must be reduced to Fe(II) before hydroxyl radicals are produced. In the

ISBN:/DL:T.1259-2011

literature such reaction is usually named as “Fenton-like” process. It has been tried to distinguish it from Fenton process mechanistically. However, it can be seen that both Fe(II) and Fe(III) species are present simultaneously in the chain reaction, independent of initial oxidation state and regardless of which is used to initiate the reaction [19].

1.1.2. Heterogeneous Fenton processes

As it was mentioned above, a major disadvantage of wastewater treatment by homogeneous Fenton processes is that iron must usually be removed from the water at the end of the process [20]. Heterogeneous Fenton processes are of particular interest, since most of the iron remains in the solid phase and hence is easily separated from the treated water. Another disadvantage of the homogeneous Fenton reaction is that the treatment has to be performed at acidic pH preferentially between 2-4.

To overcome the above drawbacks, the development of supported Fenton catalysts is recently gaining importance. The ideal solid Fenton catalyst should not be prone to iron leaching, but most of the heterogeneous Fenton catalysts developed up to now still exhibit this problem. Iron ions significantly leach from the catalyst during the reaction, which causes a loss in activity with time and generates metal ion pollution. Therefore, it is well accepted that the most important issue in the heterogeneous Fenton process is the development of a heterogeneous catalyst with high activity and long-term stability at a reasonable cost. The optimum catalytic system can be obtained considering items such as source of iron, type of support, method of preparation and catalysts pretreatment conditions. Fe/Zeolites and Fe-containing pillared clays have been widely studied as heterogeneous Fenton catalysts [20-22]. Different phases of iron oxide such as hematite (Fe_2O_3) and magnetite (Fe_3O_4) have also been tested as heterogeneous Fenton catalyst [23-25]. Magnetite, although showed high stability during the oxidation of chlorophenol, the process was

ISBN:/DL:T.1259-2011

found to be very time-consuming (7 days needed to obtained full TOC mineralization) [23]. Fe_2O_3 as nanohematite (α-Fe_2O_3) demonstrated highest heterogeneous behavior in phenol degradation [24]. However, its activity was lower than homogeneous Fe catalyst. Other transition metals like Co and Ni have been tested as supported on carbon synthesized by wet impregnation and showed high activity, while the catalysts prepared via metal doping on the carbon aerogels presented lower amount of leaching [26].

1.2. Hydrogen peroxide

Hydrogen peroxide (main reagent of the Fenton process) was first recognized by Thenard in 1818 as the product of the reaction of barium peroxide with nitric acid. Hydrogen peroxide is a versatile oxidant that is effective over the whole pH range with high oxidation potential (E_0 = 1.763 V at pH 0, E_0 = 0.878 V at pH 14) and water as the only co-product [27]. Hydrogen peroxide can oxidize a broad variety of inorganic and organic substrates in liquid-phase reactions under very mild reaction conditions. In industry, H_2O_2 is used as an efficient bleaching agent in place of chlorine containing agents. Owing to its low molecular weight, hydrogen peroxide is a more efficient oxidizing agent than other oxidants, such as nitric acid and sodium hypochlorite. H_2O_2 has an environmentally benign profile since it decomposes to give only water and oxygen which makes it one of the cleanest, most versatile chemical oxidants available.

Hydrogen peroxide is currently produced with the alkyl anthraquinone oxidation (AO) process in which hydrogen, atmospheric oxygen and an anthraquinone derivative (typically 2-ethylantraquinone) are employed in the reaction cycle, the later acting as a reaction carrier [28]. The advantage of the AO process is the very high yield of hydrogen peroxide per cycle. However, its major disadvantage comes out not only from the side reactions, which require regeneration of the solution and the hydrogenation catalyst, but also from the

separation steps involved in the removal of organic impurities from the hydrogen peroxide product; this makes it a costly and non-environmentally-friendly process.

1.2.1. Direct generation of H_2O_2

The direct synthesis of H_2O_2 from hydrogen and oxygen using an appropriate catalyst has been found as an attractive alternative route for the use of AO process [29]. The single reaction $H_2 + O_2 \rightarrow H_2O_2$ is in principle, the simplest method to form hydrogen peroxide and should lead to a reduction in the capital investment and operating cost. Nevertheless, the reaction scheme (scheme 1) is more complex because of the occurrence of simultaneous or consecutive reactions which all are thermodynamically favored and highly exothermic [27]. Among these, unwanted reactions are: the formation of water (2), the decomposition of H_2O_2 (3), and the reduction of H_2O_2 (4). Each of these reactions can be favored depending on the catalyst used, the promoters or additives in the reaction medium and the reaction conditions. Despite of plenty of researches and several patents performed till now, the process has not yet been put into practice.

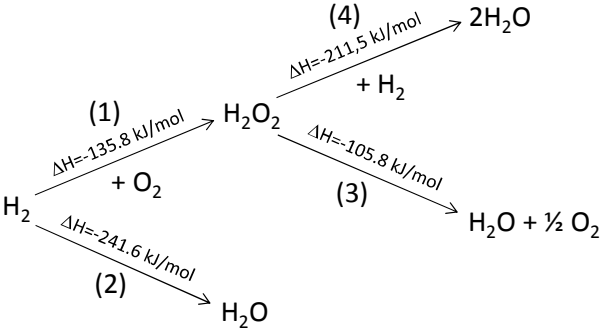

Scheme 1. Reaction pathways in the direct generation of hydrogen peroxide [27]

There are some major drawbacks to the direct synthesis of hydrogen peroxide. First, H_2/O_2 mixtures are explosive over a wide range of concentrations. The flammability limits of H_2 in O_2 are 4-94% [30]. So either the

ratio of hydrogen to oxygen needs to be carefully controlled or a diluent such as nitrogen, carbon dioxide, or argon must be added. A strategy to avoid direct contact between O_2 and H_2 reagents is the use of catalytic membrane reactors, in which pure gases can be used [31]. Also, taking into account the very low solubility of the gases, H_2 replacement with other soluble reactant can be considered as an appropriate alternative [32]. The other major problem in obtaining good selectivity for hydrogen peroxide over water is that catalysts for the production of hydrogen peroxide are also active for the combustion of hydrogen to water and the decomposition of hydrogen peroxide [27]. In addition, since pure hydrogen peroxide is highly unstable and decomposes into water and oxygen, the reaction must be conducted within an appropriate solvent. Thus, the performance of the reaction using three different phases i.e. gases (H_2 and O_2), liquid (solvent) and solid (catalyst) makes the process extremely complicated.

Palladium is the most suitable active metal known for the direct generation of hydrogen peroxide [27,33]. The metal is usually supported on a suitable oxide support such as alumina, silica, titania and carbon. Acid is often incorporated into the reaction medium in addition to the heterogeneous catalyst to delay or prevent the decomposition of hydrogen peroxide, which occurs in the presence of a base [34]. Another approach involves the addition of catalyst poisons (i.e. halides) to delay the water production and consequently increase the hydrogen peroxide selectivity [35]. Although halides show good selectivity for H_2O_2 formation, they also delay the hydrogen conversion. This suggests that the halide ions are adsorbed on the metal centers that participate in the surface reaction between hydrogen and oxygen [36]. Chloride and bromide are the most commonly employed halides. An obvious choice as promoters is the hydrogen halides, as they combine the function of the acidic proton with the effect of the anion on the catalyst center. However the presence

ISBN:/DL:T.1259-2011

of acid solutions and halide ion also favor the dissolution of the active metal, which results in deactivation of the catalyst. Colloid Pd is believed to be involved in the catalytic cycle of palladium catalysts [33]. Nevertheless, the management of a colloid would be difficult in a commercial process.

1.2.1. In situ generation of H_2O_2

A real breakthrough in H_2O_2 chemistry would be a one-pot process involving the direct synthesis of H_2O_2 from its elements and its direct application (*in situ*) in an oxidation reaction (scheme 2) [37,38]. Due to the high cost of bulk production of hydrogen peroxide and also difficulties related to the transportation and handling of high volume of hydrogen peroxide, *in situ* generation of hydrogen peroxide has been recently of interest to be used for different oxidation processes. The design of the *in situ* generation process requires considering its total compatibility with the oxidation catalyst and with the reagents/products involved in the overall reaction. The direct synthesis of hydrogen peroxide via catalytic hydrogenation of oxygen over Pd-based heterogeneous catalysts can be used for *in situ* applications owing to its performance at temperature range 0-25°C and overall pressure up to 100 atm [33]. The reaction can be carried out in aqueous/organic solvent mixture, which can be adequate for the *in situ* oxidation of water insoluble compounds. However, for example, the presence of strong acids which is essential to get high selectivity to hydrogen peroxide is incompatible with the epoxidation of olefins.

Epoxidation of olefins was one of the first application of *in situ* generated hydrogen peroxide [39], for which titanosilicate zeolites (TS-1 and TS-2) were found as the preferred catalyst for unhindered olefins [40]. Herron and Tolman for the first time reported the hydroxylation of alkanes performed with a mixture of molecular hydrogen and oxygen over small pore zeolite loaded with

ISBN:/DL:T.1259-2011

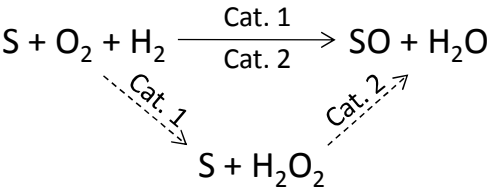

Scheme 2. Oxidation of substrate S with *in situ* generated H_2O_2 [33].

Pd(0)/Fe(II) [41]. An outstanding study was reported by Niwa et al. who showed up to 97% selectivity to phenol by oxidation of benzene using *in situ* generated H_2O_2 over palladium membrane [42].

The application of H_2 substitutes for the generation of H_2O_2 can also be used for the *in situ* generation of H_2O_2, in particular, where the use of H_2 gas may not be compatible with reaction conditions. The most well-known H_2 substitutes are hydrazine, hydroxylamine and formic acid [43-45].

The application of *in situ* generated hydrogen peroxide in wastewater treatment has been experienced limitedly. There are few works involving *in situ* generated hydrogen peroxide used for the oxidation of water contaminants [46,47].

1.3. Ozonation

Ozone, a powerful oxidizing agent (under acidic conditions $E(O_3/O_2)$ = 2.07 V), is effective for the mineralization of refractory organic compounds [48]. The ozonation of organic pollutants involves two types of oxidation reactions, either molecular ozone reactions (ozonolysis) or hydroxyl radical reactions, depending on the reaction conditions such as pH and the type of pollutant [49]. At lower pH, molecular ozone reactions are predominant, where organic compounds are subjected to the electrophilic attack of ozone molecules and decomposed into carboxylic acids as final end products. The molecular ozone reactions are selective to the organic molecule having nucleophilic moieties such as carbon-carbon double bonds, -OH, $-CH_3$, $-OCH_3$ and other nitrogen,

ISBN:/DL:T.1259-2011

oxygen, phosphorous, and sulfur bearing functional groups [50]. On the other hand, in the presence of hydroxyl anion (HO^-) at high pH (>8), ozone molecules are decomposed into free radicals ($^{\bullet}O_2^-$ and $HO_2^{\bullet}$), and subsequently produces hydroxyl radical ($OH^{\bullet}$), which will attack organic compounds [51]. The later process is classified as an AOP, because it employs hydroxyl radicals. Ozonation finds application for drinking water disinfection, bacterial sterilization and generally for organic compounds degradation, although its application to wastewater treatment is limited due to the high energy demand [52]. However, the ozonation as a pre-treatment process to transform refractory compounds into substances to be removed by conventional methods appears more economically attractive [53].

1.3.1. Catalytic ozonation

In the presence of a catalyst or in combination with UV radiation or H_2O_2, the ozonation process is more efficient in the degradation of organic compounds [48]. Homogeneous catalytic ozonation involves the use of O_3 and a dissolved metal ion like Fe^{2+} or coupled with UV radiation, or H_2O_2. Heterogeneous catalytic ozonation involves the use of O_3 and a supported metal or a metal oxide as catalyst. Such a system can be coupled with UV radiation or H_2O_2 in order to be stronger. The major advantage of a heterogeneous over homogeneous catalytic system is the ease of catalyst retrieval from the reaction media. However, the stability and durability of the catalyst under operating conditions is important. Leaching of the catalytic active species or poisoning of the active sites or fouling of the catalyst surface by intermediate reaction products are important factors which determine the stability and durability of the catalyst. Recent studies on the Co-based catalysts have shown that in the presence of all these catalysts, phenol conversion by ozonation was completed in less than 1 h [54]. However, TOC removal (%) depended on the characteristic of the catalysts. Highest efficiency in TOC removal was obtained by the CoNi-

ISBN:/DL:T.1259-2011

hydrotalcite catalyst. Among the single metal oxides, MnO_2, Al_2O_3 and Fe, Co and Ce oxides have been widely studied in catalytic ozonation [55]. MnO_2 was found to be efficient in gaseous medium [56]. Tong et al. have discovered that the possible mechanism of catalytic ozonation by MnO_2 is adsorption of organic molecule on the surface of MnO_2 and subsequent attack of ozone on adsorbed molecule [57]. In the case of Al_2O_3, Chen et al. revealed that activity of γ-Al_2O_3 in ozonation of 2-methylisoborneol is due to hydroxyl radical generation on the surface at a pH close to pH_{PZC} [58]. However, ozonation of oxalic acid in the presence of Fe_2O_3/Al_2O_3 was found to not proceed via radical formation [59]. A reaction between molecular ozone and surface complex between Fe and oxalic acid could be the responsible for oxalic acid oxidation.

2. Objectives of the project

This project is aimed to present new catalytic AOPs (specifically Fenton process and catalytic ozonation) for the degradation of organic pollutants existed in wastewaters. Owing to the difficulties related to the transportation of hydrogen peroxide, a special attention has been accounted to the *in situ* generated hydrogen peroxide (Scheme 3).

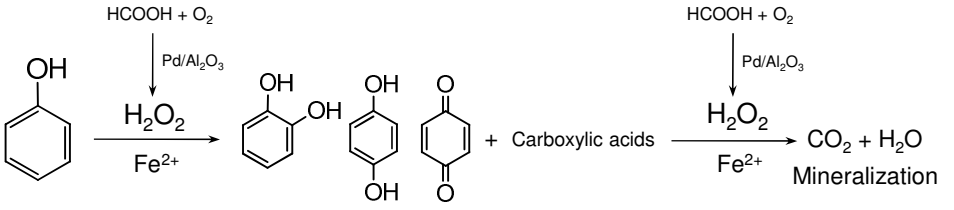

Scheme 3. Phenol (as representative of organic pollutants) degradation via Fenton process using *in situ* generated H_2O_2

Considering the previous methods for the generation of hydrogen peroxide, a new route using an appropriate substitute for H_2 is presented. Then, this

ISBN:/DL:T.1259-2011

pathway is applied as *in situ* for the degradation of organic pollutant via Fenton process. Meanwhile, the effect of second metal and support on the main catalyst is screened. Subsequently, a full heterogeneous catalytic Fenton process involving *in situ* generated hydrogen peroxide is developed. The later process is experienced for different categories of organic pollutant. The combination of such process with other techniques e.g. hydrodechlorination is also undertaken. As the last part, catalytic ozonation of pharmaceutical compounds based on dawsonite based materials is performed. The efficiency of the new process are compared with similar and known process i.e. conventional Fenton process and single ozonation.

Separately, each chapter of this thesis is subjected to the following objectives:

Chapter 1. The generation of hydrogen peroxide is performed using formic acid and oxygen over Pd/γ-Al_2O_3. Formic acid is used as substitute for hydrogen. The effect of Pd content and halide ions on the selectivity of the process is studied.

Chapter 2. The pathway for the hydrogen peroxide formation introduced in Chapter 1 is used *in situ* for the oxidation of phenol (representative for organic pollutants) in the presence of ferrous iron. The performance of this process is compared with the conventional Fenton process. The effect of some factors such as Pd content of the catalyst and temperature is studied.

Chapter 3. The effect of second metal (Au, Pt, Fe, Cu) and support (Al_2O_3, TiO_2, Carbon) on the performance of Pd in the process described in chapter 2 is studied. The studied is developed for phenol degradation via Fenton process.

Chapter 4. A full heterogeneous Pd-Fe catalytic system is designed to carry out hydrogen peroxide generation and Fenton reaction simultaneously. The catalysts are characterized using different techniques in order to evidence the mechanism of the reaction. The performance of this process is evaluated for

different categories of organic pollutants such as phenol, chlorophenols (2,4-dichlorophenol) and pharmaceuticals (clofibric acid).

Chapter 5. The degradation of chlorophenols (2,4-dichlorophenol and pentachlorophenol) involving a combination of reduction (hydrodechlorination) and oxidation (Fenton process) is studied. The heterogeneous Fenton process using *in situ* generation hydrogen peroxide presented in Chapter 4 is applied for this purpose. Formic acid behaves as source of hydrogen for both hydrodechlorination and *in situ* generation of hydrogen peroxide.

Chapter 6. Different hydrogen substitutes (formic acid, hydrazine and hydroxylamine) are applied for *in situ* generation of hydrogen peroxide. The hydrogen peroxide generated *in situ* is used in phenol degradation via Fenton process. The reactions are taken place using semi- (Pd/Al_2O_3 + Fe^{2+}) and full heterogeneous ($FePd/Al_2O_3$) catalysts and at different initial pHs. The performances of these hydrogen substitutes in this process are compared.

Chapter 7. The activity of Cu-dawsonite in catalytic ozonation of clofibric acid (a pharmaceutical compound) is studied. The catalyst is synthesized and characterized using different techniques. The performance of Cu incorporated in the structure of dawsonite in the above process is compared with dissolved homogeneous Cu^{2+} and CuO supported on alumina. The stability of Cu-dawsonite and the position of Cu within the structure of dawsonite based on the characterization and activity results are discussed.

References

[1] S. A. Parasons, M. Williams, *Advanced Oxidation Processes for Water and Wastewater Treatment,* IWA Publishing, 1st Ed., (2004) 1-6.

[2] R. Munter, *Proc. Estonian Acad. Sci. Chem.*, 50 (2001) 59–80.

[3] W. H. Glaze, J. W. Kang, D. H. Chapin, *Ozone: Sci. Eng*., 9 (1987) 335–352.

[4] J. H. Carey, *Water Pollut. Res. J. Can*., 27 (1992) 1–21.

[5] H.J.H. Fenton, *J. Chem. Soc. Trans.* 65 (1894) 899-910.

[6] F. Haber, J. Weiss, *Proc. Roy. Soc. A.*, 134 (1934) 332-351.

[7] W. G. Barb, J. H. Baxendale, P. George, , and K. R. Hargrave, *Nature*, 163 (1949) 692–694.

[8] W. G. Barb, J. H. Baxendale, , P. George, K. R. Hargrave, *Trans. Faraday Soc.*, 47 (1951a) 462–500.

[9] W. G. Barb, J. H. Baxendale, , P. George, K. R. Hargrave, *Trans. Faraday Soc.* 47 (1951b) 591–616.

[10] C. Walling, *Acc. Chem. Res.*, 8 (1975) 125–131.

[11] P. L. Houston, J. J. Pignatello, *Water. Res.*, 33 (1999) 1238-1246.

[12] A. R. Fernández-Alba, D. Hernando, A. Agüera, J. Cáceres, S. Malato, *Water. Res.* 36 (2002) 4255-4262.

[13] C. Von Sonntag, and H. P. Schuchmann, Z. B. Alfassi, ed., John Wiley and Sons, New York, (1997) 173–234.

[14] G. V. Buxton, C. L. Greenstock, W. P. Helman, A. B. Ross, *J. Phys. Chem. Ref. Data* 17, (1988) 513–886.

[15] J. J. Pignatello, *Environ. Sci. Technol.* 26 (1992) 944-951.

[16] C. F. Wells, M. A. Salam, *J. Chem. Soc. A* (1968) 24–29.

[17] M. E. Balmer, B. Sultzberger, *Environ. Sci. Technol.*, 33 (1999) 2418-2424.

[18] J.J. Pignatello, E. Oliveros, A. MacKey, *Crit. Rev. Environ. Sci. Technol.* 36 (2006) 1-84.

[19] A. Safarzadeh-Amiri, J. R. Bolton, S. R. Cater, *J. Adv. Oxid. Technol.* 1 (1996) 18-26.

[20] M. Hartmann, S. Kullmana, H. Keller, *J. Mater. Chem.* 20 (2010) 9002-9017.

[21] S. Navalon, M. Alvaro, H. Garcia, *Appl. Catal. B: Environ.* 99 (2010) 1-26.

[22] S. Perathoner, G. Centi, *Top. Catal.* 33 (2003) 207-224.

[23] X. Xue, K. Hanna, M. Abdelmoula, N. Deng, *Appl. Catal. B: Environ.* 89 (2009) 432-440.

[24] R. Prucek, M. Hermanek, R. Zboril, *Appl. Catal. A: Gen.* 366 (2009) 325-332.

[25] S. Yang, H. He, D. Wu, D. Chen, X. Liang, Z. Qin, M. Fan, J. Zhu, P. Yuan, *Appl. Catal. B: Environ.* 89 (2009) 527-535.

[26] F. Duarte, F.J. Maldonado-Hódar, A.F. Pérez-Cadenas, L.M. Madeira, Appl. Catal. B: Environ. 85 (2009) 139-147.

[27] J. M. Campus-Martin, G. Blanco-Brieva, J. L. G. Fierro, *Angew. Chem. Int. Ed.* 2006, 45, 6962-6984.

[28] W. T. Hess, *Kirk-Othmer Encyclopedia of Chemical Technology,* ed. J. K. Kroschwitz and M. Howe-Grant, Wiley, New York, 4th edn. 13 (1995) 961-995.

[29] Q. Liu, J. C. Bauer, R. E. Schaak, J. H. Lunsford, *Angew. Chem. Int. Ed.* 47 (2008) 6221-6224.

[30] C. E. Baukal, *Oxygen-Enhanced Combustion,* CRC, (1998).

[31] V. R. Choudhary, A. G. Gaikwad, S. D. Sansare, *Angew. Chem. Int. Ed.* 40 (2001) 1776-1779.

[32] T. P. Sheriff, *J. Chem. Soc. Dalton. Trans.* (1992) 1051.

[33] S. Chinta, J. H. Lunsford, *J. Catal.* 225 (2004) 249-255.

[34] R. Burch, P. R. Ellis, *Appl. Catal. B: Environ.* 42 (2003) 203-211.

[35] Q. Liu, J. H. Lunsford, *Appl. Catal. A: Gen.* 314 (2006) 94-100.

[36] V. R. Choudhary, C. Samanta, *J. Catal.* 238 (2006) 28-38.

[37] M. G. Clerici and P. Ingallina, *Catal. Today*, 41 (1998) 351.

[38] W. F. Hoelderich, Appl. Catal. A: Gen. 194 –195 (2000) 487–496.

[39] T. Hayashi, K. Tanaka, M. Haruta, *J. Catal.* 178 (1998) 566-575.

[40] M. G. Clerici, G. Bellussi, U. Romano, *J. Catal.* 129 (1991) 159-167.

[41] N. Herron, C. A. Tolman, *J. Am. Chem. Soc.* 109 (1987) 2837-2839.

[42] S. Niwa, M. Eswaramoorthy, J. Nair, A. Raj, N. Itoh, H. Shoji, T. Namba, F. Mizukami, *Science* 295 (2002) 105-107.

[43] V. R. Choudhary, C. Samanta, P. Jana, *Chem. Commun.* (2005) 5399-5401.

[44] V. R. Choudhary, P. Jana, *Catal. Commun.* 8 (2007) 1578-1582.

[45] M. S. Yalfani, S. Contreras, F. Medina, J. Sueiras, *Chem. Commun.* (2008) 3885-3887.

[46] Y.–G. Zhang, L.–L. Ma, J.–L. Li, Y. Yu, *Environ. Sci. Technol.* 41 (2007) 6264-6269.

[47] Sheriff, T.S. Cope, S. Ekwegh, M.; *Dalton Trans.* (2007) 5119-5122.

[48] L. F. Liotta, M. Gruttadauria, G. Di Carlo, G. Perrini, V. Librando, *J. Hazard. Mater.* 162 (2009) 588-606.

[49] K. Ikehata, M. G. El-Din, *Ozone Sci. Eng.* 26 (2004) 327-343.

[50] A. B. C. Adams, C. Diaper, S. A. Parsons, *Environ. Technol.* 22 (2001) 409-427.

[51] C. Gottschalk, J. A. Libra, A. Saupe, *Ozonation of Water and Waste Water,* 2nd ed. WILEY-VCH, (2010).

[52] M. Pera.Titus, V. García-Molina, M. A. Baños, J, Giménez, S. Esplugas, *Appl. Catal. B: Environ.* 47 (2004) 219-254.

[53] S. T. Hu, Y. H. Yu, *Ozone Sci. Eng.* 16 (1994) 13-28.

[54] M. Gruttadauria, L.F. Loitta, G. Di Carlo, G. Pantaleo, G. Deganello, P. Lo Meo, C. Aprile, R. Noto, *Appl. Catal. B: Environ.* 75 (2007) 281-289.

[55] J. Nawrocki, B. Kasprzyk-Hordern, *Appl. Catal. B: Environ.* 99 (2010) 27-42.

[56] S.T. Oyama, *Catal. Rev. Sci. Eng.* 42 (2000) 279-322.

[57] S.-P. Tong, W.-P. Liu, W.-H. Leng, Q.-Q. Zhang, *Chemosphere* 50 (2003) 1359-1364.

[58] L. Chen, F. Qi, B. Xu, J. Shen, K. Li, *Water Sci. Technol: Water Supply* 6 (2006) 43-51.

[59] F.J. Beltran, F.J. Rivas, R. Montero-de-Espinosa, *Water Res.* 39 (2005) 3553-3564.

UNIVERSITAT ROVIRA I VIRGILI
NEW CATALYTIC ADVANCED OXIDATION PROCESSES FOR WASTEWATER TREATMENT
Mohammad Sadegh Yalfani
ISBN:/DL:T.1259-2011

Chapter 1

Direct generation of hydrogen peroxide from formic acid and O_2 using heterogeneous Pd/γ-Al_2O_3 catalysts

Hydrogen peroxide formation is achieved with remarkable productivity at ambient conditions (25 °C and atmospheric pressure) in aqueous medium using a heterogeneous catalytic system. Formic acid is decomposed in the presence of a continuous flow of O_2 over Pd/γ-Al_2O_3 catalyst leading to the generation of hydrogen peroxide. The addition of a negligible amount of bromide ion improves the selectivity of the reaction.

ISBN:/DL:T.1259-2011

1. Introduction

Hydrogen peroxide has been known as benign and efficient oxidant for various purposes such as synthesis of organic compounds, pulp and paper industry, bleaching and also oxidation of organic pollutants in industrial wastewater via Fenton process. Hydrogen peroxide is industrially synthesized through alkyl anthraquinone as an intermediate from hydrogen and oxygen [1]. Recently, due to negative economic and environmental aspects of this process, there has been strong interest in replacing that with one in which hydrogen peroxide can be produced by direct reaction between H_2 and O_2 or as *in situ* in the reaction media [2-4]. H_2 and O_2 are among the first choices as substrate for direct generation of hydrogen peroxide [3], what can be considered as an environmentally-friendly process. In this approach, heterogeneous catalysis is recognized as a promising technique, where Pd has shown a significant performance in formation of hydrogen peroxide [3]. However, there are some drawbacks in this process, being the main ones the risk of explosivity of the O_2/H_2 mixture and the low solubility of the gases in solution, in particular hydrogen. The use of membranes to separate the reaction mixture [5] or the use of other sources of hydrogen could overcome these difficulties. Furthermore, the use of *in situ* generated H_2O_2 in oxidation processes [5,6] would open new possibilities, for which the *in situ* generation should be performed in operating conditions compatible with those of subsequent oxidation reactions. Bortolo et al. [7] found that alcohols can act as reducing agents of palladium complexes with production of hydrogen peroxide. The main drawback of this process is to use a homogeneous catalyst which has problems concerning to separation and recycling of catalyst and products from the reaction medium. Choudhary et al. [8] indicated that hydrazine can be used as hydrogen source for production of hydrogen peroxide leading a remarkable selectivity toward hydrogen peroxide. However, this system utilizes hydrazine

ISBN:/DL:T.1259-2011

which is classified as toxic and possible carcinogenic compound. It also requires addition of halide ions as prerequisite to proceed. Besides, presence of a mineral acid creating an extremely low pH is of importance in order to stabilize hydrogen peroxide. Recently, the same authors [9], proposed hydroxylamine as hydrogen source using Pd/Al_2O_3 catalyst. Although the offered system is sufficiently simple, hydroxylamine is known to be explosive.

Formic acid is a compound which has not been classified as carcinogenic neither explosive. It can be decomposed according to dehydration ($HCOOH \rightarrow CO + H_2O$) or dehydrogenation ($HCOOH \rightarrow CO_2 + H_2$) [10]. The process over supported-metal catalysts has also been investigated [11]. The studies indicated that catalytic decomposition of formic acid is predominantly inclined toward production of hydrogen and carbon dioxide when the process occurs at low temperature (< 380 K) and in aqueous medium [10,12]. Therefore, it could be utilized as a source of hydrogen in hydrogenation processes. Regarding to this fact, Hyde et al. [13] carried out hydrogenation of organic compounds using hydrogen released from decomposition of formic acid. It has also been shown that formic acid can be considered as a promising substitute for H_2 in hydrodechlorination of chlorinated organic compounds [14].

In this work, we perform generation of hydrogen peroxide in aqueous medium from formic acid and oxygen using $Pd/\gamma\text{-}Al_2O_3$ catalysts at ambient conditions. This new route could be applied to produce *in situ* H_2O_2 for the subsequent oxidation purposes. Selection of supported-Pd catalyst has been based on its appreciable results in development of hydrogen peroxide formation process and decomposition of formic acid as well [3,12]. The production rate and the selectivity of the reaction for H_2O_2 at both short and long time are of high importance in this route. The effect of halide ion on the selectivity of the reaction is also studied. According to our knowledge no result

ISBN:/DL:T.1259-2011

concerning to this route for generation of hydrogen peroxide has been published.

2. Experimental

The Pd/γ-Al_2O_3 catalysts were synthesized by conventional incipient wetness impregnation. An aqueous solution of $PdCl_2$ acidified by hydrochloric acid was added to an aqueous slurry of γ-Al_2O_3 (prepared by sol-gel method) stirring vigorously. The mixture aged stirring for 1 h, heated under vacuum at 60 °C and eventually dried at 110 °C for 12 h. The precipitate was calcined in static air at 400 °C for 3 h and reduced under a flow of pure hydrogen (20 ml/min) at 200 °C for 2 h. H_2 chemisorption was performed using a Micromeritics ASAP 2010 aparatus.

The hydrogen peroxide formation reactions were implemented at ambient conditions (T = 25 °C and atmospheric pressure) in a magnetically stirred three-necked glass reactor with a capacity of 100 ml. The volume of the reaction was always 50 ml containing 25 mmol formic acid in H_2O. The amount of catalyst was 0.1 g in all the reactions. Oxygen was passed bubbling into the reaction medium with a flow rate of 20 $ml.min^{-1}$. The temperature of the reaction was controled using water bath. H_2O_2 formation and formic acid decomposition were monitored by sampling at regular time intervals and analysing by iodometric titration and high performance liquid chromatography HPLC (Shimadzu LC-2010 equipped with a Acclaim OA column and SPD-M10A detector and using 100 mM Na_2SO_4 at pH 2.65 adjusted by methanesulphonic acid as mobile phase) respectively. The overhead exhausted gases of the reaction were analyzed online using a gas chromatography (Shimadzu GC-14B with a TEKNOKROMA Propapack R column, TCD detector and He as carrier gas) and a mass analyser (PFEIFFER VACUUM, GSD 301 O_2, Omnistar™). The reaction solution at the end of each run after filtration was analysed by atomic

absorption spectroscopty to detect leached Pd. H_2O_2 decomposition reactions were performed at ambient conditions using a 50 ml aqueous solution containing 100 ppm H_2O_2 and 0.1 g catalyst. H_2O_2 degradation was monitored by iodometric titration.

3. Results and discussion

The results illustrated in Table 1 show formation of hydrogen peroxide during the reaction of formic acid with O_2 over Pd/γ-Al_2O_3 catalysts. The reactions were carried out at ambient conditions (25 ˚C and atmospheric pressure) in aqueous medium for 1 h using various Pd content catalysts. Without using the catalyst no H_2O_2 was detected through the reaction. The highest short time production is achieved by the highest Pd content catalyst with 5% Pd. After 1 h reaction, highest H_2O_2 produced is obtained by the Pd0.5%/γ-Al_2O_3 catalyst. This catalyst also presents the highest efficiency, measured as TOF value (118 h^{-1}).

Table 1. H_2O_2 formation results during the reaction of formic acid and O_2 over Pd/γ-Al_2O_3 catalysts.

Catalyst	D^a (%)	Time (h)	Formic acid conv. (mmol)	H_2O_2 formation (mmol 10^2)	TOF^b (h^{-1})	H_2O_2 selectivity (%)
Pd5/γ-Al_2O_3	5.8	0.083	0.31	3.10		10.0
		1.0	3.60	4.20	15.4	1.2
Pd2.5/γ-Al_2O_3	12.3	0.083	0.22	1.35		6.2
		1.0	3.10	4.45	15.4	1.5
Pd1/γ-Al_2O_3	19.9	0.083	0.27	1.35		5.0
		1.0	2.52	8.90	47.6	3.5
Pd0.5/γ-Al_2O_3	25.2	0.083	0.18	0.75		4.2
		1.0	2.0	14.0	118.2	7.0
Pd0.1/γ-Al_2O_3	26.7	0.083	0.15	0.37		2.5
		1.0	1.60	2.65	105.6	1.7

^{a} Metal dispersion, ^{b} mmol H_2O_2 mmol (Pd dispersed)$^{-1}$ h^{-1}

Conversion of formic acid is decreased by reducing the Pd content in the catalysts (Table 1). Selectivity of the reaction for H_2O_2 is calculated as mmol H_2O_2 formed divided by mmol HCOOH converted. According to that, selectivity of H_2O_2 (shown in Table 1) was higher at short time for the catalysts than at

ISBN:/DL:T.1259-2011

long time. However, for Pd0.5%/γ-Al_2O_3 catalyst the H_2O_2 production showed highest selectivity (7%) at long time (1 h).

The phenomenon can be simply presumed to be firstly decomposition of formic acid over the Pd catalyst (Scheme 1-A). This process is expected to lead to production of H_2 and CO_2 at these conditions as it has been proved in the literature [12]. Analysis of the overhead gases of the reaction indicates only O_2 and CO_2. No CO and H_2 peaks were observed in the gas chromatogram. In addition, mass analysis profile of the outlet gases displays only masses related to CO_2 (44), O_2 (32), and 28 as a fragment of CO_2 (Figure 1). Only trace amount of MS (2) related to H_2 is observed indicating almost total consumption of released hydrogen. In order to further evidence the above results, we performed the decomposition of formic acid over the catalyst (Pd5%/γ-Al_2O_3) in Ar atmosphere and observed only CO_2 and H_2 corresponding masses in mass analysis profile of the outlet gases (Figure 2). These results can confirm that the formic acid decomposition on the catalyst at our reaction conditions rather follows dehydrogenation than dehydration. As second step, the introduced O_2 reacts with released H_2 to form hydrogen peroxide. Definitely, a side reaction of water formation is also expected to occur with a significant rate which drastically influences H_2O_2 selectivity.

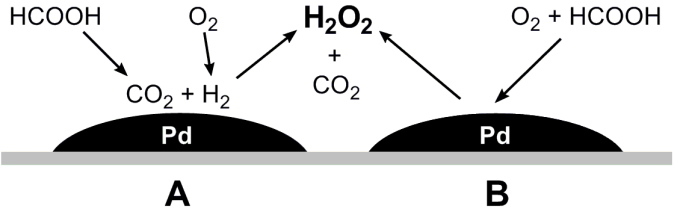

Scheme 1. Suggested approaches toward generation of H_2O_2 from formic acid and O_2 over Pd/γ-Al_2O_3; A: two steps, B: one step

ISBN:/DL:T.1259-2011

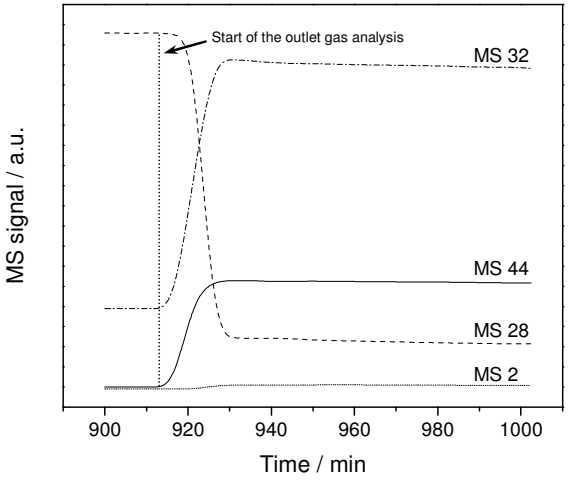

Figure 1. MS profile of the outlet gases during generation of hydrogen peroxide from formic acid and O_2 over Pd/γ-Al_2O_3

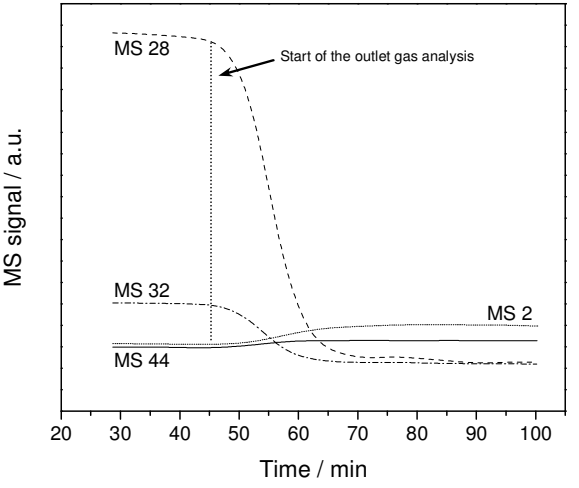

Figure 2. MS profile of the outlet gases during decomposition of formic acid over Pd/γ-Al_2O_3 in Ar atmosphere.

ISBN:/DL:T.1259-2011

Another assumption that can be considered is the direct reaction of formic acid with O_2 (Scheme 1-B) (with different stoichiometries) resulting in H_2O_2 or H_2O ($HCOOH + O_2 \rightarrow H_2O_2 + CO_2$ or $HCOOH + 1/2O_2 \rightarrow H_2O + CO_2$). In this case, water formation occurs by direct reaction of HCOOH and oxygen as well as decomposition of hydrogen peroxide. Most importantly, decomposition rate of formic acid was remarkably higher in comparison with the reaction carried out in the absence of oxygen. Thus, in the presence of oxygen, decomposition of formic acid is accelerated.

Table 2. H_2O_2 formation results during the reaction of formic acid and O_2 over $Pd/\gamma\text{-}Al_2O_3$ catalysts in presence of O_2.

Catalysts	KBr (mol)	Time (h)	Formic acid conv. (mmol)	H_2O_2 formed (mmol 10^2)	H_2O_2 selectivity (%)
$Pd5/\gamma\text{-}Al_2O_3$	10^{-4}	0.083	0.22	0.74	3.4
		1.0	0.36	0.99	2.8
$Pd5/\gamma\text{-}Al_2O_3$	10^{-5}	0.083	0.19	1.97	10.4
		1.0	0.70	14.30	20.5
$Pd5/\gamma\text{-}Al_2O_3$	10^{-6}	0.083	0.38	4.45	11.7
		1.0	3.55	6.70	1.9
$Pd1/\gamma\text{-}Al_2O_3$	10^{-5}	0.083	0.28	0.74	2.7
		1.0	0.43	3.45	8.0
$Pd0.5/\gamma\text{-}Al_2O_3$	10^{-4}	0.083	0.44	0.25	<1
		1.0	0.54	1.48	2.8
$Pd0.5/\gamma\text{-}Al_2O_3$	10^{-5}	0.083	0.23	1.23	5.4
		1.0	0.68	2.71	4.0
$Pd0.1/\gamma\text{-}Al_2O_3$	10^{-5}	0.083	0.21	0.99	4.7
		1.0	0.36	1.23	3.4

In the previous works of generation of H_2O_2, it has been strongly mentioned the essential requirement of halide ion and mineral acid presence in order to achieve the process with high selectivity [3,8]. As it is shown in Table 2, addition of different dosages of bromide ion to the reaction medium displays interesting changes in the H_2O_2 production process. Firstly, decomposition of formic acid especially at long time is appreciably diminished. Considering that decomposition of formic acid occurs prior to hydrogen peroxide formation, it could be described that halide ions block the active sites of the catalyst to

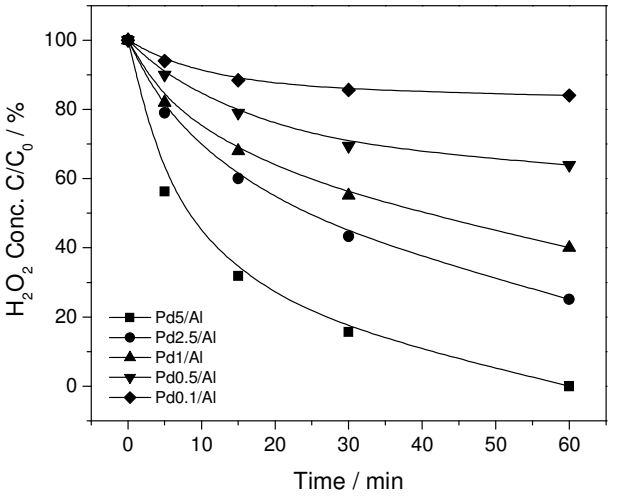

Figure 3. H_2O_2 decomposition profile over Pd/γ-Al_2O_3 catalysts.

adsorb formic acid and hamper this trend. In other words, halide ion behaves as poison for formic acid decomposition reaction. In order to confirm the above hypothesis, we fulfilled the catalytic decomposition of formic acid in Ar atmosphere at 50 °C (to observe clearly the phenomenon) using Pd5%/γ-Al_2O_3 with and without Br^- ion (10^{-4} mol). In the presence of Br^- decomposition rate of formic acid was clearly lower than in the absence of Br^-. Similar trend was observed for the decomposition of H_2O_2, mainly at low Br^- content. Consequently, bromide can control decomposition of H_2O_2 and improve its selectivity. As shown in Table 2, by decreasing the concentration of bromide to 10^{-5} mol in the reaction medium, H_2O_2 selectivity using Pd5%/γ-Al_2O_3 reaches to a worthwhile number of 21% at long time. Further decreasing of bromide to 10^{-6} mol results again in increasing of formic acid decomposition and thereupon decreasing of H_2O_2 selectivity. H_2O_2 selectivity for the catalysts with lower Pd content (as shown in Table 2) was influenced by bromide but not in the same extent as for Pd5%/γ-Al_2O_3.

Productivity of the catalysts with lower Pd amount can also be described regarding to their ability to decompose hydrogen peroxide. As shown in Figure 3 decomposition rate of hydrogen peroxide is abated by decreasing the Pd amount in catalysts. In other words, hydrogen peroxide molecules demonstrate more resistance when they are exposed to the low Pd catalysts.

Our catalytic system shows a marked stability property because no Pd leaching was detected in aqueous medium after the end of each run. Hence, the catalyst can be easily recovered at the end of the reaction.

4. Conclusion

As conclusion, we attained a new route to produce hydrogen peroxide with several advantageous properties including simplicity, cleanness and most important environment-friendly. It performs at ambient conditions and in aqueous medium. The productivity and selectivity of the system are noteworthy. In presence of negligible amount of bromide ion the selectivity of H_2O_2 increases remarkably. Nevertheless, both productivity and selectivity of the system have still a significant potential for improvement. The decomposition of formic acid to H_2 and CO_2 at ambient conditions [10,12], introduces formic acid as eligible replacement for pure hydrogen in hydrogen peroxide formation process. This hydrogen peroxide generation approach could be proposed to be used for oxidation of organic compounds.

Acknowledgement

This work was funded by the URV projects no. AIRE 2006/02, and also AECI, ref. A/5188/06.

References

[1] W. T. Hess, *Kirk-Othmer Encyclopedia of Chemical Technology*, ed. J. K. Kroschwitz and M. Howe-Grant, Wiley, New York, 4th edn., (1995), vol. 13, 961-995.

[2] J. M. Campos-Martin, G. Blanco-Brieva and J. L. G. Fierro, *Angew. Chem. Int. Ed.*, 45 (2006) 6962-6984.

[3] J. H. Lunsford, *J. Catal.*, 216 (2003) 455-460.

[4] M. G. Clerici and P. Ingallina, *Catal. Today*, 41 (1998) 351-364.

[5] S. Niwa, M. Eswaramoorthy, J. Nair, A. Raj, N. Itoh, H. Shoji, T. Namba and F. Mizukami, *Science*, 295 (2002) 105-107.

[6] Y. –G. Zhang, L. –L. Ma, J. –L. Li And Y. Yu, *Environ. Sci. Technol.*, 41 (2007) 6264-6269.

[7] R. Bortolo, D. Bianchi, R. D'Aloisio, C. Querci and M. Ricci, *J. Mol. Catal. A: Chem.*, 153 (2000) 25-29.

[8] V. R. Choudhary, C. Samanta and P. Jana, *Chem. Commun.*, (2005) 5399-5401.

[9] V. R. Choudhary and P. Jana, *Catal. Commun.*, 8 (2007) 1578-1582.

[10] N. Akiya and P. E. Savage, *AICHE J.*, 44 (1998) 405-415.

[11] T. van Herwijnen, R. T. Guczalski and W. A. de Jong, *J. Catal.*, , 63 (1980) 94-101.

[12] E. M. Cordi and J. L. Falconer, *J. Catal.* 162 (1996) 104-117.

[13] J. R. Hyde and M. Poliakoff, *Chem. Commun.*, (2004) 1482-1483.

[14] F. –D. Kopinke, K. Mackenzie, R. Koehler and A. Georgi, *Appl. Catal. A*, 271 (2004) 119-128.

UNIVERSITAT ROVIRA I VIRGILI
NEW CATALYTIC ADVANCED OXIDATION PROCESSES FOR WASTEWATER TREATMENT
Mohammad Sadegh Yalfani
ISBN:/DL:T.1259-2011

Chapter 2

Phenol degradation by Fenton's process using catalytic *in situ* generated hydrogen peroxide

The recent reported pathway using oxygen and formic acid at ambient conditions has been utilized to generate hydrogen peroxide in situ for the degradation of phenol. An alumina supported palladium catalyst prepared via impregnation was used for this purpose. Almost full destruction of phenol was carried out within 6 h corresponding to the termination of 100 mM formic acid at the same time. In addition, a significant mineralization (60%) was attained. A simulated conventional Fenton process (CFP) using continuous addition of 300 ppm H_2O_2 displayed maximum 48% mineralization. Study of different doses of formic acid showed that decreasing the initial concentration of formic acid caused faster destruction of phenol and its toxic intermediates. The catalytic in situ generation of hydrogen peroxide system demonstrated interesting ability to oxidize phenol without the addition of Fenton's catalyst (ferrous ion). Lower Pd content catalysts (Pd1/Al and Pd0.5/Al) despite of producing higher hydrogen peroxide amount for bulk purposes, did not reach the same efficiency as the Pd5/Al catalyst in phenol degradation. The later catalyst showed a remarkable repeatability so that more than 90% phenol degradation along with 57% mineralization was attained by the used catalyst after twice recovery. Higher temperature (45°C) gave rise to faster degradation of phenol resulting to almost the same mineralization degree as obtained at ambient temperature. Meanwhile, Pd leaching studied by atomic absorption proved excellent stability of the catalysts.

1. Introduction

Chemical oxidation and its developed form, advanced oxidation processes (AOPs) have been assigned an outstanding priority over other wastewater treatment methods e.g. adsorption and stripping techniques, due to their ability to mineralize organic pollutants. Different possible routes for OH• radicals production such as Fenton and Fenton-like offered by AOPs cover wide range of treatment processes with specific conditions [1-2]. Among the various approaches of generation of hydroxyl radical, Fenton reaction is one of the cleanest and most efficient processes to eliminate particularly toxic compounds in wastewaters and soil as well [3]. Fenton reaction involves generation of hydroxyl radical via hydrogen peroxide and ferrous ion, known as Fenton's reagent [2]. The application of Fenton's reagent as an oxidant for wastewater remediation is attractive due to the fact that iron is a highly abundant and non-toxic element, and hydrogen peroxide breaks down to environmentally benign products [4].

In the last decades, there has been great interest to produce hydrogen peroxide *in situ* within the reaction medium in order to promote efficiency of the subsequent oxidation reaction and lowering the relevant costs of hydrogen peroxide transportation as well [5-16]. *In situ* produced hydrogen peroxide can be consumed prior to decomposition to H_2O and O_2 leading to higher yield and selectivity toward the favorite reaction direction. In addition, the oxidation process would be proceeded under an appreciable controlled rate due to the lack of undesired bulk feeding of hydrogen peroxide. The *in situ* generating approaches should be specifically designed according to the physical and the chemical features of the subsequent oxidation process. Initially, the systems containing hydrogen and oxygen as substrates and metal-supported-titanium-silicate (TS-1) as catalyst were offered for hydroxylation and epoxidation purposes [5,7,8]. Afterwards, the conversion of benzene to phenol over

ISBN:/DL:T.1259-2011

palladium membrane presented by Niwa et al. displayed a break-through in *in situ* generation of H_2O_2 demonstrating an outstanding selectivity (up to 97%) for phenol [11]. Recently, oxidation of propane has been carried out with high selectivity toward oxygenates compounds through gold supported TS-1 [15,16]. In all above cases, the reaction mechanism is strongly postulated to be passing through an H_2O_2 intermediate. Indeed, the assumption has been evidenced by the direct generation of hydrogen peroxide from H_2 and O_2 over the similar catalytic systems [17,18]. However, the common point of the above studies is to use H_2-O_2 mixture which involves an inherent risk of explosion. To eliminate this drawback, replacing H_2 with a safer source could be an interesting alternative. Hydrazine and hydroxylamine have been offered for such a purpose but neither can be considered as a suitable replacement for hydrogen due to their toxicity or explosivity [19,20]. Very recently, we have reported a simple, clean and environment-friendly route for the generation of hydrogen peroxide via formic acid and oxygen [21]. In this method, formic acid (as replacement for H_2) and oxygen at full ambient conditions react over a supported-Pd catalyst leading to hydrogen peroxide generation. One of the main advantages of this new approach is its ability to be applied for *in situ* purposes. As referred above, there are several works related to chemically *in situ* generation of hydrogen peroxide, but concerning degradation of organic pollutant compounds, other than few reports [22], the rest of the works have been mostly carried out through electrochemical processes [23].

In this work, we demonstrate the application of *in situ* hydrogen peroxide generated from formic acid and oxygen for degradation of phenol as model pollutant compound. In fact, in this process, hydrogen peroxide is consumed as soon as it is produced to oxidize phenol. The efficiency of the system is measured as phenol decomposition rate during the reaction and the amount of total organic carbon (TOC) removed as well. The effect of factors such as

temperature and catalyst Pd content is studied. A comparison between our system and continuous and batch CFP is carried out.

2. Experimental

2.1. Catalyst preparation and characterization techniques

The alumina supported-Pd catalysts with Pd content range 0.1-5 wt% (denoted as Pd0.1/Al, Pd0.5/Al, Pd1/Al, Pd2.5/Al and Pd5/Al respectively) were synthesized through conventional impregnation. An acidic solution of $PdCl_2$ was added to a slurry solution of γ-Al_2O_3 (prepared by sol-gel). The mixture was stirred and aged for 1 h. Water was removed by rotary vapor at 55 °C. The precipitate was dried at 110 °C and then was calcined at 400 °C for 3 h. Finally, the catalyst was reduced under a flow of pure hydrogen (20 ml min^{-1}) at 200 °C for 2 h.

Table 1. Textural and structural properties of the synthesized catalysts

Catalyst	Pd loading (wt%)	XRD phases	BET ($m^2.g^{-1}$)	D (%)	d_{VA} (nm)
γ-Al_2O_3	0	γ-Al_2O_3	389	-	-
Pd0.1/Al	0.1	γ-Al_2O_3	218	26.7	4.2
Pd0.5/Al	0.5	γ-Al_2O_3	224	25.2	4.4
Pd1/Al	1.0	γ-Al_2O_3	214	19.9	5.6
Pd2.5/Al	2.5	γ-Al_2O_3	206	12.8	8.7
Pd5/Al	5	Pd(0), γ-Al_2O_3	205	5.8	19.2

The catalysts were characterized by X-ray powder diffraction (XRD), N_2 adsorption and H_2 chemisorption. X-ray diffraction of the samples was carried out using a Siemens D5000 diffractometer by nickel-filtered Cu Kα radiation. The patterns were recorded over a range of 2θ angles from 5° to 70°. In all the patterns, as summarized in Table 1, the broad peaks corresponding to the structure of γ-Al_2O_3 can be observed. The characteristic reflections of Pd(0) are

ISBN:/DL:T.1259-2011

recognizable clearly only in the pattern of Pd5/Al sample. N_2 adsorption was performed using a Micromeritics ASAP 2010 apparatus at 77 K. First, the samples were degasified at 120 °C for 12 h. Total surface area was calculated by the BET method. As shown in Table 1, pure γ-Al_2O_3 has a surface area nearly 400 m^2 g^{-1}. Impregnation with the $PdCl_2$ acidic solution and the subsequent treatments cause a slump in the surface area of the final synthesized samples. H_2 chemisorption was also acquired by a Micromeritics ASAP 2010. Before analysis at 100 °C, a pretreatment program including evacuation at 100 °C, oxidation under O_2 flow at 350 °C, evacuation at 100 °C and 350 °C, reduction under H_2 flow at 350 °C and evacuation at 100 °C respectively was fulfilled. Metal dispersion was obtained by the ratio of the gas (H_2) uptake to the total Pd content assuming an adsorption stoichiometry of H:Pd = 1:1. Particle size of the catalysts was calculated by the following equation [24]:

$$d_{VA} = 6\ (\upsilon_m / a_m) / D$$

where d_{VA} is the mean particle size, υ_m is the volume occupied by an atom m (for Pd is 14.70 Å^3), a_m is the surface area occupied by an atom m on a polycrystalline surface (for Pd is 7.93 Å^2) and D is the metal dispersion.

2.2. Catalytic tests

The phenol degradation reactions were implemented at ambient conditions (25 °C and atmospheric pressure) in a magnetically stirred three-necked glass reactor with a capacity of 100 ml. The reaction details are as follows unless it is mentioned specifically. The volume of the reaction was always 50 ml containing phenol (100 ppm), ferrous iron (10 ppm) and the catalyst (0.1 g). Formic acid was injected with different concentrations (40-500 mM). The initial pH of the solution has been 2.2-2.5 depending on the formic acid concentration. Oxygen was passed bubbling into the reaction medium with a flow rate of 20 ml min^{-1}. The temperature of the reaction was controlled using a water bath. Without

any exception, all the reactions were performed at darkness in order to avoid any interfering effect of existing light. Phenol degradation and formic acid decomposition were monitored by sampling at regular time intervals and analysing by high performance liquid chromatography HPLC (Shimadzu LC-2010 equipped with a SPD-M10A Diode array UV-vis detector). A Varian OmniSpher C18 column and a solution containing Milli-Q H_2O and acetonitrile (60:40) at pH 3.80 adjusted by phosphoric acid as mobile phase were used to analyse phenol and the aromatic intermediates at wavelength 254 nm. An Acclaim OA column and a mobile phase containing 100 mM Na_2SO_4 at pH 2.65 adjusted by methanesulphonic acid were used to analyse organic acid at wavelength 210 nm. TOC for each sample was measured by a Shimadzu TOC-5000A. The reaction solution at the end of each run after filtration was analysed by atomic absorption spectroscopy to detect leached Pd.

Continuous Fenton's reaction for phenol degradation was simulated using almost the same reaction conditions (100 ppm phenol, 10 ppm Fe^{2+}, adjusted pH 3-3.5 and ambient conditions) as we used for the *in situ* ones. For this purpose, 300 or 600 ppm H_2O_2 was injected continuously via a peristaltic pump (Watson-Marlow 205CA) during a period of 6 h. In the batch experiments, a total of 300 or 600 ppm H_2O_2 was injected concurrently into the solution (with the above mentioned conditions) at the start of the reaction and the reaction proceeded for 1 h. For each run, sampling was carried out at regular time intervals.

3. Results and discussion

3.1. Hydrogen peroxide generation from formic acid and O_2

Hydrogen peroxide can be produced through the reaction of formic acid and oxygen over supported-Pd catalysts [21]. The process is carried out within completely ambient conditions and attains a respectable productivity. Simply, formic acid is catalytically decomposed into CO_2 and H_2 and simultaneously O_2

reacts with released H_2 to form H_2O_2. Although another assumption of direct reaction of O_2 with formic acid resulting to H_2O_2 should be taken into account. The results of generation of hydrogen peroxide from formic acid and oxygen shown in Figure 1-A demonstrate a sharp rate of hydrogen peroxide formation for the highest Pd content catalyst (Pd5/Al) at 5 minutes of the reaction. The rate becomes moderate through the reaction time till 1 h, demonstrating severe competition between formation and decomposition of hydrogen peroxide. This high production value at 5 minutes can reflect somewhat real activity of the catalyst for the generation of hydrogen peroxide, because by proceeding the reaction it seems that the decomposition of H_2O_2 overcomes its generation.

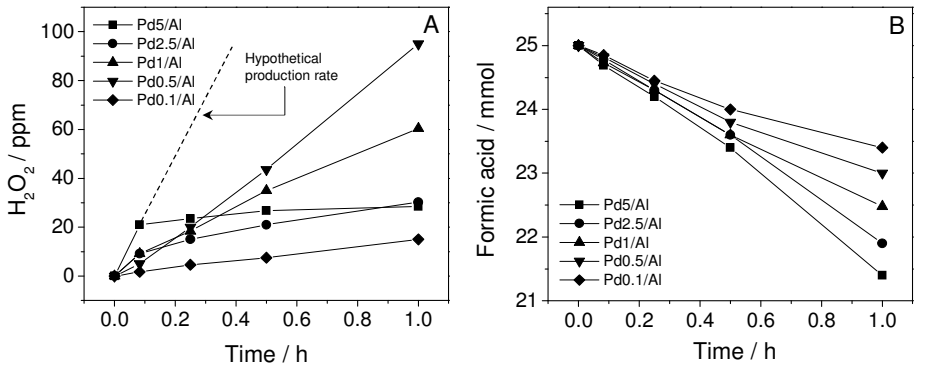

Figure 1. 1. A: H_2O_2 formation profile during the reaction of O_2 and formic acid over Pd/Al catalysts at ambient conditions. B: Formic acid decomposition profile over Pd/Al catalysts during H_2O_2 formation reaction.

Therefore we can hypothesize a theoretical production rate of H_2O_2 by extrapolating the line passing through the points at 0 and 5 minutes. Decreasing the Pd content to 0.1% leads to reducing of H_2O_2 production at 5 minutes whereas an outstanding promotion is observed after 1 h reaction markedly for the Pd0.5/Al catalyst (as high as 100 ppm H_2O_2). Over lower Pd content catalysts, the H_2O_2 formation profile becomes closer to linearity during the whole reaction. In general, over the catalyst, two favorable reactions occur,

ISBN:/DL:T.1259-2011

i.e. decomposition of formic acid and formation of hydrogen peroxide, depending the progress of the later on the rate of the former. Nevertheless, the side reactions of H_2O formation, H_2O_2 decomposition to H_2O and O_2 and H_2O_2 hydrogenation to H_2O influence the productivity and the selectivity of the reaction undesirably. Referring to the metal particle size of the catalysts presented in Table 1, it can be seen that the catalysts with smaller Pd particles are able to generate hydrogen peroxide in 1 h with higher rate than the ones with bigger particles, despite of the higher Pd content loaded on the later ones. On the other hand, increasing Pd content results to higher decomposition rate of formic acid (Figure 1-B). Taking into consideration of such a complicated system, the optimum Pd0.5/Al catalyst is offered for the bulk production of hydrogen peroxide within 1 h reaction. But as our main purpose is to generate H_2O_2 *in situ* for the subsequent oxidation reaction that catalyst may not be the adequate one, because for the *in situ* application, higher production rate at short time is of high importance. Hence, the Pd5/Al catalyst can be more eligible for the above purpose than the other ones due to its ability to decompose formic acid with higher rate and further production of hydrogen peroxide at short times.

3.2. Phenol degradation

Assuming the Pd5/Al as the most appropriate catalyst for the *in situ* application, the phenol degradation reactions were performed at full ambient conditions and using that and ferrous ion as Fenton's catalyst. The concentration of ferrous ion was elected according to the limits established by Directive 91/271/CE, which is 10 mg l^{-1}. Since degradation of toxic compounds at low concentrations (especially less than 100 ppm) is of high importance [25], we conducted all our reactions starting with a solution containing 100 ppm phenol.

ISBN:/DL:T.1259-2011

Table 2. Phenol degradation results obtained using *in situ* generated H_2O_2 over the Pd5/Al catalyst.

Run no.	F.A. int. conc.* (mM)	t (h)	F.A. conv. (%)	Phenol conv. (%)	TOC removed (%)
1	500	6	33	88.3	N.A.
2	200	6	69	94.8	N.A.
3	100	6	100	98.2	60.7
4	60	5	100	94.9	57.9
		6	100	95.1	66.3
5	40	4	100	82.5	55.3
		6	100	86.3	66

* Formic acid initial concentration

The main results have been summarized in Table 2. Different initial doses of formic acid were fed into the reaction medium. During direct generation of hydrogen peroxide an initial concentration of 500 mM was found to be favorable. Decreasing that amount to the lower ones caused reducing the yield of the process. Contrarily, *in situ* generated hydrogen peroxide initiated with 500 mM formic acid leads to maximum 88% degradation of phenol after 6 h, and no complete consumption of formic acid is attained, whereas decreasing initial concentration of formic acid to 100 mM results in almost full degradation of phenol and no formic acid remains within the reaction medium. It seems that during *in situ* generation of hydrogen peroxide high concentration of formic acid may deactivate the catalyst to degrade phenol by avoiding phenol to be exposed to the generated hydrogen peroxide or by consumption of generated H_2O_2 or $OH^{\bullet}$ by formic acid itself. Entire disappearance of formic acid from the solution enabled us to analyse TOC utterly associated to phenol degradation process and thereupon to monitor the phenol mineralization achieved by the system. Based on that, a 60% mineralization was gained after 6 h. Further reducing the initial concentration of formic acid down to 60 and 40 mM, leads to the entire decomposition of formic acid after 5 and 4 h and the mineralization degrees are 58% and 55%, respectively. By termination of

formic acid, oxidation of phenol obviously diminishes, while mineralization proceeds up to 66% after 6 h. The reason can be the extended decomposition of the intermediates, in particular carboxylic acids, over the catalyst.

Considering 14 mol H_2O_2 required for the entire mineralization of phenol (according to the reaction below)

$$C_6H_6O + 14\ H_2O_2 \rightarrow 17\ H_2O + 6\ CO_2$$

and 60% mineralization achieved, an approximate amount of 300 ppm H_2O_2 is estimated that has been produced through the *in situ* process. The number represents the apparent amount of produced H_2O_2 which has thoroughly participated in the mineralization of phenol. The real amount of the generated H_2O_2, which definitely must be much more than 300 ppm, is indistinct. A great part of H_2O_2 is decomposed as soon as generated, may be consumed to oxidize the formic acid feed, or to oxidize phenol and intermediates without any mineralization. Figure 2 displays the phenol degradation profiles using different initial doses of formic acid during a reaction time of 6 h. At 5 minutes, a sharp decreasing-increasing of phenol concentration is observed which can be attributed to a fast adsorption-desorption of phenol on the catalyst. This explanation was evidenced by simple exposing an aqueous phenol solution (100 ppm) to the catalyst for a period of 1 h applying the same conditions as used for degradation reactions. The variations of phenol concentration in such a system have been depicted in the inset of Figure 2. It is clearly observed that phenol disappears quickly and then appears gradually until its initial concentration is apparently detected. In fact, by addition of the solution containing phenol to the catalyst, phenol is partially adsorbed on the support (alumina). In turn, owing to the low adsorption tendency of phenol on alumina [26], it returns to the solution as a reversible process and recreates the initial concentration of phenol. In presence of formic acid, due to the strong

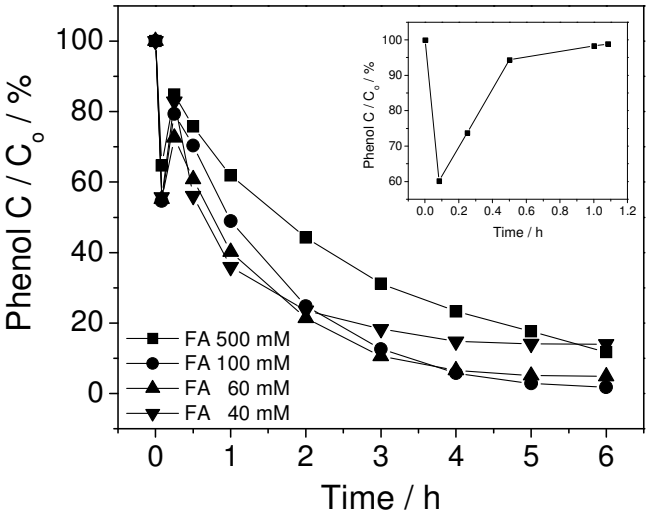

Figure 2. Phenol degradation profile using *in situ* generated H_2O_2 at different initial concentrations of formic acid. Inset: variations of phenol concentration in presence of only 0.1 g Pd5/Al catalyst.

adsorption of carboxylic acid on alumina [27], the replacement of phenol molecules with formic acid's ones on the catalyst surface occurs and phenol releases back into the solution faster. Followed by the mentioned adsorption-desorption, by reducing the initial dose of formic acid the oxidation of phenol proceeds faster. The difference is obviously observed at 1 h, where remaining phenol, 62% for the reaction started with 500 mM formic acid drops to 36% for the reaction started with 40 mM formic acid. Finally, by arriving to the low concentration of phenol, the oxidation rate is retarded due to the kinetic aspects [28].

In order to compare the *in situ* generated H_2O_2 system with CFP, continuous and batch Fenton's reactions for phenol degradation were performed using the same reaction conditions as we used for the *in situ* ones. Firstly, the Fenton reactions were experienced using 300 ppm H_2O_2 continuously and batchwise. The results shown in Figure 3-A indicate disappearance of phenol in less than 3

ISBN:/DL:T.1259-2011

h for the continuous run which corresponds to a mineralization of 31%. The oxidation was extended till 6 h resulting to maximum 48% mineralization. In the batch run (Figure 3-B), although a fast collapse of phenol is observed, mineralization did not go beyond 46% despite of lasting the reaction till 1 h. Increasing the H_2O_2 concentration to 600 ppm (1.2 times the stoichiometric amount required for complete mineralization of phenol) in continuous run (Figure 3-C) did not promote the yield of mineralization despite of faster oxidation of phenol. The batch reaction with 600 ppm (Figure 3-D) even arrived to worse result of mineralization that was 36% after 6 h. The reason of such a phenomenon has been already elucidated [29] by the fact that hydrogen peroxide acts as free-radical scavenger itself at high concentrations, thereby inhibits proceeding the oxidation process. Figure 4 displays the corresponding final filtered solutions after the end of each reaction i.e. *in situ* system (A), continuous (B) and batch (C) CFP using 300 ppm H_2O_2. *In situ* system degrades phenol through a slower but more controlled process which arrives to a nearly colorless solution. Continuous CFP, although is able to decompose the whole phenol at shorter time, eventually a pale brown solution remains which reflects the presence of toxic aromatic intermediates. The batch system also acts fast on phenol but lower mineralization and pale brown solution is obtained. It has been concluded that the observed color through a phenol degradation process depends on the level of oxidation achieved [30].

As it has been mentioned in the literature, one of the main drawbacks of Fenton's process is its weak capacity to degrade some of the intermediates which are produced during the phenol oxidation [31]. These compounds, which are known as recalcitrant, include mostly organic acids such as oxalic, maleic and acetic acids. As mineralization is mostly the result of oxidation of such organic acids to CO_2 and H_2O, it seems to be logical to state that the difference in mineralization between CFP and *in situ* system could be attributed to the

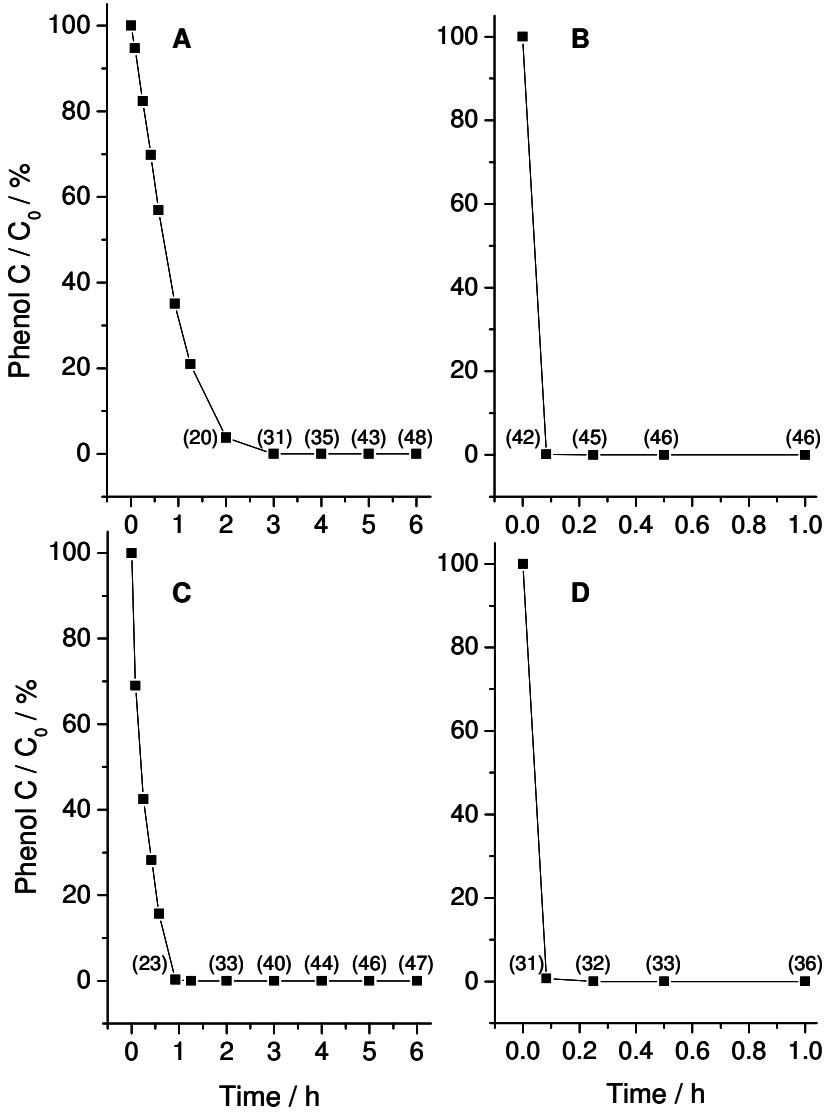

Figure 3. A: Phenol degradation profile by continuous CFP using 300 ppm H_2O_2; B: Phenol degradation profile by batch CFP using 300 ppm H_2O_2; C: Phenol degradation profile by continuous CFP using 600 ppm H_2O_2; D: Phenol degradation profile by batch CFP using 600 ppm H_2O_2; the numbers in parentheses are %TOC removed.

ISBN:/DL:T.1259-2011

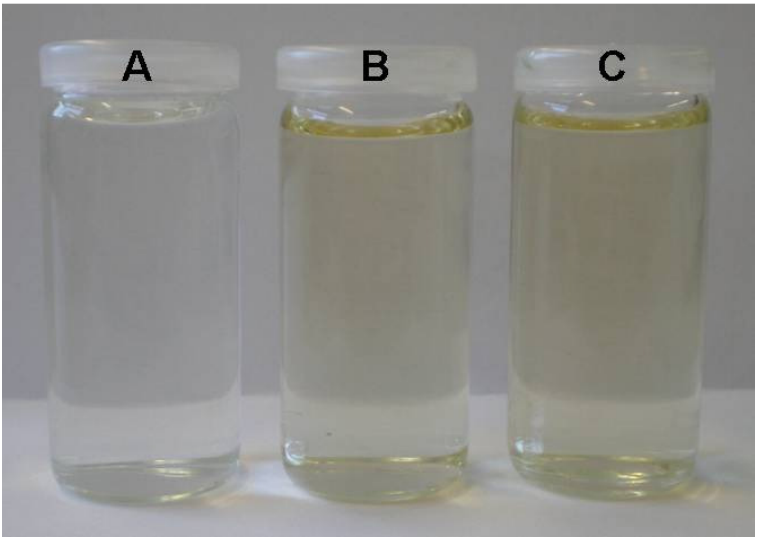

Figure 4. Filtered solutions at the end of phenol degradation reactions obtained by A: *in situ* system (100 mM initial concentration of F.A.); B: continuous CFP (300 ppm H_2O_2); C: batch CFP (300 ppm H_2O_2)

ability of the later to degrade further the recalcitrant organic acids. However, this assumption needs further investigation to be properly approved.

Figure 5 demonstrates phenol removal profile in the similar *in situ* system described above but without the presence of ferrous ion. 42% phenol degradation along with 6% mineralization is achieved, suggesting that hydrogen peroxide can oxidize phenol directly (ca. 10% in 2 h, results not shown) and especially that the catalyst can play the role of ferrous ion in converting H_2O_2 to hydroxyl radicals. In fact, in presence of ferrous ion, occurrence of the above phenomenon beside the formation of hydroxyl radical via Fenton's process can positively affect the general efficiency of the reaction.

Formic acid in this system behaves as a source of hydrogen to produce hydrogen peroxide, besides providing the necessary acidic pH. The compound can have another important advantageous side effect which has been proposed by Ferraz et al. [32]. It has been shown both computationally and empirically

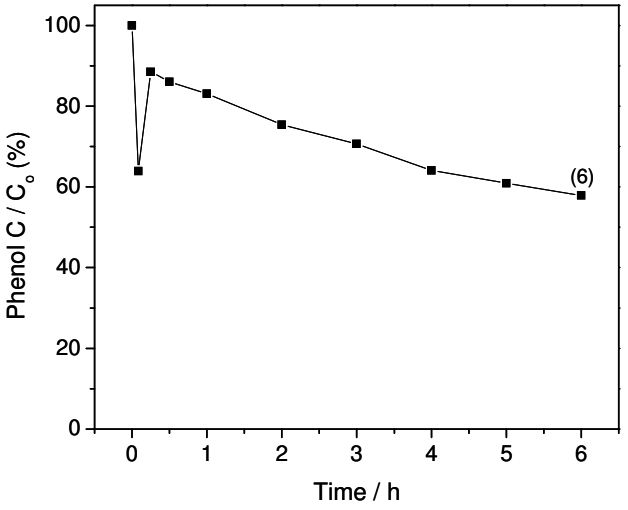

Figure 5. Phenol degradation profile by *in situ* generated H_2O_2 in absence of ferrous ion (100 mM initial F.A. concentration); the number in parenthesis is %TOC removed.

that organic acids and specifically formic acid can enhance the efficiency of Fenton's process in the degradation of organic compounds. In other words, formic acid can interact with H_2O_2 to lead to better formation of hydroxyl radical. Another promoter of the reaction can be oxygen which has been generally verified to be as supplemental bulk oxidant or a rate accelerator [2]. However, exceptionally, in the case of formic acid, oxygen can play an inhibiting role by terminating the Fenton cycle [33].

The alumina supported-Pd catalyst used for this work shows excellent stability, since no Pd leached into the solution was detected by atomic absorption analysis after the end of each run. This advantage makes possible the recovery of the catalyst at the end of the reaction. The recovered and re-recovered catalysts by filtration and drying at 110 °C for 12 h were utilized for phenol degradation reaction and surprisingly displayed very interesting behavior. These results have been shown in Figure 6. Higher decomposition

rate of formic acid is observed compared to the fresh catalyst, giving rise to an impact on phenol degradation. Nearly 70% conversion for phenol is attained within the first hour of the reaction. Nevertheless, mineralization achieved at the end of the reaction is a little lower in comparison with the fresh catalyst. The above phenomenon can be rationalized as the fresh Pd catalyst during the first run not only does not loose its activity but also improves it since the H_2 released from the decomposition of formic acid can re-reduce likely oxidized and even non-reduced Pd sites and avoid deactivation of the catalyst.

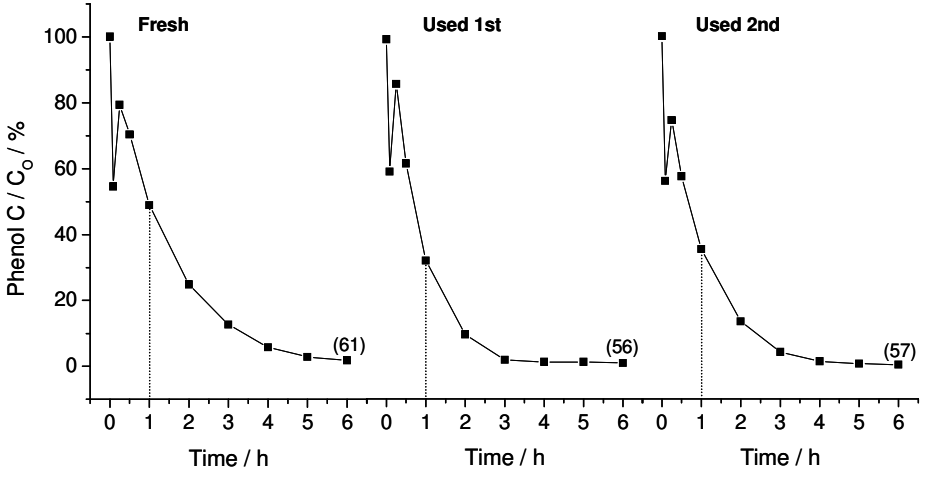

Figure 6. Phenol degradation profile obtained by *in situ* generated H_2O_2 over fresh and used Pd5/Al catalyst (100 mM initial F.A. concentration). The numbers in parentheses are %TOC removed.

3.3. Evolution of intermediates

Different pathways have been proposed for oxidation of phenol in aqueous phase [34]. In general, phenol degradation pursues a sequential process passing through formation of several intermediates. In Fenton's process, initially phenol hydroxylation occurs which results in dihydroxylbenzenes such as hydroquinone, resorcinol and catechol [35]. Formation of resorcinol based on substitution rules in organic chemistry is implausible. These compounds

ISBN:/DL:T.1259-2011

undergo a further oxidation leading to quinone compounds which are: p-benzoquinone and o-benzoquinone. The later two quinones are in redox equilibrium with their corresponding hydroquinones [36]. In turn, phenolic ring is collapsed to produce low molecular weight carboxylic acids like maleic, oxalic and acetic acids which are mineralized to water and carbon dioxide. Figure 7 displays concentration profile of catechol as representative of aromatic intermediate compounds. Catechol is more resistant to degradation than quinones [37] and therefore its variations during the reaction can be interesting. Moreover, in our system, we could not follow quantitatively the other aromatic intermediates by HPLC, because the retention times of hydroquinone and p-benzoquinone overlied on each other and their individual analysis was difficult. By starting the reaction, catechol is produced and its concentration within the reaction medium increases, which depends directly on the rate of phenol degradation. Gradually, catechol concentration undergoes decomposition and competes with its formation. Using 100 mM formic acid, the catechol concentration reaches to a maximum which then slips to near 1 ppm after 6 h. This peak corresponds to 50% degradation of phenol after 1 h reaction (see Figure 2). With lower formic acid concentrations, higher amount of catechol is produced, up to nearly 30 ppm. Then, decomposition of catechol is predominant, leading to a decrease of its concentration down to 2 to 5 ppm after 6 h. Using 500 mM formic acid, catechol graph appears as a hillock form indicating that oxidation process is mild. The color changes during the degradation reaction can also reflect remediation of the intermediates which possess higher toxicity than phenol itself [38]. In conventional Fenton, when the reaction is carried out batchwise, the color of the solution changes from colorless to dark brown as soon as the addition of hydrogen peroxide. The dark brown color gradually misses its intensity and after 1 h a pale brown color

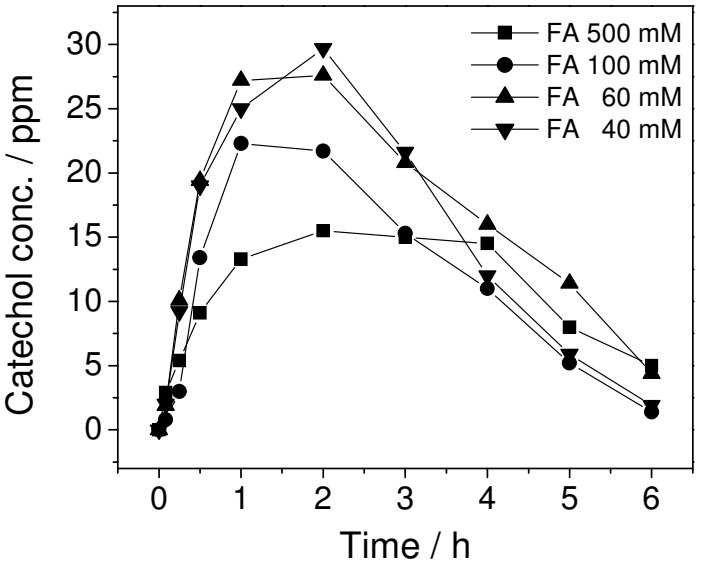

Figure 7. Evolution of catechol during phenol degradation using different initial concentrations of formic acid.

remains (Figure 4-C). The continuous Fenton's process indicates appearance of pale brown color by addition of hydrogen peroxide which is constant until the end of the reaction (Figure 4-B). The color can be arisen from different sources such as, the quinhydrone complex, the Fe^{3+}-catecholate complex, Fe^{3+}-oxalate complex and polymeric species resulted from aromatic condensations. At these conditions no peaks related to the above colored compounds are detected in the HPLC chromatogram. In our *in situ* H_2O_2 system, the solution is almost colorless at the end of the reaction after the catalyst filtration (Figure 4-A) which reflects higher capacity of the system to oxidize the aromatic intermediates. Therefore, it can be concluded that *in situ* generated H_2O_2 system is able to degrade phenol and its toxic intermediates with higher efficiency with respect to CFP.

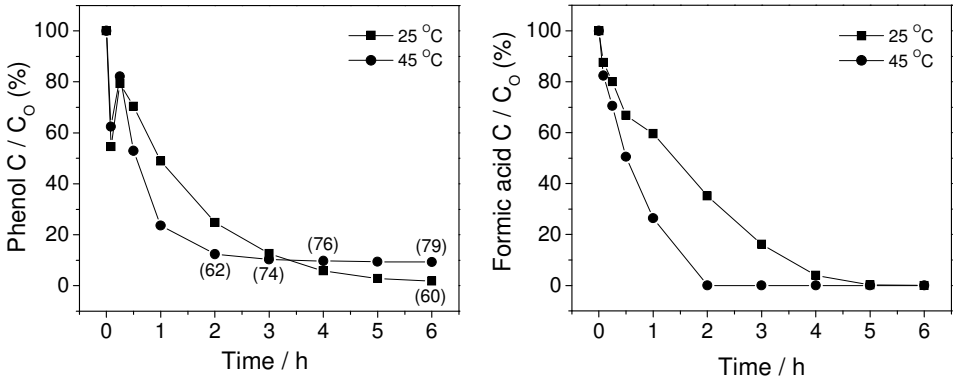

Figure 8. A: Phenol degradation profiles using *in situ* generated H_2O_2 over Pd5/Al at different temperatures (100 mM initial concentration of F.A.). B: Formic acid decomposition profiles during the above reactions. The numbers in parentheses are %TOC removed.

3.4. Effect of temperature

Since both decomposition of formic acid and oxidation of phenol are promoted by elevating the temperature [39,29], we studied the effect of higher temperature on phenol degradation via *in situ* generated H_2O_2 reaction. Figure 8 illustrates a comparison between phenol and formic acid decomposition carried out at 25 and 45 °C. Increasing the temperature to 45 °C gives rise to decomposition of formic acid with higher rate than that at 25 °C. Further decomposition of formic acid generates more H_2O_2 which subsequently decomposes with promoted rate. As it is observed, after 1 h, the oxidation of phenol reaches to nearly 75%, but, by termination of formic acid after 2 h, oxidation of phenol is suppressed and around 9 ppm of phenol remains at the end of the reaction. After 2 h 62% as TOC removed is obtained, while at ambient condition and with the same initial dose of formic acid, 6 h are needed to achieve this degree of mineralization. At 45º, after the termination of formic acid, mineralization proceeds up to 79% after 6 h. The same phenomenon was observed for the systems started with 40 and 60 mM (section 3.2) formic acid at ambient conditions. The interesting point is that phenol is not affected by the

catalyst after termination of formic acid, indicating possible degradation of aromatic intermediates and carboxylic acids. By comparison of the high temperature system with that at ambient, it can be simply viewed that at 45 °C almost similar efficiency is achieved but three times faster than at 25 °C considering mineralization as measure.

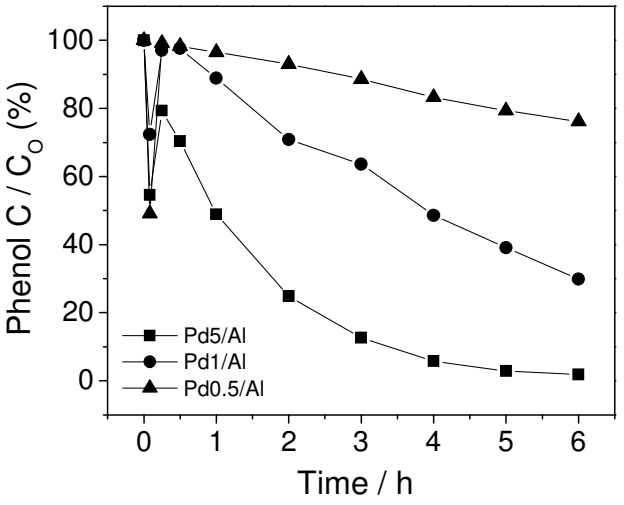

Figure 9. Phenol degradation profiles by *in situ* generated H_2O_2 using different Pd loaded catalysts.

3.5. Effect of Pd content

As it has been mentioned in our recent report [21], decreasing of Pd content over alumina can enhance the productivity for direct formation of hydrogen peroxide, in particular for bulk purposes. Since for *in situ* application a catalyst with ability to produce hydrogen peroxide at short time is anticipated to be more desired, we fulfilled our reactions using Pd5/Al catalyst. In order to evidence the above view, we tested the lower Pd content catalysts for phenol degradation via *in situ* generated hydrogen peroxide. The results displayed in Figure 9 indicate that by decreasing Pd content, phenol degradation rate

reduces. For example, the Pd0.5/Al catalyst, which had represented highest productivity within 1 h, could not compete with Pd5/Al and a maximum of 24% for phenol degradation after 6 h is yielded. These observations support the idea previously suggested (section 3.1) that real production rate of hydrogen peroxide for the Pd5/Al catalyst should be displayed by extrapolating the production rate passing from zero point and 5 minutes (as shown in Figure 1).

On the way to support the above assumption, the productivity of hydrogen peroxide production obtained as *in situ* (300 ppm) is more than one order of magnitude higher than that of direct generation (24 ppm) after 6 h, considering as well that 100 mM formic acid was used for the *in situ* system with respect to 500 mM for direct generation.

4. Conclusions

We applied hydrogen peroxide generation via oxygen and formic acid system to produce hydrogen peroxide *in situ* for degradation of phenol by Fenton's reaction. The system indicated significant ability to mineralize phenol and its intermediates. A maximum of 60% mineralization was achieved in comparison with the 48% obtained by the simulated continuous and 46% by batch CFP. These results can highlight the advantage of *in situ* approaches for the oxidation process with respect to even continuous feeding of the oxidant. The productivity of hydrogen peroxide during *in situ* generation is remarkably enhanced compared to the direct process for bulk production. The catalyst possesses excellent stability as no Pd leached was detected at the end of each run. In addition, repeatability of the catalyst is significant as it shows almost the same activity by performing the reaction twice with the recovered catalyst.

Acknowledgements

This work was funded by the URV projects no. AIRE 2006/02, and also AECI, ref. A/5188/06 and MICINN project no. CTM 2008-02453.

References

[1] R. Andreozzi, V. Caprio, A. Insola, R. Marotta, *Catal. Today* 53 (1999) 51-59.

[2] J. J. Pignatello, E. Oliveros, A. MacKay, *Crit. Rev. Environ. Sci. Technol.* 36 (2006) 1-84 and references therein.

[3] S. Esplugas, J. Giménez, S. Contreras, E. Pascual, M. Rodríguez, *Water Res.* 36 (2002) 1034-1042.

[4] C.W. Jones, *Applications of Hydrogen Peroxide and Derivatives*, RSC, 1999, pp. 207-230.

[5] T. Tatsumi, K. Yuasa, H. Tominaga, *J. Chem. Soc., Chem. Commun.* (1992) 1446-1447.

[6] M. G. Clerici, P. Ingallina, *Catal. Today* 41 (1998) 351-364.

[7] R. Meiers, U. Dingerdissen, W.F. Hölderich, *J. Catal.* 176 (1998) 376-386.

[8] R. Meiers, W.F. Hölderich, *Catal. Lett.* 59 (1999) 161-163.

[9] E.D. Park, Y.–S. Hwang, J.S. Lee, *Catal. Commun.* 2 (2001) 187-190.

[10] J.R. Monnier, *Appl. Catal. A: Gen.* 221 (2001) 73-91.[11] S. Niwa, M. Eswaramoorthy, J. Nair, A. Raj, N. Itoh, H. Shoji, T. Namba, F. Mizukami, *Science* 295 (2002) 105-107.

[12] J.E. Remias, T.A. Pavlosky, A. Sen, *J. Mol. Catal. A: Gen.* 203 (2003) 179-192.

[13] G.D. Vulpescu, M. Ruitenbeek, L.L. van Lieshout, L.A. Correia, D. Meyer, P.P.A.C Pex, *Catal. Commun.* 5 (2004) 347-351.

[14] G. Li, J. Edwards, A.F. Carley, G. Hutchings, *Catal. Commun.* 8 (2007) 247-250.

[15] J.J. Bravo-Suárez, K.K. Bando, T. Akita, T. Fujitani, T.J. Fuhrer, S.T. Oyama, *Chem. Commun.* 2008, 3272-3274.

[16] J.J. Bravo-Suárez, K.K. Bando, T. Fujitani, S.T. Oyama, *J. Catal.* 257 (2008) 32-42.

[17] J.M. Campos-Martin, G. Blanco-Brieva, J.L.G. Fierro, *Angew. Chem., Int. Ed.* 45 (2006) 6962-6984.

[18] J.H. Lunsford, *J. Catal.* 216 (2003) 455-460.

[19] V.R. Choudhary, C. Samanta, P. Jana, *Chem. Commun.* (2005) 5399-5401.

[20] V.R. Choudhary, P. Jana, *Catal. Commun.* 8 (2007) 1578-1582.

[21] M.S. Yalfani, S. Contreras, F. Medina, J. Sueiras, *Chem. Commun.* (2008) 3885-3887.

[22] Y.–G. Zhang, L.–L. Ma, J.–L. Li, Y. Yu, *Environ. Sci. Technol.* 41 (2007) 6264-6269.

[23] I. Sirés, F. Centellas, J.A. Garrido, R.M. Rodríguez, C. Arias, P.L. Cabot, E. Brillas, *Appl. Catal. B: Environ.* 72 (2007) 373-381 and references therein.

[24] G. Bergeret, P. Gallezot, *Handbook of Heterogeneous Catalysis* (Edited by: G. Ertl, H. Knözinger and J. Weitkamp) Wiley-VCH, 1997, Vol. 2, 439.

[25] Y.–F. Han, N. Phonthammachai, K. Ramesh, Z. Zhong, T. White, *Environ. Sci. Technol.* 42 (2008) 908-912.

[26] C.M. Cirtiu, H.O. Hassani, N.–A. Bouchard, P.A. Rowntree, H. Ménard, *Langmuir* 22 (2006) 6414-6421.

[27] J.T. Hall, K.P. Hansma, *Surf. Sci.* 76 (1978) 61-76.

[28] N. Kang, D.S. Lee, J. Yoon, *Chemosphere* 47 (2002) 915-924.

[29] R. Alnaizy, A. Akgerman, *Adv. Environ. Res.* 4 (2000) 233-244.

[30] F. Mijangos, F. Varona, N. Villota, *Environ. Sci. Technol.* 40 (2006) 5538-5543.

[31] R.J. Bigda, *Chem. Eng. Prog.* (1995) 62-66.

[32] W. Ferraz, L.C.A. Oliveira, R. Dallago, L. da Conceição, *Catal. Commun.* 8 (2007) 131-134.

[33] C.K. Duesterberg, W.J. Cooper, T.D. Waite, *Environ. Sci. Technol.* 39 (2005) 5052-5058.

[34] A. Santos, P. Yustos, A. Quintanilla, S. Rodríguez, F. García-Ochoa, *Appl. Catal. B: Environ.* 39 (2002) 97-113.

[35] J.A. Zazo, J.A. Casas, A.F. Mohedano, M.A. Gilarranz, J. J. Rodríguez, *Environ. Sci. Technol.* 39 (2005) 9295-9302.

[36] H. Alt, H.Binder, A. Köhling G. Sandstede, *Angew. Chem., Int. Ed.* 10 (1971) 514-515.

[37] D.H. Bremner, A.E. Burgess, D. Houllemare, K.–C. Namkung, *Appl. Catal. B: Environ.* 63 (2006) 15-19.

[38] A. Santos, P. Yustos, A. Quintanilla, F. García-Ochoa, J. A. Casas, J. J. Rodríguez, *Environ. Sci. Technol.* 38 (2004) 133-138.

[39] E.M. Cordi, J.L. Falconer, *J. Catal.* 162 (1996) 104-117.

UNIVERSITAT ROVIRA I VIRGILI
NEW CATALYTIC ADVANCED OXIDATION PROCESSES FOR WASTEWATER TREATMENT
Mohammad Sadegh Yalfani
ISBN:/DL:T.1259-2011

Chapter 3

Effect of support and second metal in catalytic *in situ* generation of hydrogen peroxide by Pd-supported catalysts: Application in the removal of organic pollutants by means of the Fenton process

A catalytic system for the generation of H_2O_2 from formic acid and oxygen at ambient conditions has been developed. Pd-supported catalysts (Pd/C, Pd/TiO_2 and Pd/Al_2O_3) have been tested, showing that for bulk purposes Pd/Al_2O_3 is more favourable while for in situ applications Pd/TiO_2 seems to be preferable. However, when these catalysts were tested in the in situ H_2O_2 generation for the oxidation of phenol by means of the Fenton process (in the presence of ferrous ion), Pd/TiO_2 did not demonstrate the expected results, whereas Pd/Al_2O_3 showed to be an efficient catalyst. Therefore, Pd/Al_2O_3 is offered as a good catalyst for Fenton's reactions with in situ generated H_2O_2. In order to optimize the operating cost of the process, different initial concentrations of formic acid have been tested with Pd/Al_2O_3, and it has been seen that lowering the initial amount of formic acid favours the efficiency of the process. The effect of the addition of a second metallic (Pt, Au, Fe, Cu) active phase was studied. Concerning H_2O_2 generation, best results were obtained with a Pd-Au catalyst for bulk production (long time) while for in situ application Pd-Fe showed interesting results. The Pd-Fe catalyst also performed similar to the semi-homogeneous Fenton system involving Pd/Al_2O_3 and ferrous ion in the degradation of phenol. Therefore, Pd-Fe catalyst offered an interesting prospect for making a full heterogeneous catalyst for Fenton reaction involving in situ generation of H_2O_2.

ISBN:/DL:T.1259-2011

1. Introduction

During the last decade there has been a growing interest in the bulk or *in situ* (within the reaction medium for oxidation reactions) generation of hydrogen peroxide from H_2 and O_2 [1-6], which is an environmentally-friendly process. In these systems, heterogeneous Pd-supported catalysts have shown a good performance. The use of *in situ* generated H_2O_2 could improve the efficiency of the subsequent oxidation reactions, which can also be performed at a more controlled rate. It avoids the safety problems associated to the storage and handling of large amounts of H_2O_2 too. Nevertheless, there are some drawbacks in those systems, such as the risk of explosivity of the H_2-O_2 mixture and the low solubility of the gases in solution, especially hydrogen. Therefore, the use of other sources of H_2 in solution is of high interest. In the literature there have been some attempts such as the use of hydrazine [7] and hydroxylamine [8], but these compounds are classified as toxic and possible carcinogenic or explosive, what makes necessary to look for other options. Formic acid (FA) can also be a source of hydrogen, as it has already been demonstrated in the hydrogenation of organic compounds [9], the hydrodechlorination of chlorinated organic compounds [10] or the catalytic reduction of nitrates in water [11]. Recently, we have developed a catalytic system for the generation of H_2O_2 from formic acid and oxygen using a Pd/Al_2O_3 catalyst [12]. This system could be applied in *in situ* oxidation reactions.

The addition of a second metal to Pd has been studied in order to improve the activity and the selectivity of the catalysts for the direct generation of H_2O_2 [13,14]. Gold is the one that has been widely tested for this reaction [15-18], showing a significant promotion in the rate of formation and selectivity for hydrogen peroxide compared to the single Pd catalyst. Also, with smaller extensiveness, addition of Pt to Pd in order to enhance the efficiency of direct synthesis of H_2O_2 has been investigated [19,20].

ISBN:/DL:T.1259-2011

In the Fenton reaction, H_2O_2 is one of the main sources of the operating costs, thus the possible replacement of bulk feeding by *in situ* generated H_2O_2 can be attractive. Few references have been found in the literature about the use of *in situ* generated H_2O_2 for the degradation of organic pollutants in water [21,22] and most of them are based on electrochemical processes [23]. In this work we have studied the effect of different supports on the catalytic generation of H_2O_2 from formic acid and oxygen over Pd-supported catalysts. The subsequent application of the *in situ* produced H_2O_2 has been the degradation of a model organic pollutant (i.e. phenol) in aqueous medium by means of the Fenton process in the presence of ferrous ion. On the most appropriate support, the effect of the addition of a second metal to Pd was investigated. The selection of the second metal was based on the ability of the metal to make a full heterogeneous catalyst for the Fenton reaction (Fe and Cu) and also for promotion of H_2O_2 productivity and selectivity (Au and Pt). Phenol has been chosen as model compound in order to test the feasibility of this new catalytic advanced oxidation process (AOP), as its degradation by different AOPs has been extensively studied. Efficiency of the system has been measured as percentage of removal and mineralization of the target compound. The initial concentration of formic acid has been optimised.

2. Materials and methods

Pd/Al_2O_3 (Pd5/Al) and Pd/TiO_2 (Pd5/Ti) were synthesized by conventional impregnation. An aqueous solution of $PdCl_2$ acidified by hydrochloric acid was added to an aqueous slurry of γ-Al_2O_3 or TiO_2 (prepared by sol-gel method), stirring vigorously. Pd content was always 5 wt%. Bimetallic catalysts were prepared by co-impregnation of γ-Al_2O_3 by an acidic solution of $PdCl_2$ and the other metal precursor: H_2PtCl_6 (Pd2.5Pt2.5/Al) and H_2AuCl_4 (Pd2.5Au2.5/Al). Content of each metal was 2.5 wt% (therefore total metal content was 5 wt%). Other two bimetallic catalysts incorporating Fe and Cu were prepared by co-

impregnation of □-Al_2O_3 with an acidic solution of $PdCl_2$ and $Fe(NO_3)_3.9H_2O$ or $Cu(NO_3)_2.3H_2O$ containing 5 wt%Pd and 1 wt%Fe or 1 wt%Cu (Pd5Fe1/Al and Pd5Cu1/Al, respectively). In all the cases, the final slurry solutions were aged under stirring for 1 h, heated under vacuum at 60ºC and dried at 110ºC for 12 h. The precipitates obtained were calcined in static air at 400ºC for 3h and afterwards reduced under H_2 flow (20 ml/min) at 200ºC for 2 h. Pd 5wt%/C (Pd5/C) was purchased from Esteve Química, S.A.

XRD patterns were obtained using a Siemens D5000 diffractometer by a nickel-filtered Cu-Kα radiation (λ=1.54 Å). The angular 2θ diffraction range was between 5 and 80º. The data were collected with an angular step of 0.02º at 4s per step and sample rotation. TEM images were acquired using a JEOL JEM-1011 microscope operating at 80 KV. The samples were mounted on a carbon-coated copper grid by placing a few droplets of a suspension of the ground sample in acetone, followed by evaporation at ambient conditions.

H_2O_2 generation reactions were performed at ambient conditions (atmospheric pressure, T=25±2ºC controlled by a water bath) in a magnetically stirred 100-ml three-necked glass reactor for 1 h. The volume of reaction was always 50 ml and the initial amount of formic acid 25 mmol. The amount of catalyst was 0.1 g and oxygen passed bubbling into the reaction medium with a flow rate 20 ml/min. H_2O_2 concentration was monitored by iodometric titration and formic acid decomposition by HPLC (Shimadzu LC-2010), equipped with an Acclaim OA column and diode array detector (SPD-M10A) using 100 mM Na_2SO_4 at pH 2.65 adjusted by methanesulphonic acid as mobile phase at λ=210 nm.

Fenton reactions were carried out at ambient conditions (25ºC and atmospheric pressure) in a magnetically stirred 100-ml three-necked glass reactor. The volume of the reaction was always 50 ml, phenol initial concentration 100 ppm, 0.1 g of catalyst, 10 ppm of ferrous ion, and formic acid concentration in the range 40-500 mM. Initial pH of the solution was 2.2-2.5

ISBN:/DL:T.1259-2011

depending on the initial formic acid concentration. Oxygen flow rate was 20 ml/min. Formic acid, phenol and intermediates were analysed by HPLC (Shimadzu LC-2010) and diode array detector (SPD-M10A). Formic acid and organic acids were analysed as explained above, and phenol and aromatic intermediates with a Varian OmniSpher C18 column and acetonitrile/H_2O (40/60) at pH 3.80 adjusted by phosphoric acid as mobile phase, at λ=254 nm. Total organic carbon (TOC) was monitored by a Shimadzu TOC-5000A analyser. The reaction solution at the end of each run was analysed after filtration by atomic absorption spectroscopy to detect metal leaching.

3. Results and discussion

3.1. Effect of support on H_2O_2 generation

Formic acid can be decomposed according to dehydration ($HCOOH \rightarrow CO + H_2O$) or dehydrogenation ($HCOOH \rightarrow CO_2 + H_2$), and this process is directed predominantly towards the production of hydrogen and CO_2 when is performed over Pd based catalyst at low temperature (<400K) and in aqueous medium [24]. Under our tested operating conditions, FA is decomposed over Pd to CO_2 and H_2 (confirmed by the analysis of the overhead gases released during decomposition of FA under Ar atmosphere), which further reacts with O_2 to produce H_2O_2 [12]. Also the direct reaction of FA with oxygen resulting in H_2O_2 ($HCOOH + O_2 \rightarrow CO_2 + H_2O_2$) or H_2O ($HCOOH + \frac{1}{2}\ O_2 \rightarrow CO_2 + H_2O$) may occur, because it was observed that the decomposition rate of formic acid is enhanced in the presence of oxygen when compared with experiments performed in absence of oxygen (results not shown).

Pd-supported catalysts (Pd5/C, Pd5/Ti and Pd5/Al) were tested in the generation of hydrogen peroxide by means of the catalytic decomposition of FA in the presence of oxygen. Although the supports themselves were not able to convert FA appreciably, they influenced strongly the process of H_2O_2 generation (see Table 1). At short time (5 min reaction) Pd5/Ti achieved the highest

ISBN:/DL:T.1259-2011

productivity (132 mmol $H_2O_2/g_{Pd}.h$), followed by Pd5/Al. At longer times the H_2O_2 generation rate becomes more moderate due to the competitive reaction of H_2O_2 decomposition over the catalyst. The best results after 1 h reaction were attained by Pd5/Al (8.4 mmol $H_2O_2/g_{Pd}.h$). No hydrogen peroxide was detected when Pd5/C was used, probably due to the high activity of this catalyst in the decomposition of H_2O_2 as soon as it is produced.

Table 1. Catalysts performance in hydrogen peroxide formation by formic acid and oxygen.

Catalyst	Time (min)	Formic acid conv. (mmol)	H_2O_2 available (10^{-2} mmol)	H_2O_2 product. (mmol H_2O_2 $g_{(Pd)}^{-1}$ h^{-1})	H_2O_2 select. (%)[d]
Pd/Al	5	0.31	3.09	74.5	10
	60	3.6	4.19	8.4	1.15
Pd/Ti	5	0.25	5.47	131.8	21.9
	60	4.2	2.48	5.0	<1
Pd/C	5	3.2	0	0	0
	60	18.3	0	0	0
γ-Al_2O_3[a]	5	0	0	0	0
	60	T[b]	T	T	T
TiO_2[a]	5	0	0	0	0
	60	1.1	0.74	1.48[c]	<1

[a] Amount of catalyst: 0.5 g; [b] Trace; [c] mmol H_2O_2 $g_{(cat)}^{-1}$ h^{-1}; [d] mmolH_2O_2 formed/mmol HCOOH converted

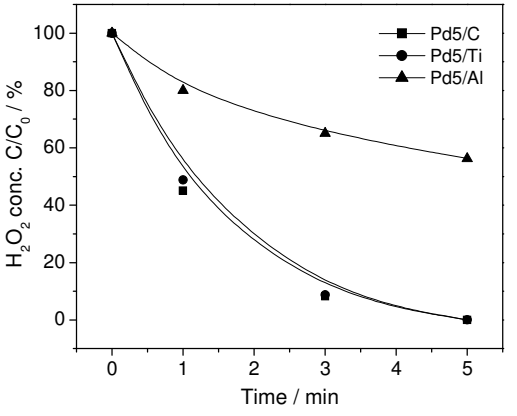

Figure 1. H_2O_2 decomposition profile over supported-Pd catalysts (initial H_2O_2 conc= 100 ppm, 0.1 g catalyst, 25°C).

ISBN:/DL:T.1259-2011

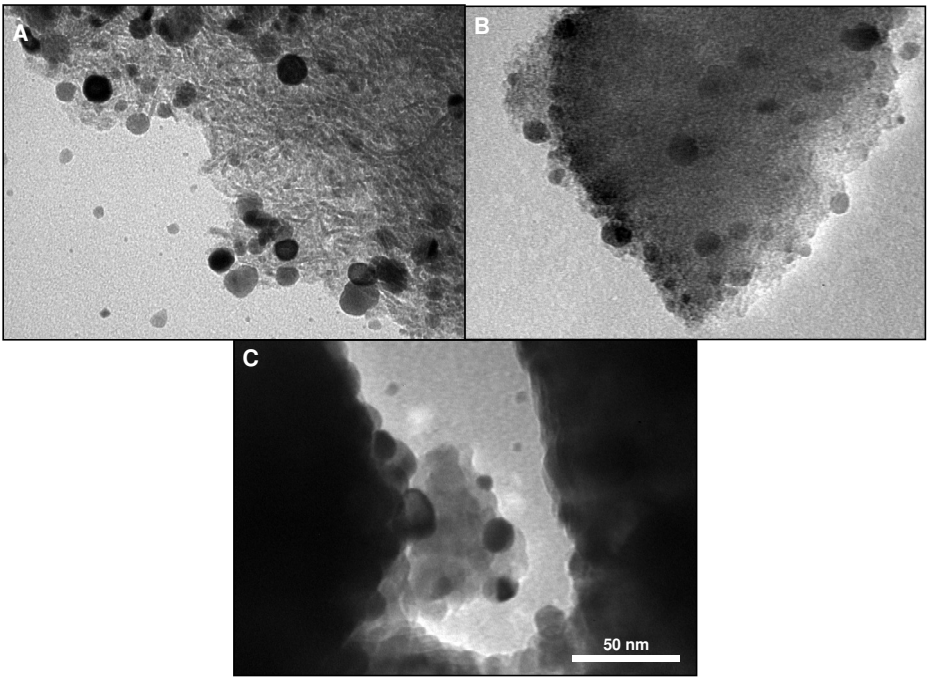

Figure 2. TEM images of A) Pd5/Al, B) Pd5/C and C) Pd5/Ti.

In fact, the study of the decomposition of H_2O_2 (100 ppm H_2O_2, 0.1 g catalyst, 25ºC) over the Pd-supported catalysts showed (Figure 1) that Pd5/Al offers more stability for H_2O_2: whereas almost full decomposition of H_2O_2 happened over Pd5/Ti and Pd5/C in less than 5 minutes, lifetime of H_2O_2 molecules over Pd5/Al was enhanced up to 1 h (40% decomposition after 5 min). Differences in Pd particle size could be responsible for this behaviour [17]. The average size of Pd particles measured by TEM (see Figure 2) was within the close range of 10 to 20 nm for Pd5/C, Pd5/Ti and Pd5/Al. It can also be observed that on carbon, Pd particles present a more uniform distribution. Therefore, although smaller metal particles usually are more active, it can be suggested that here Pd particle size may not play the key role in the observed activity of Pd-supported catalyst. However, the role of the support in controlling the activity of Pd in decomposition of H_2O_2 can be even more important, e.g. affecting the

ISBN:/DL:T.1259-2011

Pd(0)/Pd^{2+} ratio. At the light of the results presented above, Pd5/Al is expected to be adequate for bulk purposes, while for *in situ* applications Pd5/Ti appeared to be the most appropriate option.

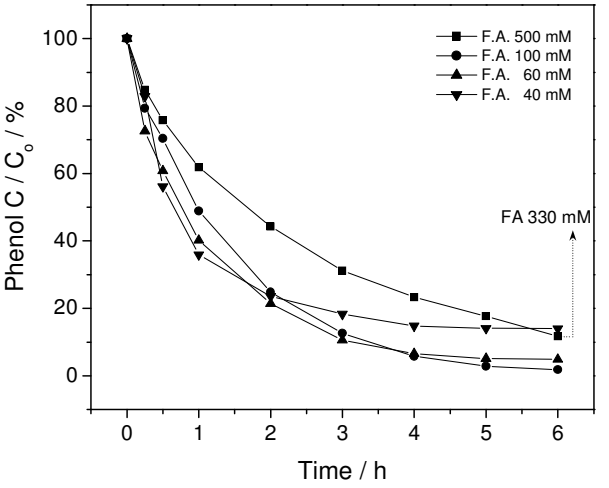

Figure 4. Degradation of phenol with *in situ* generated H_2O_2 starting with different initial formic acid concentrations (initial phenol conc= 100 ppm, 0.1 g catalyst, 25°C).

In order to optimize the cost of the process, the effect of using different initial concentrations of FA was studied (in the range 40-500 mM, see Figure 4) with a Pd5/Al catalyst. It was seen that by decreasing the initial concentration of FA down to 100 mM, phenol was decomposed at a higher rate. While reactions performed with 500 mM FA led to a removal of 88% phenol after 6 h reaction and no complete consumption of FA was attained, when the process was initiated with 100 mM FA almost full oxidation of phenol was achieved and no FA remained in solution, what allowed us also to measure the TOC exclusively associated to the degradation of phenol (when FA is present, it contributes to the TOC value, and therefore the amount of carbon associated to the degradation of phenol cannot be measured). It is worth to note that the possible amount of FA produced from the degradation of 100 ppm of phenol is much lower than the FA supplied to the system. Therefore, its contribution to

the overall process is very minor. TOC measurement could be performed as well in experiments carried out with 60 and 40 mM initial FA concentration. Almost complete removal of CC was achieved when working with 100 mM FA after 6h of reaction, together with a 60% mineralization. Further decreasing the initial FA concentration down to 40 mM led to a mineralization degree of 55% after 4 h (when FA finished as well). It is interesting to note that after finishing FA, the mineralization proceeded up to 66% at 6h of reaction, probably due to the extended decomposition of intermediates over the catalyst. At the light of the results it was also seen that the amount of H_2O_2 available by *in situ* generation is more than 10 times higher than the amount available by bulk generation (without subsequent consumption of H_2O_2), based on the degree of mineralization achieved.

Comparing with the conventional Fenton process (CFP) it is worthy to mention that, although this system shows a lower degradation rate, the degree of mineralization achieved is higher, as maximum percentages of TOC removal by CFP are ca. 45-50% [22-25]; concerning intermediates, this system is also more efficient in the removal of toxic intermediates, as evidenced by the lack of colour of the solution [26]. Nevertheless, the degradation rate can also be enhanced by increasing the temperature of operation [22]. Since the mineralization achievement does not increase by even higher H_2O_2 feeding in the case of CFP, using catalytic *in situ* generated H_2O_2 instead of CFP might be taken into consideration. However, a full economic balance requires involving other items such as catalyst, materials, time of treatment, etc. which is out of the scope of the current work. For example, further studies to find a catalyst with a lower noble metal content and higher activity is a subject of future work.

Although FA can also react with hydroxyl radicals and could interfere the oxidation of phenol, reaction rate constants are different by one order of magnitude. Rate constants with OH radicals are $6.6.10^9$ $M^{-1}.s^{-1}$ [27] and $1.4.10^8$

$M^{-1}.s^{-1}$ [28] for phenol and formic acid, respectively. Therefore, when not very high concentrations of formic acid are used, phenol oxidation by $^{\bullet}OH$ proceeds faster than formic acid oxidation.

3.2. Effect of the addition of a second metallic active phase. Heterogenization of the catalytic system.

As it has been shown in the literature that the addition of Au to a Pd-supported catalyst improves the rate and selectivity of hydrogen peroxide generation, two bimetallic catalysts (Pd-Au and Pd-Pt) supported on alumina with a total metal content of 5 wt%, were prepared and tested in the process of generation of hydrogen peroxide from formic acid and oxygen. Besides them, two other catalysts incorporating the active phase for H_2O_2 decomposition into hydroxyl radicals (Pd-Fe and Pd-Cu) were also prepared for a full heterogenization of the Fenton catalytic system. They were prepared to be tested in the Fenton reaction, but they were previously tested in the generation of H_2O_2 (i.e. without phenol) in order to see the effect of Fe and Cu in this process. For these two catalysts, the amount of Pd was 5 wt% and the amount of Fe or Cu 1 wt%. Table 2 summarizes results achieved at short and long time related to the amount of FA converted, the amount of H_2O_2 generated and the selectivity (%) towards H_2O_2.

As it can be seen, the incorporation of Cu, Fe and Au did not affect significantly the conversion of FA while in the presence of Pt, FA decomposition is increased remarkably. However, this increase was not translated into a higher amount of H_2O_2 produced (see Figure 5). It seems that Pt enhances the activity of the catalyst in both FA and H_2O_2 decomposition. Therefore Pt is not a good active metal for this reaction at least in such a proportion with Pd. Lio et al. [19] has shown that the addition of small amounts of Pt (2.5 atom%) to Pd increases only the formation rate of H_2O_2. It has been also found that small amount of Pt added to Pd on sulphated zirconia is able to increase the

selectivity for H_2O_2 [20]. In the both above cases, it has been mentioned that further increasing of Pt content has a reverse effect on the reaction.

Table 2. Effect of the addition of a second metal in the generation of hydrogen peroxide by formic acid and oxygen.

Catalyst	Time (min)	Formic acid conv. (mmol (%))	H_2O_2 available (10^{-2} mmol)	H_2O_2 selectivity (%)[a]
Pd5/Al	5	0.31 (1.24)	3.09	10
	60	3.6 (14.40)	4.19	1.2
Pd2.5Au2.5/Al	5	0.33 / (1.32)	2.0	6.0
	60	0.81 (3.24)	6.7	8.2
Pd2.5Pt2.5/Al	5	0.78 (3.12)	0.7	0.9
	60	16.37 (65.5)	0.5	<0.1
Pd5Fe1/Al	5	0.35 (1.4)	4.5	12.8
	60	2.41 (9.6)	2.2	0.9
Pd5Cu1/Al	5	0.31 (1.24)	2.4	7.7
	60	4.49 (17.9)	4.2	0.9

[a] mmolH_2O_2 formed/mmol HCOOH converted

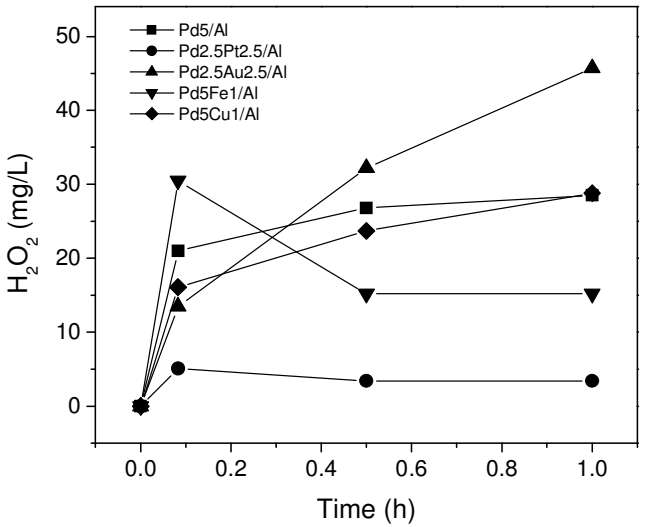

Figure 5. Production of H_2O_2 over the bimetallic catalysts (initial FA conc= 500 mM, 0.1 g catalyst, 25°C).

ISBN:/DL:T.1259-2011

At longer times, Au shows an interesting ability to enhance the production of H_2O_2, as it was stated in the literature [17,19], whereas at short time Fe is the one which demonstrated the highest capacity for H_2O_2 production, something that is required for *in situ* applications.

These bimetallic catalysts were also tested in the oxidation of phenol by the Fenton process with *in situ* generated hydrogen peroxide. In these tests, initial FA concentration was 100 mM. In the case of Pd2.5Au2.5/Al and Pd2.5Pt2.5/Al, 10 mg/L of ferrous ion was added to the initial reaction solution. None of the bimetallic catalysts could improve the degradation rate obtained by the Pd5/Al catalyst (Figure 6). Pd-Pt and Pd-Au showed similar phenol oxidation rate during the first hour of reaction. Later disappearance of phenol is almost suppressed over Pd-Pt, due to termination of FA after 1h. Pd and Cu did not show a complementary effect, resulting in a poorest achievement in the degradation of phenol. Further study of the structure of the catalyst is needed to explain this behaviour. In order to monitor the amount of TOC, some experiments with lower amount of FA (40 mM) were carried out. In these tests it was observed that, although the oxidation rate is slightly lower, the Pd5-Fe1/Al achieved similar mineralization rates to the system with the monometallic catalyst and ferrous ion. Using this catalyst, 72% phenol removal and 51% mineralization was attained after 4 h (when FA was finished) which proceeded up to 68% after 6 h reaction. This bimetallic catalyst clearly showed a synergistic effect of Pd and Fe in the production of hydrogen peroxide followed by its decomposition to hydroxyl radicals on the surface of catalyst. Therefore, complete heterogenization of the catalytic system is accomplished achieving a good performance in the mineralization of the organic pollutant. Concerning the Pd-Au system, it presented similar degradation rates to Pd5Fe1/Al, however the mineralization degrees were lower, as after 8 hours of reaction only a 47% TOC removal was obtained.

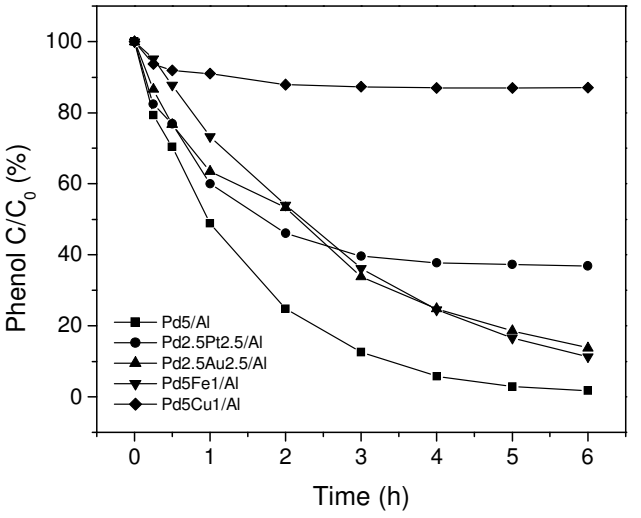

Figure 6. Degradation of phenol by the Fenton process with *in situ* generated H_2O_2 by the bimetallic catalysts (initial phenol conc= 100 ppm, initial FA conc= 100 mM, 0.1 g catalyst, 25°C).

In the Pd5Fe1/Al catalyst, leaching of Pd and Fe was measured by atomic absorption at the end of the reaction. No Pd was detected in solution. Concerning iron, concentration of iron in solution was 0.86 mg/L. At the light of this low concentration and based on a test performed with catalyst Pd5/Al in the presence of 1 mg/L of ferrous ion (results not shown), contribution of possible homogeneous reaction to the total mineralization degree is very minor.

4. Conclusions

Among the Pd-supported catalysts tested, Pd5/Al has shown to be an efficient catalyst in the *in situ* generation of H_2O_2 by formic acid and oxygen and its subsequent application in the oxidation of phenol by Fenton process. Lowering initial concentration of FA down to 100 mM favours the efficiency of the system. Addition of a second metal demonstrated different effects. In the presence of Pt, FA decomposition was enhanced, but also the decomposition of the produced H_2O_2 was increased. Pd-Au catalyst showed an interesting improvement in productivity and selectivity for bulk production of H_2O_2, as it was expected reviewing the recent reports in the literature, but was not

appropriate for the Fenton process as the mineralization degrees obtained were lower. On the contrary, Pd-Fe catalyst offered an interesting prospect for making a full heterogeneous catalyst for Fenton reaction involving *in situ* generation of H_2O_2.

Acknowledgments

The funding provided by URV (AIRE 2006/02), the Spanish Ministry of Science and Innovation (CTM2008-02453), Generalitat de Catalunya-CIDEM (VALTEC 08-1-0052) and ICREA ACADEMIA programme are acknowledged.

References

[1] M.G. Clerici, P. Ingallina, *Catal. Today*, 41 (1998) 351-364.

[2] R. Burch P.R Ellis. *Appl. Catal. B: Environ.* 42 (2003) 203-211.

[3] J.H. Lunsford, *J. Catal.* 216 (2003) 455-460.

[4] J.M. Campos-Martin, G. Blanco-Brieva, J.L. Fierro, *Angew. Chem. Int. Ed.* 45 (2006) 6962-6984.

[5] C. Samanta, V.R. Choudhary, *Appl. Catal. A: Gen.* 330 (2007) 23-32.

[6] J.J. Bravo-Suárez, K.K. Bando, T. Akita, T. Fujitani, T.J. Fuhrer, S.T. Oyama, *Chem. Commun.* (2008) 3272-3274.

[7] V.R. Choudhary, C. Samanta and P. Jana, *Chem. Commun.* (2005) 5399-5401.

[8] V.R. Choudhary, P. Jana *Catal. Commun.* 8 (2007) 1578-1582.

[9] J.R. Hyde, M. Poliakoff, *Chem. Commun.* (2004) 1482-1483.

[10] F.-D. Kopinke, K. Mackenzie, R. Koehler, A. Georgi, *Appl. Catal. A: Gen.* 271 (2004) 119-128.

[11] A. Garron, F. Epron, *Water Res.* 39 (2005) 3073-3081.

[12] M.S. Yalfani, S. Contreras, F. Medina, J. Sueiras, *Chem. Commun.* (2008) 3885-3887

[13] S. Abate, S. Melada, G. Centi, S. Perathoner, F. Pinna, G. Strukul, *Catal. Today* 117(2006) 193-198.

[14] V.R. Choudhary, C. Samanta, T.V. Choudhary, *Appl. Catal. A: Gen.* 308 (2006) 128-133.

[15] P. Landon, P.J. Collier, D. Chadwick, A.J. Papworth, A. Burrows, C.J. Kiely, G.J. Hutchings, *Phys. Chem. Chem. Phys.* 5 (2003) 1917-1923.

[16] J.K. Edwards, B.E. Solsona, P. Landon, A.F.. Carley, A. Herzing, C.J. Keily, G.J. Hutchings, *J. Catal.* 236 (2005) 69-79.

[17] J.K. Edwards, B.E. Solsona, E.N. Ntainjua, A.F. Carley, A. Herzing, C.J. Kiely, G.J. Hutchings, *Science*, 323 (2009) 1037-1041.

[18] J.C. Pritchard, Q. He, E.N. Ntainjua, M. Piccinini, J.K. Edwards, A.A. Herzing, A.F. Carley, J.A. Moulijn, C.J. KIely, G.J. Hutchings, *Green Chem.* 12 (2010) 915-921.

[19] Q. Lio, J.C. Bauer, R.E. Schaak, J.H. Lunsford, *Appl. Catal. A: Gen.* 339 (2008) 130-136.

[20] G. Bernardotto, F. Menegazzo, F. Pinna, M. Signoretto, G. Cruciani, G. Strukul, Appl. Catal. A: Gen. 358 (2009) 129-135.

[21] Y.-G. Zhang, L.-L. Ma, J.-L. Li, Y. Yu, *Environ. Sci. Technol.* 41 (2007) 6264-6269.

[22] M.S. Yalfani, S. Contreras, F. Medina, J. Sueiras, , *Appl. Catal. B: Environ.* 89 (2009) 519-526.

[23] I. Sirés, F. Centellas, J.A. Garrido, R.M. Rodríguez, C. Arias, P.L. Cabot, E. Brillas, *Appl. Catal. B: Environ.* 72 (2007) 373-381.

[24] E.M. Cordi, J.L. Falconer, *J. Catal.* 162 (1996) 104-107.

[25] J.A. Zazo, J.A. Casas, A.F. Mahedano, M.A. Gilarranz, J.J. Rodriguez, *Environ. Sci. Technol,* 39 (2005) 9295-9302.

[26] F. Mijangos, F. Varona, N. Villota, *Environ. Sci. Technol,* 40 (2006) 5538-5543.

[27] N. Kang, D.S. Lee, J. Yoon, *Chemosphere*, 47 (2002) 915-924.

[28] G.H. Rossetti, E.D. Albizzati, O.M. Alfano, *Ind. Eng. Chem. Res.* 41 (2002) 1436-1444.

UNIVERSITAT ROVIRA I VIRGILI
NEW CATALYTIC ADVANCED OXIDATION PROCESSES FOR WASTEWATER TREATMENT
Mohammad Sadegh Yalfani
ISBN:/DL:T.1259-2011

Chapter 4

Simultaneous *in situ* generation of hydrogen peroxide and Fenton reaction over Pd-Fe Catalysts

High mineralization degree of organic compounds can be achieved by a novel environmentally-friendly full heterogeneous Pd-Fe catalytic system, which involves in situ generation of hydrogen peroxide from formic acid and oxygen, and oxidation of organic compounds by Fenton process in a one-pot reaction. The alumina-supported Pd-Fe catalyst synthesized via consecutive co-precipitation (first Fe then Pd) was found as the most favourite one in which low tendency to Pd-Fe alloy formation is in favour of the process. The catalyst is highly stable due to the lack of Fe and Pd leaching during the reactions.

1. Introduction

The Fenton process is known as one of the most efficient advanced oxidation processes for the degradation of organic pollutants [1]. However, the overall performance of the process is influenced by its low mineralization capacity due to the formation of recalcitrant intermediates [2]. The conventional Fenton process (CFP) requires soluble ferrous ion and H_2O_2. Ferrous ion as a homogeneous catalyst requires further treatment due to the formation of sludge. H_2O_2 is usually provided by bulk feeding, which usually does not yield high efficiency. Very recently, the Fenton process has shown good performance with catalytic *in situ* generated hydrogen peroxide [3]. *In situ* produced hydrogen peroxide can be consumed at an appreciable controlled rate prior to decomposition to H_2O and O_2, which leads to an improved performance of H_2O_2 in the favorite reaction direction [4]. Here, we demonstrate for the first time that the Pd-Fe catalytic coupling is able to achieve a nearly total degree of mineralization for the Fenton reaction within a full heterogeneous catalytic system under very mild conditions. The catalytic system involves the simultaneous generation of hydrogen peroxide from formic acid and oxygen, the formation of hydroxyl radicals and the oxidation of organic compounds.

2. Experimental

2.1. Materials preparation

The alumina-supported Pd-Fe catalysts were synthesized via co- and successive impregnation. Co-impregnation procedure was firstly to prepare an acidic solution containing certain amount of palladium chloride and iron nitrate 9-hydrate corresponding to 5% Pd and 1% Fe with respect to alumina (the catalyst denoted as Pd5FeCI). The solution was added to slurry solution of γ-Al_2O_3 (prepared by sol-gel) while stirring vigorously. The slurry was aged stirring for 1 h at ambient conditions. Water was removed by rotary vapor at

ISBN:/DL:T.1259-2011

55°C. The precipitate was dried at 110°C and then was calcined at 400°C for 3 h. Finally, the catalyst was reduced under a flow of pure hydrogen (20 ml min^{-1}) at 200°C for 2 h. The catalyst is denoted as Pd5FeCI.

Successive-impregnation was performed in two steps. First alumina was impregnated with a solution of iron nitrate or acidic solution of palladium chloride. Similar pretreatment explained above including water removing by rotary vapor, drying at 110°C and calcination at 400°C for 3 h was fulfilled. In the second step, the second metal solution (Pd or Fe) was added to the slurry solution of the calcined sample, followed by the above pretreatment program. After final calcination, the samples were reduced under a flow of pure hydrogen (20 ml min^{-1}) at 200 or 400°C for 2 h. The catalyst prepared firstly by Fe is denoted as FePd5 and the one prepared firstly by Pd as Pd5Fe. The Pd and Fe metal contents in the above three samples were 5 and 1 wt%, respectively. A reference Pd5Al sample was also prepared containing 5 wt% Pd on alumina.

2.2. Characterization techniques

The catalysts were characterized by XRD, H_2 chemisorption, HRTEM, TPR and XPS. X-ray diffraction of the samples was carried out using a Siemens D5000 diffractometer by nickel-filtered Cu Kα radiation. The patterns were recorded over a range of 2θ angles from 5° to 70°. In all the patterns, as summarized in Table S2, the broad peaks corresponding to the structure of γ-Al_2O_3 can be observed. The characteristic reflections of Pd(0) are recognizable clearly only in the pattern of Pd5/Al sample. H_2 chemisorption was also acquired by a Micromeritics ASAP 2010. Before analysis at 100 °C, a pretreatment program including evacuation at 100 and 200°C, reduction under H_2 flow at 200 °C and evacuation at 100 °C respectively was fulfilled.

Temperature program reduction (TPR) analyses were performed in a ThermoFinnigan (TPORD 110) apparatus equipped with a thermal conductivity

detector (TCD). The sample was purged with argon flow before the analysis. The analysis was carried out using a 3% H_2/Ar gas flowing at 20 ml min^{-1} by heating from room temperature to 900°C with a ramp of 10°C min. Water produced during TPR was trapped in CaO + Na_2O (Soda lime) before reaching the TCD. H_2 consumption was quantified by measuring the peak area and comparing against the standards curve made using CuO known samples.

High-Resolution Transmission Electron Microscopy (HRTEM) on the reduced samples was carried out at 200 kV with a JEOL JEM 2100 instrument equipped with a LaB_6 source and an Energy Dispersive X-ray analyzer (EDX, Oxford Instruments). The point-to-point resolution of the microscope was 0.20 nm. Samples were deposited on holey-carbon-coated Cu grids from alcohol suspensions. For each sample, particle size distribution histograms were obtained over 100-200 individual particles.

X-ray photoelectron spectroscopy (XPS) was performed with a SPECS system equipped with an Al anode XR50 source operating at 150 W and a Phoibos 150 MCD-9 detector. Sample powders were pelleted and fixed mechanically into a special sample holder without glue or tape. Spectra were recorded with pass energy of 25 eV at 0.1 eV steps at a pressure below 5×10^{-9} mbar and binding energies were referred to the C 1s signal. The system was equipped with an HPC-20 reaction chamber. *In situ* reduction treatments were carried out at 1 bar under an atmosphere of pure hydrogen supplied via a MKS mass flow controller. The temperature was provided with an infrared source and was measured directly on the sample holder with a thermocouple. The temperature was raised smoothly and the sample was maintained at each temperature for 10 minutes. After each treatment, samples were transferred from the reaction cell to the analysis chamber under high vacuum (below 5×10^{-8} mbar). The C 1s peak from the adventitious carbon was used as an internal reference with a binding energy of 284.8 eV. The atomic percentage of each

element was determined by dividing the peak area of the most intense XPS signal of each element by the corresponding sensitivity factor and expressing it as a fraction of the sum of all normalized peak areas. High resolution XP spectra were acquired by Gaussian/Lorentzian curve fitting after S-shape background subtraction.

2.3. Catalytic tests

The phenol degradation reactions were implemented at ambient conditions (25 °C and atmospheric pressure) in a magnetically stirred three-necked glass reactor with a capacity of 100 ml. The reaction details are as follows unless it is mentioned specifically. The volume of the reaction was always 50 ml containing phenol (100 ppm), ferrous iron (10 ppm, only added in the tests with Pd5Al) and the catalyst (0.1 g). Formic acid was injected with a concentration of 40 mM. Oxygen was passed bubbling into the reaction medium with a flow rate of 20 ml min^{-1}. The temperature of the reaction was controlled using a water bath. Without any exception, all the reactions were performed at darkness in order to avoid any interfering effect of existing light. Phenol degradation and formic acid decomposition were monitored by sampling at regular time intervals and analysing by high performance liquid chromatography HPLC (Shimadzu LC-2010 equipped with a SPD-M10A Diode array UV-vis detector). A Varian OmniSpher C18 column and a solution containing Milli-Q H_2O and acetonitrile (60:40) at pH 3.80 adjusted by phosphoric acid as mobile phase were used to analyse phenol and the aromatic intermediates at wavelength 254 nm. An Acclaim OA column and a mobile phase containing 100 mM Na_2SO_4 at pH 2.65 adjusted by methanesulphonic acid as mobile phase were used to analyse formic acid at wavelength 210 nm. TOC for each sample was measured by a Shimadzu TOC-5000A. The reaction solution at the end of each run after filtration was analysed by atomic absorption spectroscopy to detect leached Pd and Fe.

3. Results and discussion

The palladium loading was chosen from the study of H_2O_2 generation from formic acid and O_2 over alumina-supported Pd catalysts with different Pd loads. The results showed that the highest H_2O_2 productivity at the initial time of the reaction which is more adequate for *in situ* applications was achieved using Pd5Al [3,5]. Our experiments indicate that this productivity was further enhanced in the presence of Fe (See Figure1).

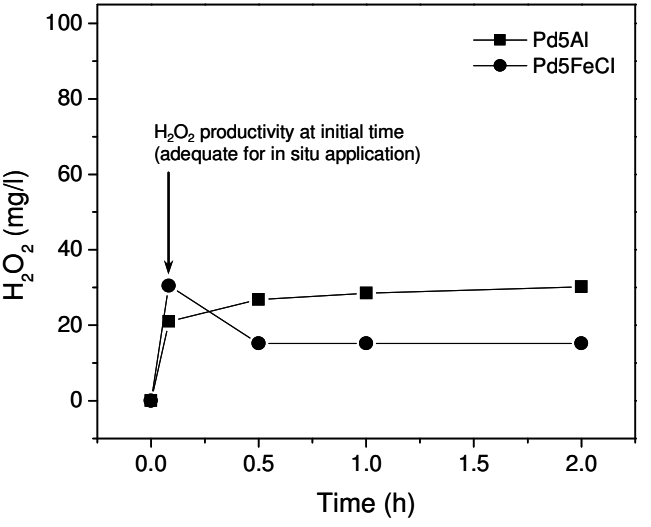

Figure 1. H_2O_2 generation from formic acid and O_2 over Pd5Al and Pd5FeCI. Reactions were performed at ambient conditions (25°C and atmospheric pressure) in a three necked glass reactor containing 50 ml Milli-Q water, 500 mM formic acid, 100 mg catalyst and O_2 with a flow rate of 20 ml/min. H_2O_2 evolution was measured by iodometric titration and formic acid by HPLC.

Phenol as a model pollutant was degraded by the Fenton reaction over Pd-Fe catalysts at ambient conditions using H_2O_2 generated *in situ* from formic acid and O_2. The results by the Pd-Fe catalysts are compared with the corresponding reaction using the Pd5Al catalyst in the presence of 10 ppm of Fe^{2+} (homogeneous Fenton catalyst) and CFP using 300 ppm H_2O_2 (the amount estimated to be produced *in situ* by formic acid and O_2 over Pd5Al within 6 h)

ISBN:/DL:T.1259-2011

[3] and 10 ppm of Fe^{2+} (Table 1). The reaction rate coefficients (k_{obs}) for formic acid and phenol decompositions are calculated by fitting data to a pseudo-first-order kinetics during the first hour. Formic acid decomposition rates for all of the catalysts are within a very narrow range, which indicates that Fe does not interfere in formic acid decomposition by Pd [6]. Phenol degradation over the PdFeCI catalyst proceeds at a rate 2.4 times lower than with Pd5Al. The catalyst also shows lower mineralization activity. Although the Pd5Fe catalyst oxidizes phenol at a lower rate, its performance in mineralization is slightly better. However, the FePd5 catalyst competes with Pd5Al in phenol oxidation and shows outstanding pollutant compound mineralization ability, especially in comparison with CFP, which is unable to exceed 50% [2c]. A higher H_2O_2 feeding increases the rate at which phenol disappears, but it results in a lower degree of mineralization [2b]. Over Pd5Al and Pd-Fe catalysts, formic acid is finished at 4 h, but the mineralization proceeds even in the absence of formic acid. This phenomenon can be attributed to the ability of the catalysts to mineralize intermediates. The stability of FePd5 was proved by adding 20 mM of formic acid as soon as the initial 40 mM was finished, i.e. at 4 h. Figure 2 shows the phenol degradation profile of this reaction. This graph demonstrates that the second stage of the reaction proceeds at a rate similar to that of the initial phenol oxidation. This proves that the catalyst remains active after 4 h and that the system is capable of degrading even very low concentrations of pollutant. Most importantly, the achievement of a very high degree of mineralization suggests that such a system has the potential to completely remove all organic intermediates. FePd5 was the most appropriate Pd-Fe catalyst because no measurable leached Pd or Fe remained at the end of each run. Application of the later process was expanded for the degradation of 2,4-dichlorophenol (DCP, as representative of chlorophenols) and clofibric acid (CFA, as representative of pharmaceutical compounds). The results are shown

in Figure 3-a and 3-b. In the case of DCP, the reaction is started with a high rate so that 95% of DCP is destructed within 2h. Second addition of formic acid gives rise to proceeding the reaction with similar rate. By termination of formic acid decomposition of DCP is stopped. For CFA, similar trend is observed but the mineralization degree achieved is lower.

Table 1. Phenol degradation results by CFP and over Pd5Al and Pd-Fe catalysts.

Catalyst	t (h)	Ph. conv. (%)	TOC[a] rem. (%)	$k_{obs(FA)}$[b] (min^{-1})	$k_{obs(Ph)}$[c] (min^{-1})	Pd leached / $mg.l^{-1}$ (%)	Fe leached /$mg.l^{-1}$(%)
10 mg/l Fe^{2+}[d]	4	100	45	-	1.90×10^{-2}	-	-
	6	100	47		*(R^2 = 0.9821)*		
Pd5Al + 10 mg/l Fe^{2+}	4	85.3	55	1.38×10^{-2}	1.71×10^{-2}		
	6	86.3	66	*(R^2 =0.9996)*	*(R^2 = 0.9950)*	0	-
Pd5FeCl	4	72.2	47	1.29×10^{-2}	7.00×10^{-3}		
	6	73.6	62	*(R^2 = 0.9956)*	*(R^2 = 0.9945)*	0	0.86 (4.3)
Pd5Fe	4	91.4	57	1.39×10^{-2}	1.04×10^{-2}		
	6	93.2	72	*(R^2 = 0.9983)*	*(R^2 = 0.9992)*	0	1.46 (7.3)
FePd5	4	91.2	68	1.33×10^{-2}	1.26×10^{-2}		
	6	92.1	78	*(R^2 = 0.9905)*	*(R^2 = 0.9998)*	0	<0.1

[a] Total organic carbon, [b,c] Rate coefficients of formic acid and phenol decomposition for the first 1 h of reaction, respectively, [d] CFP using 300 ppm H_2O_2.

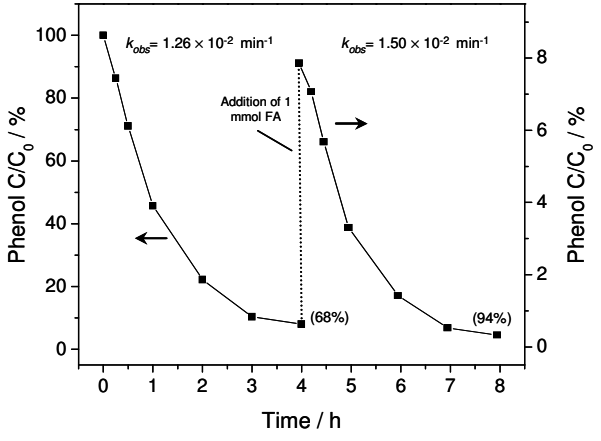

Figure 2. Phenol degradation profile over FePd5 performed in two steps; the numbers in parentheses are the corresponding TOC percentages removed at that time.

UNIVERSITAT ROVIRA I VIRGILI
NEW CATALYTIC ADVANCED OXIDATION PROCESSES FOR WASTEWATER TREATMENT
Mohammad Sadegh Yalfani
ISBN:/DL:T.1259-2011

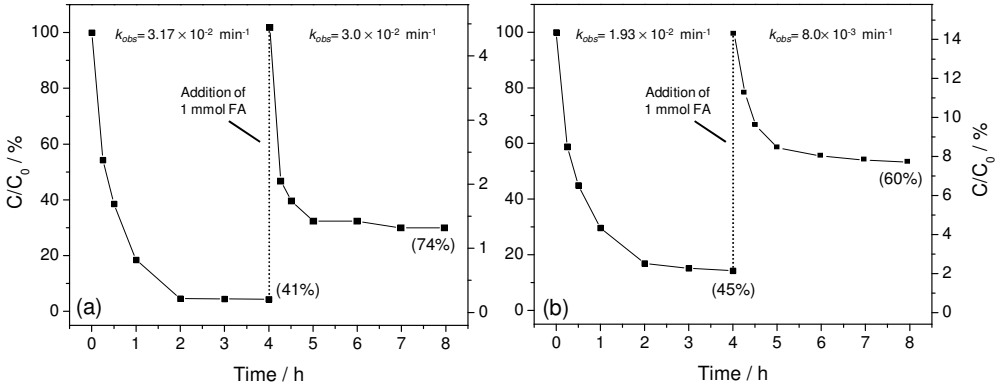

Figure 3. DCP and CFA degradation profiles over FePd5 performed in two steps; the numbers in parentheses are the corresponding TOC percentages removed at that time.

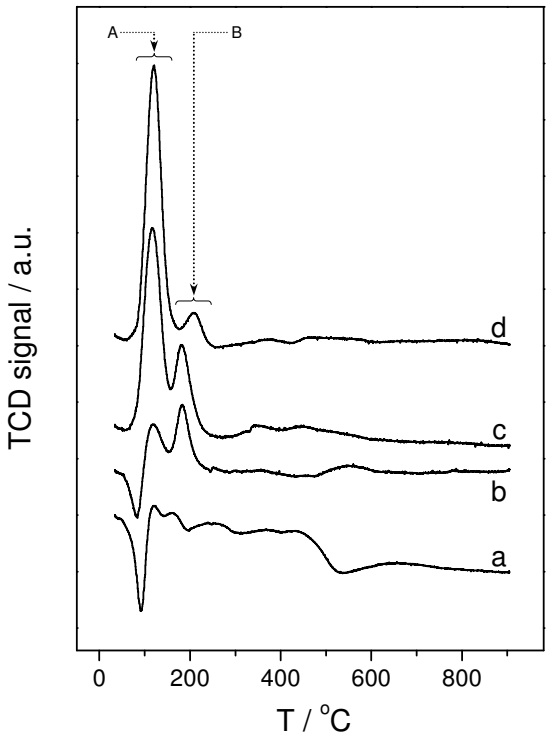

Figure 4. TPR thermograms of the samples: a) Pd5Al, b) FePd5, c) Pd5Fe and d) Pd5FeCl

ISBN:/DL:T.1259-2011

The catalysts were characterized in order to explain the differences observed in catalytic activity. Figure 4 contains TPR profiles of the samples, that shows for the Pd5Al sample only a desorption peak of β-PdH, which means an almost total reduction of PdO at ambient temperature.[7] In the presence of Fe, the disappearance of the β-PdH desorption peak is accompanied by the growth of peaks at areas A and B, which means that iron suppresses β-PdH formation.[8] In contrast, the reduction of Fe shifts to lower temperatures. In the TPR thermograms of the Pd5FeCI and Pd5Fe samples, the peak of area A shows much more H_2 consumption (8.4 and 7 times respectively) than the thermogram of the FePd5 sample (see Table 2). High merging for the Pd and Fe species is expected in the Pd5FeCI sample, which was synthesized by co-impregnation. It can be concluded that the peak appearing in area A corresponds to the simultaneous reduction of palladium and iron oxides, resulting in the generation of Pd-Fe alloy [9,10]. The remarkable narrowness of the peak can be attributed to the uniform and well-dispersed iron and palladium oxide particles that yielded to very fine Pd-Fe alloy particles. The second reduction in area B can be attributed to the partial iron oxide reduction still being affected by Pd. The Pd5Fe sample has a relatively high tendency towards Pd-Fe alloy formation. In contrast, for the FePd5 sample, owing to the existence of β-PdH, much of the Pd has not merged with the Fe, and thus least tendency to alloy formation is observed.

Table 1. H_2 consumption during TPR analysis of the Pd-Fe samples.

Catalyst	H_2 consumption (μmol/g)					
	PdβH (40-100°C)	A (80-170°C)	B (150-260°C)	A/B	Pd Theo.	Fe Theo.
Pd5Al	52.3	1.2	1.6	0.75	466	0
Pd5FeCI	Trace	315	12.2	25.8	466	268
Pd5Fe	Trace	263	86	3.1	466	268
FePd5	3.8	37.5	54.8	0.7	466	268

In accordance with the TPR data, a HRTEM analysis of Pd5FeCI and Pd5Fe (Figure 5-A and 5-B) revealed lattice fringes at 2.20 Å for both samples. This value is within the (111) lattice fringes of the PdFe and Pd_3Fe alloys at 2.19 Å and 2.22 Å, respectively, and slightly below the value of the (111) crystallographic plane of metallic Pd (2.24 Å). In addition to alloy particles, individual metallic Pd particles dispersed on alumina crystallites are also detectable in these two samples, but no isolated Fe-containing phases are observed. In contrast, the HRTEM analysis of the FePd5 sample (Figure 5-C) indicates the presence of metallic Pd and Fe_2O_3, which is identified by lattice fringes at 1.84 Å and 2.21 Å ascribed to (024) and (113) crystallographic planes, respectively.

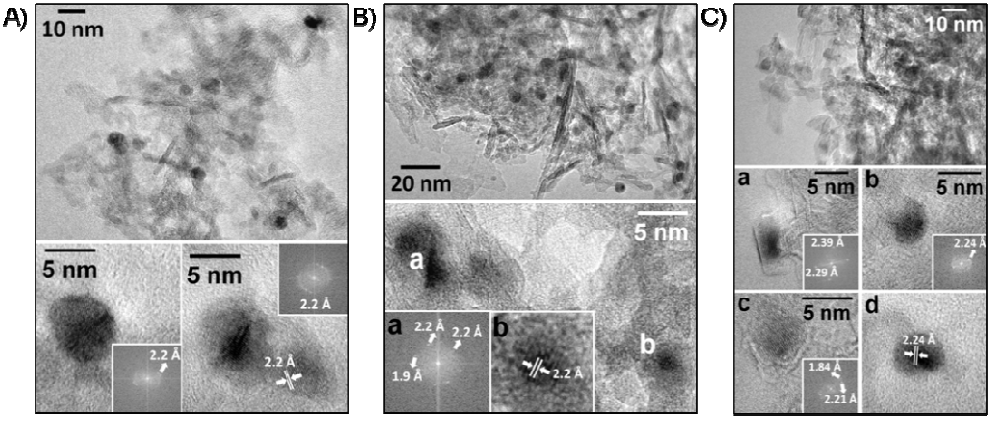

Figure 5. HRTEM images of the following samples: A) Pd5FeCI, B) Pd5Fe and C) FePd5.

In situ surface analysis by XPS during the reduction of the samples shows considerable reduction of PdO at 100°C (>70% in all cases) (See Table 3), whereas the amount of reduced- surface iron is much higher for FePd5 (18.4%) than for Pd5Fe or Pd5FeCI (0% and 6.5%, respectively). Interestingly, reduction at 200°C increases the amount of Fe reduced by up to 25.4% for FePd5 and, at the same time, slightly decreases the amount of Pd reduced (from

ISBN:/DL:T.1259-2011

Table 3. XPS quantitative results of the calcined and reduced Pd-Fe samples

Catalyst	Binding energy (eV)				Elements contributions (%)			
	Pd(0)3d5/2	*Pd(δ^+)3d5/2*	*Fe(0)2p3/2*	*Fe(δ^+)2p3/2*	*Pd(0)*	*Pd^{n+}*	*Fe(0)*	*Fe^{n+}*
Pd5FeCI calc.	-	335.8	-	710.6	0	100	0	100
Pd5FeCI red. 100 °C	335.0	336.4	706.3	711.4	80.9	19.1	6.5	93.5
Pd5FeCI red. 200 °C	334.8	335.9	705.8	711.0	75.1	24.9	20.3	79.7
Pd5Fe calc.	-	336.6	-	710.5/715.7	0	100	0	100
Pd5Fe red. 100 °C	335.4	336.9	-	711.2/717.0	72.7	27.3	0	100
Pd5Fe red. 200 °C	335.4	336.7	705.7	710.6	77.5	22.5	7.2	92.8
FePd5 calc.	-	336.1	-	710.7	0	100	0	100
FePd5 red. 100 °C	335.4	336.8	706.8	711.5	75	25	18.4	81.6
FePd5 red. 200 °C	335.2	336.4	706.3	710.8	72.9	27.1	25.4	74.6

ISBN:/DL:T.1259-2011

75% to 72.9%), which suggests that the reduction of Fe_2O_3 occurs via electron transfer between metallic Pd and Fe_2O_3 particles. At this temperature, the amount of reduced-surface iron increases to a lower extent for Pd5Fe and Pd5FeCI samples (7.2 and 20.3%, respectively). Thus, the order of sequential impregnation during the preparation of samples plays an important role in the final characteristics of the surface, which may account for the different activity in the Fenton reaction. The binding energy recorded for the $Fe^{(+\delta)}$p3/2 core level is very close to that of Fe_2O_3/Al_2O_3 (710.8 eV). This indicates that ionic iron species on the surface of the samples are mostly Fe^{3+} [11]. Also, on the surface of Pd-Fe alloy particles, Fe is mostly present as Fe^{3+}, as was shown by Chen et al. [12].

Therefore, according to the above characterizations, firstly, close proximity and high interaction between the Pd and Fe species is observed. High stability of both metals indicated by leaching results can be due to such interaction. Secondly, for the Pd5FeCI and Pd5Fe samples, much of the Fe participates in alloy formation, whereas a weak tendency towards alloy formation is observed for FePd5. In contrast, the main species found for this sample are metallic Pd and Fe_2O_3.

The preference of the Pd-Fe catalysts in mineralization with respect to the Pd5Al-ferrous ion coupling and CFP can be elucidated by a mechanistic model. In CFP, H_2O_2 is decomposed into hydroxyl radicals by dissolved ferrous ions. In a homogeneous system using the Pd5Al-ferrous ion, the hydrogen peroxide generated should be released into the solution to reach a soluble ferrous ion for radical formation. Over Pd-Fe catalysts, the mechanism can take the form of a spillover effect (Scheme 1) [13]. For surface species, the spillover effect mostly involves metallic Pd and Fe_2O_3. Based on that, formic acid decomposes to CO_2 and H_2 over metallic Pd, which is followed by reaction with O_2, leading to H_2O_2 formation. Then, surface chemisorbed H_2O_2 diffuses onto the Fe_2O_3 surface and,

depending on the oxidation state of the Fe, is decomposed into •OH or •O_2H radical [14]. In the last stage, the organic molecule approaches the radical and is oxidized to the oxidation products. Surface diffusion of activated H_2O_2 may also take place via alumina support. No spillover of chemisorbed H_2O_2 has been reported. It is important to say that the Pd-Fe alloy may not favor the Fenton reaction; a close conjunction of metallic Pd and Fe_2O_3 particles would be more suitable. This conclusion is based on the better results obtained by the FePd5 catalyst.

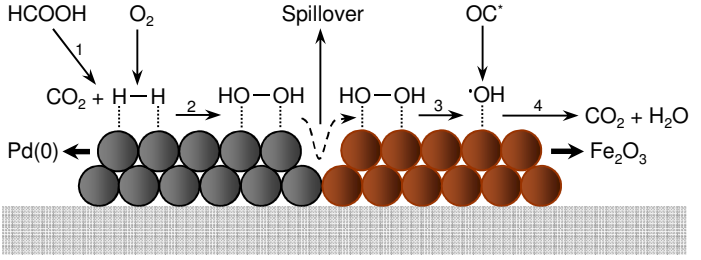

Scheme 1. Mechanism of the phenol degradation reaction via *in situ* generated H_2O_2 including: 1) Decomposition of formic acid to CO_2 and H_2, 2) Reaction of O_2 with surface H_2 to generate H_2O_2, 3) Decomposition of chemisorbed H_2O_2 into radicals, 4) Oxidation of organic compounds by surface radicals.
OC*: organic compound,

4. Conclusions

In summary, a nearly total mineralization of phenol was achieved by a Fenton reaction over a Pd-Fe catalytic system. H_2O_2 was generated *in situ* by formic acid and O_2 at ambient conditions. Degradation of chlorophenols and pharmaceutical compounds was also tested which indicated extensive capacity of the catalytic system in degradation of other categories of organic pollutants. The catalysts showed outstanding ability in a multi-step process that included H_2O_2 generation and the Fenton reaction. The catalysts are highly stable, as shown by the lack of Pd and Fe leaching, which represents a full heterogeneous Fenton process. These results suggest promising prospects for a one-pot full mineralization of organic pollutants.

Acknowledgement

This work was funded by MICINN projects CTM2008-02453 and CTQ2009-12520 and CIDEM project VALTEC 08-1-0052.

References

[1] R. Andreozzi, V. Caprio, A. Insola, R. Marotta, *Catal. Today* 53 (1999) 51-59; S. Esplugas, J. Giménez, S. Contreras, E. Pascual, M. Rodríguez, *Water Res.* 36 (2002) 1034-1042; J.J. Pignatello, E. Oliveros, A. MacKay, *Crit. Rev. Environ. Sci. Technol.*, 36 (2006) 1-84; E. Brillas, I. Sirés, M. Oturan, *Chem. Rev.* 109 (2009) 6570-6631.

[2] a) R.J. Bigda, *Chem. Eng. Prog.* 1995, 62-66; b) R. Alnaizy, A. Akgerman, *Adv. Environ. Res.* 4 (2000) 233-244; c) J.A. Zazo, J.A. Casas, A.F. Mohedano, M.A. Gilarranz, J.J. Rodriguez, *Environ. Sci. Technol.* 39 (2005) 9295-9302; d) A. Santos, P. Yustos, S. Rodriguez, E. Simon, F. Garcia-Ochoa, *J. Hazard. Mater.* 146 (2007) 595-601.

[3] M.S. Yalfani, S. Contreras, F. Medina, J. Sueiras, *Appl. Catal. B: Environ.* 89 (2009) 519-526.

[4] M.G. Clerici, P. Ingallina, *Catal. Today* 41 (1998) 351-364; R. Meiers, U. Dingerdissen, W.F. Hölderich, *J. Catal.* 176 (1998) 376-386; J.R. Monnier, *Appl. Catal. A: Gen.* 221 (2001) 73-91; S. Niwa, M. Eswaramoorthy, J. Nair, A. Raj, N. Itoh, H. Shoji, T. Namba, F. Mizukami, *Science* 295 (2002) 105-107; J.M. Campos-Martín, G. Blanco-Brieva, J.L.G. Fierro, *Angew. Chem. Int. Ed*. 45 (2006) 6962-6984; J.J. Bravo-Suárez, K.K. Bando, T. Akita, T. Fujitani, T.J. Fuhrer, S.T. Oyama, *Chem. Commun.* (2008) 3272-3274.

[5] M.S. Yalfani, S. Contreras, F. Medina, J. Sueiras, *Chem. Commun.* (2008) 3885-3887.

[6] E.M. Cordi, J.L. Falconer, *J. Catal.*, 162 (1996) 104-117.

[7] F. Pinna, F. Menegazzo, M. Signoretto, P. Canton, G. Fagherazzi, N. Pernicone, *Appl. Catal. A: Gen.* 219 (2001) 195-200.

[8] F.J. Berry, L.E. Smart, P.S. Sai Prasad, N. Lingaiah, P. Kanta Rao, *Appl. Catal. A: Gen.* 204 (2000) 191-201.

[9] T.B. Flanagan, W.A. Oates, *Annu, Rev. Mater. Res.* 21 (1991) 269-304.

[10] H. Lieske, J. Völter, *J. Phys. Chem.* 89 (1985) 1841-1842.

[9] F. Pinna, M. Selva, M. Signoretto, G. Strukul, F. Boccuzzi, A. Benedetti, P. Canton, G. Fagherazzi, *J. Catal.* 150 (1994) 356-367.

[10] G. Leitz, M. Nimz, J. Völter, K. Lázár, L. Guczi, *Appl. Catal.* 45 (1988) 71-83.

[11] A.P. Grosvenor, B.A. Kobe, M.C. Biesinger, N.S. McIntyre, *Surf. Inteface. Anal.* 36 (2004) 1564-1574.

[12] J. Chen, X.K. Sun, M.C. Yang, J. Xu, W.X. Chen, W.D. Wei, Z.Q. Hu, *Appl. Surf. Sci.* 72 (1993) 267-271.

[13] W.C. Conner, J.L. Folconer, *Chem. Rev.* 95 (1995) 759-788.

[14] S.-S. Lin, M.D. Gurol, *Environ. Sci. Technol.* 32 (1998) 1417-1423.

UNIVERSITAT ROVIRA I VIRGILI
NEW CATALYTIC ADVANCED OXIDATION PROCESSES FOR WASTEWATER TREATMENT
Mohammad Sadegh Yalfani
ISBN:/DL:T.1259-2011

Chapter 5

Chlorophenol degradation using a one-pot reduction-oxidation process

Chlorophenol degradation was achieved using a combination of hydrodechlorination and heterogeneous Fenton-like oxidation. The process was conducted at ambient conditions (25 ± 2°C, atmospheric pressure) as a one-pot reaction involving formic acid as H_2 source for both hydrodechlorination of chlorophenols and H_2O_2 formation. An alumina-supported Pd-Fe catalyst was applied, which is able to decompose formic acid at the Pd sites, forming H_2 and CO_2, and additionally H_2O_2 in the presence of O_2. At the same time, due to presence of iron sites on the catalyst, the H_2O_2 formed can be utilized for a Fenton-like oxidation reaction. Three different reaction protocols were tested, including: (i) consecutive reduction-oxidation with an initial oxygen-free phase adjusted by He purging (CRO-He), (ii) consecutive reduction-oxidation with initially oxygen-limited conditions (CRO) and (iii) simultaneous reduction-oxidation where O_2 flowing was started at the beginning of the reaction (SRO). 2,4-dichlorophenol (DCP) and pentachlorophenol (PCP) were selected as representatives for the group of chlorophenols. For DCP degradation, CRO-He and SRO showed similar efficiencies with respect to the mineralization degree (up to 70%), whereas SRO achieved a better detoxification as observed in bioluminescence tests. The CRO-He reaction over the catalyst used showed only a small decrease in its activity during the oxidation stage, with no further change after the catalyst had been recovered twice. For PCP degradation, a self-inhibition effect was observed for the SRO process, indicating that PCP is hardly degradable by catalytic oxidation. In this case, the CRO-He process, which was facilitated by initial transformation of PCP into phenol and its subsequent oxidation, clearly produced a cleaner medium. This was also confirmed by the results of the toxicity measurements. The catalyst indicated a promising stability based upon the Pd and Fe leaching results measured at the end of each run.

ISBN:/DL:T.1259-2011

1. Introduction

Chlorophenols constitute an important category of organic pollutants. These compounds are introduced into the environment as a result of several human activities such as disinfection, herbicide and pesticide production, and wood preservation [1]. Therefore, there have been many attempts in recent years to find an appropriate way to degrade chlorophenols [2-3]. Conventional methods such as biological treatments, incineration and adsorption may not lead to complete toxicity removal. However, chemical treatment processes including hydrodechlorination (HDC) and wet oxidation have drawn the attention of many researchers because of their ability to degrade these contaminants [2,4].

HDC is, at best, only a detoxification process which, however, does not break down the hydrocarbon structure of the pollutant. The final aqueous solution needs further treatment in order to achieve the complete removal of organic compounds. Phenol is the main product of catalytic HDC of chlorophenols in aqueous solution [5]. However, depending on reaction conditions such as solvent, source of hydrogen, temperature and pressure, the products cyclohexanone, cyclohexanol and even cyclohexane can also be produced [6,7]. Due to the remaining toxicity of phenol, additional treatment is required in order to achieve a complete detoxification. Pd-based catalysts are well known as the most efficient catalysts for HDC, because of their ability to promote C-Cl bond cleavage, to absorb and store hydrogen dissociatively, and their low sensitivity towards chloride poisoning [4,8].

Usually, H_2 is used as reductant in the HDC reaction. However, its application has several disadvantages, such as low solubility in water and strict safety requirements for transportation and handling. Therefore, attempts have been made to replace H_2 by another hydrogen source. A wide band of hydrogen donor compounds have been tested, including borohydride salts [9], hydrazine [10], and alcohols [11]. Some zero-valent metals and bimetallic reductants can

ISBN:/DL:T.1259-2011

also be applied without external supply of H_2 [12,13]. However, the release of the corroded metal into the solution requires an additional treatment. Also, the catalyst in bimetallic systems such as Pd on Fe(0) gradually loses its activity due to corrosion. The application of formic acid has shown very interesting and competitive results with respect to H_2 [14-16]. It is decomposed into H_2 and CO_2 over the Pd catalyst at ambient conditions [17]. In addition, it is safe to handle and is not categorized as a hazardous compound. Although it is more expensive than H_2 on a per reduction equivalent basis, it may be an appropriate replacement for gaseous hydrogen in HDC reactions.

On the other hand, by means of catalytic gas-phase oxidation of chlorophenols using O_2 and V_2O_5/TiO_2 as a catalyst, nearly complete mineralization of chlorophenols can be achieved [18]. However, a phase transfer of the chlorophenols from the water into the gas phase and relatively high temperatures (≥200°C) are required for this process. Wet oxidation using hydrogen peroxide proceeds under milder conditions without any phase transfer [19]. The so-called advanced oxidation processes (AOPs), in which hydroxyl radicals play the role of the oxidant, are well-known [2]. Al Momani et al. have reported that the photo-Fenton reaction in acidic solution showed the best performance for DCP degradation in comparison with other AOPs, e.g. UV radiation, UV/H_2O_2, and Fenton reaction [20]. The Fenton reaction involving H_2O_2 and Fe^{2+} is the oldest AOP. The main drawbacks of this process are the narrow working pH range (3-3.5) and the formation of iron sludge after the final neutralization of the treated water. In order to overcome these shortcomings, the development of heterogeneous Fenton-like processes for application at a wider pH range has received increasing attention [21-23]. In practice, the oxidation of chlorophenols can be associated with the formation of toxic intermediates [24,25]. Adjustment of appropriate process conditions in order to obtain complete detoxification can be more demanding in such a case.

ISBN:/DL:T.1259-2011

In addition, the rate constant of hydroxyl radical attack on chlorophenols decreases with increasing number of chlorine substituents, which means that higher-chlorinated chlorophenols are more resistant to oxidation [26].

Looking at the above-described general characteristics of HDC and catalytic wet oxidation, it becomes obvious that these two reactions can be complementary to each other for the degradation of chlorophenols. In the suggested combined approach, HDC undertakes an essential detoxification while catalytic oxidation carries out destruction of the remaining hydrocarbon structure. In this paper, we demonstrate the combination of HDC (reduction) and a Fenton-like process for the degradation of chlorophenols over a bimetallic Pd-Fe catalyst within a one-pot reaction. The oxidation reaction proceeds with H_2O_2 generated *in situ*, which leads to a higher efficiency compared with bulk feeding in Fenton reactions [27]. Formic acid and O_2 are the only reagents which have to be added. Formic acid links HDC and oxidation by producing H_2 *in situ* for both HDC of the contaminants and H_2O_2 formation [28]. The whole process is carried out under ambient conditions (25 ± 2°C and atmospheric pressure). The catalyst selection was based on the ability of Pd-based catalysts to decompose formic acid and generate H_2O_2. Furthermore, anchoring iron species on the surface of the support is a means to avoid the problem of iron sludge formation which is typical for homogeneous Fenton reactions [29]. DCP and PCP were selected for this investigation as representatives of chlorophenols with low and high numbers of chlorine substituents. The combination of HDC and oxidation was conducted in various ways (CRO-He, CRO, SRO), favouring either the consecutive or the simultaneous occurrence of the two reaction types. In order to do so, the availability of oxygen for H_2O_2 formation was adjusted, either by removal of oxygen or by active oxygen flowing starting at different time points during the reaction. The efficiency of the new system was evaluated by measuring chlorophenol

ISBN:/DL:T.1259-2011

removal, mineralization degree and toxicities of the treated solutions to the luminescent bacteria *Vibrio fischeri*.

2. Experimental

2.1. Catalyst preparation

All the materials were purchased from Merck (Darmstadt, Germany). The alumina-supported Fe-Pd catalyst (denoted as $FePdAl_2O_3$) was synthesized via conventional wet impregnation. First, γ- Al_2O_3 was impregnated by an aqueous solution containing a certain amount of $Fe(NO_3)_3{\cdot}9H_2O$, followed by solvent evaporation and drying in a rotary evaporator. Then, the solid was calcined at 400°C in air for 3 h. Afterwards, the calcined solid was impregnated with Pd, using an acidified aqueous $PdCl_2$ solution. The same pre-treatment was performed as for iron impregnation. Finally, the solid was reduced by H_2 at 200°C for 2 h. The metal contents applied for Pd and Fe on the alumina support were 5 and 1 wt%, respectively. For the catalyst activity tests, only the $FePdAl_2O_3$ catalyst obtained after the final reduction step was applied, but for the calcined catalyst (i.e. a sample without reduction) several characterization methods were also applied.

2.2. Catalyst characterization

The synthesized solid was characterized by means of X-ray diffraction (XRD), temperature-programmed reduction (TPR) and UV-vis spectroscopy in the diffuse reflectance mode (UV-vis DRS). XRD analyses of the calcined and reduced samples were acquired using a Siemens D5000 diffractometer with nickel-filtered Cu Kα radiation. The patterns were recorded over a range of 2θ angles from 5° to 70°.

TPR was performed in a ThermoFinnigan (TPORD 110) apparatus equipped with a thermal conductivity detector (TCD). The sample was purged with an argon flow before the analysis. The analysis was carried out using a 3% H_2/Ar

ISBN:/DL:T.1259-2011

gas at a flow rate of 20 mL/min, heating from 25 to 900°C with a ramp of 10 °C/min. Water produced during TPR was trapped in CaO + Na_2O (Soda lime) in order to prevent it from reaching the TCD.

UV-vis DRS spectra of the calcined and the reduced samples were acquired using a Varian Cary 3 spectrophotometer equipped with a diffuse reflectance accessory.

2.3. Catalyst activity tests

Catalytic reactions were performed in a 250 mL three-necked batch reactor. In all cases, the catalyst (1g/L) was initially suspended in 100 mL of a solution of the chlorophenol under study in deionized water (DCP: C_0 = 306 μM or PCP: C_0 = 27 μM).

To perform CRO-He, this suspension was initially purged with He for 10 minutes. The system was then closed, avoiding exposition to the atmosphere, and formic acid (C_0 = 20 mM) was injected in order to start the HDC reaction. After 5 minutes, the system was opened to the ambient atmosphere and pure oxygen was passed through the solution with a flow rate of 20 mL/min, starting the oxidation stage.

In the case of CRO, the reaction was started by adding formic acid without initial purging by He. During the first 30 min, the system was stirred and open to the ambient atmosphere. After that, pure oxygen was passed through the suspension with a flow rate of 20 mL/min.

For the SRO protocol, at zero time, formic acid was injected into the suspension containing chlorophenol and the catalyst, and O_2 flowing with a rate of 20 mL/min was maintained during the whole reaction time.

The reactions were carried out under ambient conditions (25 ± 2°C and atmospheric pressure). Sampling was performed at regular time intervals. The chlorophenol conversion was monitored by means of high-performance liquid chromatography (HPLC - Hewlett Packard Series 1100) using a diode array

ISBN:/DL:T.1259-2011

detector and an Adsorbosphere XL C18 5U 250 × 4.6 mm column. The eluent for quantifying phenol, DCP and PCP consisted of a mixture of Milli-Q H_2O (adjusted to pH = 4 by phosphoric acid) and acetonitrile with proportions in the range of 60/40 to 20/80. The samples were also analyzed qualitatively by GC/MS (Shimadzu GC/MS-QP 2010) equipped with a HP5 MS (30 m × 0.25 µm × 0.32 mm) column. In order to allow GC/MS analysis of polar intermediates (such as dihydroxylated benzenes) a derivatization procedure using ethyl chloroformate as described by Husek and Simek was applied [30]. This method converts phenols into their corresponding ethyl phenyl carbonates, which are amenable to GC/MS analysis. Formic acid and chloride ion concentrations were obtained by means of an ion chromatograph (Dionex IC 25A, type DX 320) equipped with an Ion PAC AS15 column and an Ion PAC AG15 pre-column using 50 mM KOH as mobile phase. Total organic carbon (TOC) was measured with a Shimadzu 5050 TOC analyzer.

2.4. Lumistox luminescent bacteria toxicity test

The luminescent bacteria assay was performed following the ISO 11348-2 guideline (ISO Guideline, 1998) with the Dr. Lange Lumistox® system (Hach-Lange, Berlin, Germany) and the *Vibrio fischeri* bacterial strain NRRL-B-11177. The samples were amended with 2 % NaCl via 1:2 dilution with 4 % NaCl solution, resulting in a maximal sample concentration of 50 %, and the pH was adjusted to pH 7.0 ± 0.2 if necessary. Due to a test-inherent dilution step with the bacteria, the maximal sample concentration was 50 %. The bacteria were exposed to the samples for 30 min, the luminescence was recorded, and the inhibition of luminescence in comparison to the respective 2 % NaCl- controls was used as the effect endpoint. NaCl (7.5% w/v) and $ZnSO_4x\ 7H_2O$ (19.7 mg/L) served as positive controls. Each data-point in the figures gives the mean of two technical replicate measurements. The data were further analysed, following

the above ISO guideline, and were fitted using logistic curve fitting models (Origin software, version 8.5).

3. Results and discussion

3.1. Catalyst characterization

XRD patterns of the calcined and the reduced $FePdAl_2O_3$ show clearly the diffractions related to γ-alumina. The peaks attributed to metallic Pd in the reduced sample and iron oxide (Fe_2O_3), in both the calcined and the reduced samples, were influenced by the signals of the alumina support and thus can be sorely identified.

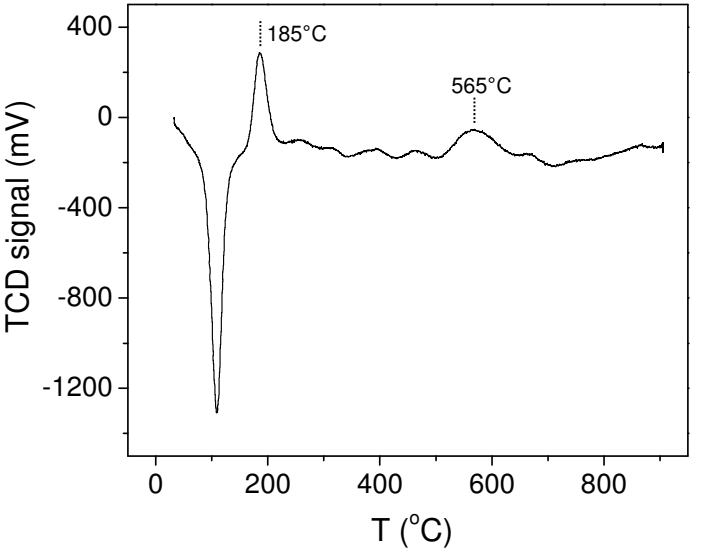

Figure 1. TPR thermogram of calcined $FePdAl_2O_3$ sample.

The TPR thermogram of the calcined $FePdAl_2O_3$ sample in Figure 1 shows a large desorption peak related to PdβH. The existence of this peak indicates that most of the Pd was reduced at ambient temperature without leaving any signal on the TPR profile [31,32]. The smaller positive peak around 185°C can be

attributed to the reduction of Fe species, which might also have been accompanied by the reduction of a small proportion of the Pd. As has already been reported, in the presence of Pd, reduction of Fe can shift to lower temperatures [33]. Co-reduction of Pd and Fe at 185°C may be due to the Pd-Fe interaction on the support, leading to the formation of a Pd-Fe alloy [33,34]. The rest of the Fe, which has no interaction with the Pd, is reduced at higher temperature, displaying a maximum H_2 consumption at 565°C.

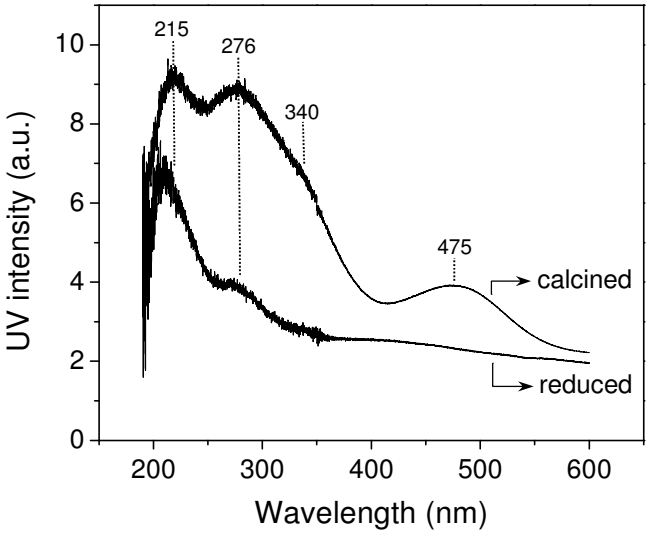

Figure 2. UV-vis spectra of calcined and reduced $FePdAl_2O_3$ sample.

The UV-vis DRS spectra shown in Figure 2 for the calcined sample are in accordance with the presence of Fe(III) and PdO species. The absorption band around 475 nm is assigned to the d-d transition of PdO [35,36]. This indicative peak of PdO disappeared in the spectra of the reduced sample. The absorption peaks appearing at wavelengths within the range of 200 to 300 nm could be attributed to isolated Fe(III) ions or Pd-O charge transfer [37,36]. Another absorption, appearing as a shoulder at 340 nm, can be assigned to small

ISBN:/DL:T.1259-2011

oligomeric clusters of Fe(III) oxide [37]. After reduction, the relative intensity of the sub-bands with maxima at about 280 nm and 340 nm decreases, which may be due to the reduction of PdO and/or the partial reduction of Fe(III) species affected by the proximity to Pd [38]. The lack of absorption at wavelengths higher than 400 nm implies the absence of large Fe_2O_3 particles, at least for the reduced sample [39]. A general view of the absorption peaks of Fe(III) in the reduced sample resembles the reference spectra of γ-Fe_2O_3 [37].

The above characterization results indicate that the active sites of the catalyst contain mostly metallic Pd and Fe_2O_3. There is little merging of Pd and Fe species to form a Pd-Fe alloy. Nevertheless, a small but plausible interaction between Pd and Fe is observed, which causes the reduction of part of the Fe_2O_3 to be shifted to lower temperatures.

3.2. Degradation of 2,4-dichlorophenol

Degradation of DCP was carried out using three different protocols involving HDC and heterogeneous Fenton-like oxidation. In the CRO-He reaction, the reaction suspension was initially free of dissolved O_2 due to the He purging, so that no oxidation reaction was possible. The profile of this reaction, shown in Figure 3-A, indicates that the dechlorination of DCP using formic acid is complete within less than 5 minutes. Complete dechlorination of DCP is accompanied by the release of the corresponding total molar amount of chloride and 95% of the stoichiometric amount of phenol as reduction products. Cyclohexanone was found at low concentration; this can close the mass balance for the reduction stage. Prolongation of the HDC process can give rise to further formation of cyclohexanone and cyclohexanol, which are less readily oxidizable than phenol [40]. Fast HDC reactions of chlorinated aromatic compounds over Pd catalysts with formic acid as H-source are known from previous studies [14,16]. The presence of chlorophenol, as consumer of the

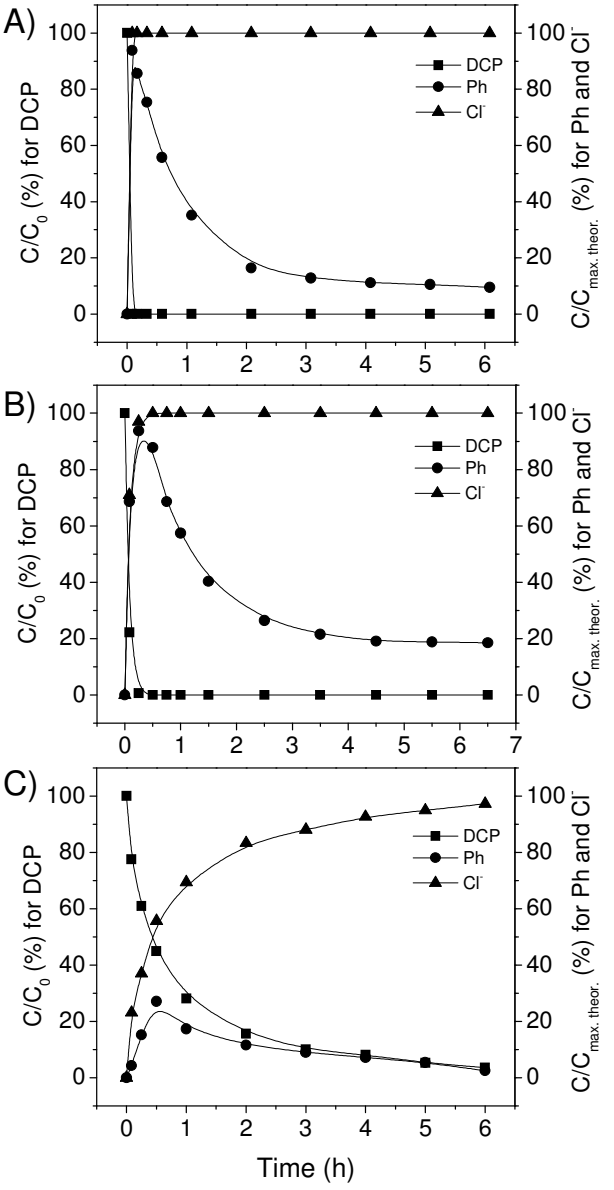

Figure 3. DCP degradation via three protocols. A: CRO-He, B: CRO, C: SRO ($C_{0,DCP}$ = 306 μM, C_{cat} = 1 g/L, $C_{0,FA}$ = 20 mM, V_{O2} = 20 mL/min). Concentrations of phenol (Ph) and chloride were normalized to the maximum theoretical concentrations according to the reaction stoichiometry (C/C_{max}).

hydrogen produced, can promote the decomposition of formic acid [14]. In addition, it has been found that both conversion of chlorophenols and formic acid decomposition are accelerated with increasing Pd content of the catalysts [41,28]. Therefore, the fast disappearance of DCP in the presence of a high HCOOH/DCP molar ratio (66) and a catalyst with a high Pd loading (5 wt%) is not unexpected.

The oxidation stage starts when activated hydrogen produced by the decomposition of formic acid reacts with O_2 over the Pd to form hydrogen peroxide. The H_2O_2 produced is then consumed *in situ* for the oxidation through Fenton-like reactions on the iron oxide species. After 6 h of reaction, the degradation of phenol reached 90%. At the same time, a total mineralization degree of 70% (TOC) was achieved. Benzoquinone was detected as a side-product during the oxidation reaction but disappeared within the 6 h of reaction time. Nearly 95% of the formic acid was decomposed within a reaction period of 2 h, which corresponds to the total dechlorination of DCP and a conversion degree of more than 80% for the phenol intermediate. The rest of the formic acid was decomposed at a slower rate until the reaction was stopped after 6 h. The initial concentration of formic acid was set at 20 mM, a value with which we obtained the most appropriate results. Our previous experiments had shown that starting the reaction with higher concentrations of formic acid gave rise to a decrease in the phenol degradation rate [27]. Formic acid competes with phenol in the reaction with OH radicals since their rate constants are similar [42,43]. Nevertheless, as can be seen from the profile (Figure 3-A), after 2 h, in the presence of low concentrations of formic acid, the degradation of phenol is almost suppressed. Therefore, in order to reach even higher conversion degrees for phenol, further sequential additions of formic acid are required.

ISBN:/DL:T.1259-2011

In the second protocol (CRO), the reaction was started by adding formic acid to the system containing the catalyst and DCP in deionized water, which was in equilibrium with ambient air and thus had a dissolved oxygen concentration of about 9 mg/L. During the first 5 minutes of CRO-He, H_2 produced by formic acid decomposition was exclusively used for HDC, but in CRO it could also react with dissolved O_2. As shown in Figure 3-B, dissolved O_2 has a negative influence on the HDC rate of DCP. The maximum concentrations of phenol and chloride are reached after 30 min, compared to less than 5 min in CRO-He. After 30 minutes, oxygen was passed through the solution, oxidizing the generated phenol. After 6 h of oxygen flowing, 80% phenol degradation along with 62% carbon mineralization was achieved. As stated above, in this protocol the O_2 flowing, which is necessary for an efficient utilization of formic acid for the oxidation stage, is started with 30 minutes' delay. Therefore, some of the formic acid was lost before its usage for H_2O_2 formation, resulting in a decrease of the total mineralization degree observed after 6 h oxidation reaction in comparison to CRO-He.

In the SRO reaction, formic acid was added to the solution after the oxygen flowing had been started in order to allow a simultaneous reduction-oxidation process. Formic acid plays the role of a H_2 source for both HDC and *in situ* H_2O_2 generation. As is shown in Figure 3-C, phenol as a main product reaches a maximum of 28% of the maximum possible concentration after 30 minutes, while at the same time DCP conversion was 55%. According to the literature, phenol is not usually detected among the main intermediates of the DCP oxidation by Fenton or photo-assisted Fenton reactions [44-45]. Therefore, the phenol produced can be attributed to the HDC reaction. In addition, a trace amount of cyclohexanone was detected, which again proves the occurrence of HDC. Obviously, reduction and oxidation reactions proceed simultaneously under these conditions.

ISBN:/DL:T.1259-2011

Two reactions compete for the hydrogen produced by formic acid decomposition: the reduction of DCP, forming phenol and HCl (ΔG_{298K} -120.3 kJ/mol), and the reduction of O_2, generating H_2O_2 (ΔG_{298K} -105.6 kJ/mol) [46,47]. Both reactions are thermodynamically favorable. The competition for hydrogen is regulated by the relative rate constants of the above-mentioned reactions and the available concentrations of the two oxidants, i.e. the competition is kinetically controlled. DCP may be subjected to HDC on Pd sites and oxidation at the same time, whereby the oxidation mechanism is still a matter of speculation. The active oxidants may be either radicals such as the hydroxyl radical formed over the iron sites, or highly oxidized species such as ferryl Fe^{4+}. Fast evolution of phenol within the first hour of reaction gives evidence of HDC, whereas dichlorobenzenediols detected in significant concentrations prove the direct oxidation of DCP in Fenton-like reactions [25,45]. In addition, monochlorinated and chlorine-free benzenediols were detected as well. Obviously, reduction and oxidation of DCP and its intermediates are in close competition under the conditions of the SRO protocol. Apparently, transition of chemisorbed H_2O_2 from the Pd surface to the catalytically active iron sites is an important step. Both reduction and oxidation reactions become slower at the end of the reaction period due to the decreasing formic acid concentration.

The clear difference between the former two protocols (CRO-He and CRO) and SRO is the lack of complete DCP dechlorination for the latter. This lack, however, opens pathways for the formation of chlorinated, partially oxidized intermediates with unknown toxicity potentials. The efficiency of DCP degradation by the three reduction-oxidation protocols was evaluated using TOC analysis data at the end of each run. The results, shown as a column chart in Figure 4, indicate that considerable mineralization degrees can be achieved

ISBN:/DL:T.1259-2011

using any of the tested procedures, comparable with the results in the literature [20,44].

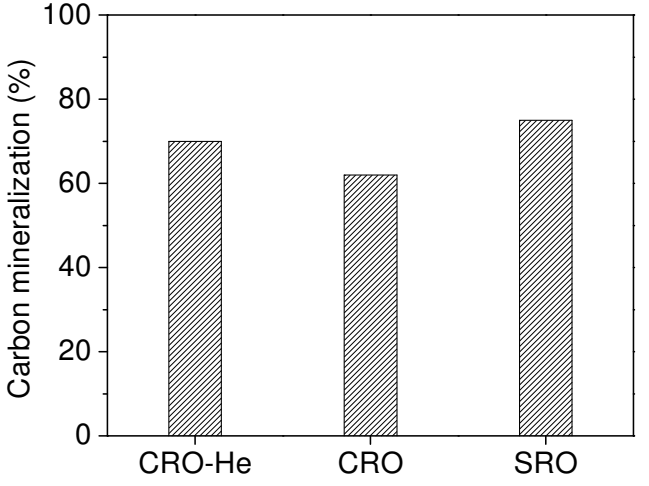

Figure 4. Carbon mineralization degree (%) obtained in DCP degradation using three different protocols, as determined from reduction in TOC after 6 h of reaction.

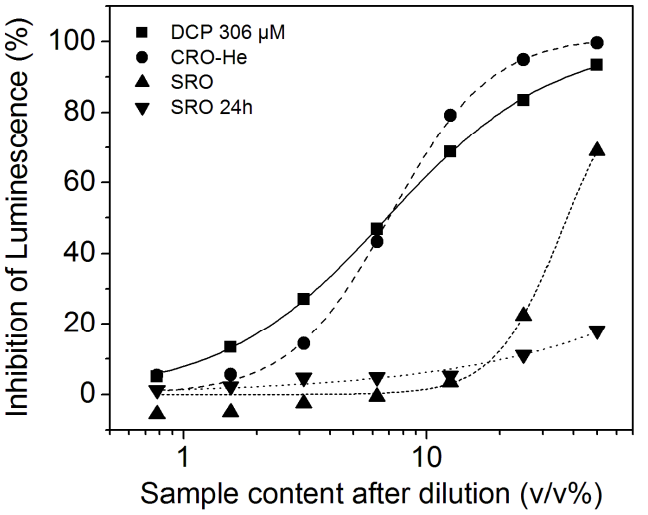

Figure 5. Toxicity measurements of the original DCP solution (306 µM) and final solutions of DCP treatment using CRO-He and SRO protocols ($C_{0,DCP}$ = 306 µM).

ISBN:/DL:T.1259-2011

As a second measure for evaluating the performance, the toxicity of the final solutions of the CRO-He and SRO protocols for *Vibrio fischeri* was studied by measuring the percentage inhibition of bioluminescence compared to that of the original DCP (306 μM) solution. The results graphed in Figure 5 show that, for the CRO-He reaction after 6 h, the toxicity of the solution was still similar to that of the original DCP solution, whereas for the SRO with the same amount of formic acid added and the same reaction time, the toxicity of the solution was drastically lower. In the latter reaction, more formic acid was available for the oxidation reaction. Obviously, in the case of CRO-He, toxic chlorine-free intermediates are still present after 6 h of reaction. The remaining toxicity of the CRO-He sample may be due to non-degraded 1,4-benzoquinones in low concentrations (~0.5 mg/L) which are produced during the oxidation of phenol. 1.4-Benzoquinones have shown a very high toxicity relative to phenol and even chlorophenols [48]. EC_{50} (defined as the effective nominal concentration of toxicant that reduces the intensity of light emission by 50% in the applied test) is measured for DCP as 3.5 mg/L. The EC_{50} for 1,4-benzoquinone is around 70 and 630 times lower than those of DCP and phenol, respectively [49]. In the case of SRO, the final solution showed low toxicity, especially at a sample concentration below 12 %. Further treatment (addition of 10 mM formic acid along with prolonging the reaction time up to 24 h) yielded a further decrease in toxicity of the final solution, as can be seen in Figure 5. It is worthy of note that 1,4-benzoquinone may not be produced easily during the oxidation of DCP, owing to its chlorinated para-position [44]. In the SRO protocol, phenol as precursor of 1,4-benzoquinones does not reach such high concentrations as in the CRO-He protocol. Nevertheless, 1,4-benzoquinones are labile intermediates and their occurrence in the treated water can be avoided by long enough treatment times.

ISBN:/DL:T.1259-2011

During the experiments described above, the pH of the solution had an increasing trend from 2.7, measured after the addition of formic acid, to 3.6 at the end of the reaction. The original pH of the solution containing DCP and the catalyst was 4.6, which indicates an acidic character of the catalyst. An aqueous solution of 306 μM DCP has a pH of 5.5. There are many reports on HDC of chlorophenols which recommend using a basic pH, adjusted by addition of a hydroxide or an amine, to scavenge the protons released during HDC by H_2 and to avoid catalyst poisoning by chloride [5,50-52]. The increased dissociation of chlorophenols in alkaline solution is supposed to positively influence the competitive binding of phenolate vs. chloride to the catalyst. However, it has been shown for HDC of chlorobenzene with formic acid over Pd/Al_2O_3 that this process is rather resistant to chloride poisoning: low concentrations of Cl^- ($\leq$ 20 mg/L) are completely tolerated, and even at high concentrations (500 mg/L) only a minor inhibition effect is observed [14]. In our study, the concentration of the released Cl^- did not exceed 30 mg/L (resulting from chlorophenols degradation and release of a few ppm Cl^- from the $FePdAl_2O_3$ catalyst which remained from the $PdCl_4^{-2}$ precursor). Furthermore, decomposition into H_2 and CO_2, which is a key step for the intended reduction-oxidation process, is considerably faster for formic acid than for formate [14].

The stability of the catalyst was studied by performing the CRO-He reaction in a second run with the previously used catalyst. For this purpose, after a 6 h reaction period, the used catalyst was recovered by centrifugation and dried at 100°C. The results of the reactions with the used catalyst are shown in Figure 6 and compared with the fresh one. Like the fresh one, the used catalyst could also dechlorinate DCP in less than 5 minutes. Oxidation of phenol by the used catalyst proceeded at a slightly lower rate and consequently lowered mineralization degree. A significant activity loss was only observed for the fresh catalyst. After the first recovery, all succeeding recycling runs (up to two)

did not affect the catalyst activity. These findings are in conformity with the hypothesis that a small and labile fraction of the catalyst is lost or inactivated during the first run. In subsequent usage, the catalyst maintains a constant activity. Most importantly, no detectable leaching of Pd was observed during the reactions, as was to be expected considering the known stability of Pd in the pH range studied [27]. The sum of detectable concentrations of dissolved iron in all reactions did not exceed 2% of the total iron on the catalyst, which is acceptable.

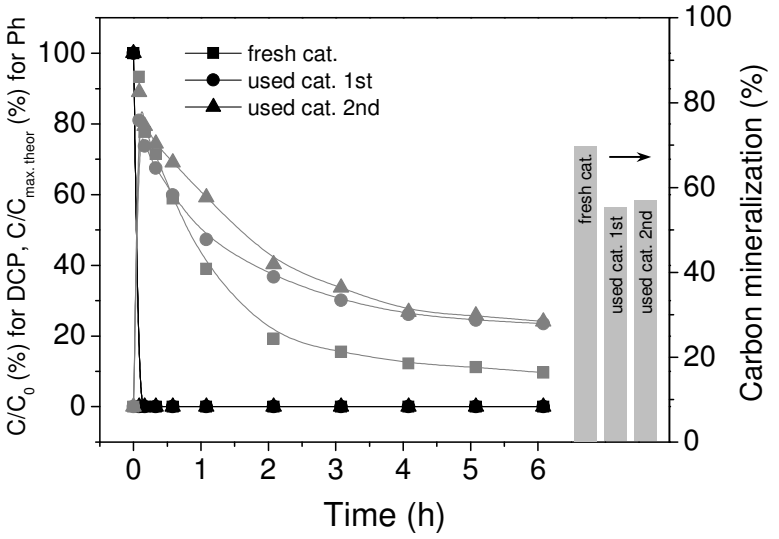

Figure 6. Concentration profiles of the CRO-He reactions using fresh and used catalysts. Concentration of phenol (Ph, grey symbols) normalized to the maximum theoretical concentration according to the reaction stoichiometry (C/C_{max}), and relative concentration of DCP (black symbols).

The selection of the $FePdAl_2O_3$ catalyst was based on the recent results obtained for a series of Pd-Fe samples prepared via co- and consecutive impregnation [53]. Characterization of these samples demonstrated that the one prepared via co-impregnation contained the highest amount of Pd-Fe alloy, whereas the sample prepared via consecutive impregnation (first Fe and then

ISBN:/DL:T.1259-2011

Pd) had the lowest content of alloy. The experiments of Fenton-like reactions using H_2O_2 generated *in situ* with these catalysts proved that the alloy formation does not favor the desired reaction pathway. Therefore, the $FePdAl_2O_3$ catalyst with the lowest tendency to alloy formation was found to be the most appropriate. In contrast to the bimetallic Pd-Fe system already used in HDC [12-13], the current Pd-Fe system behaves differently. Here, Pd and Fe species operate individually without any interference in their functions. Formic acid decomposition and H_2O_2 formation occur over Pd. H_2O_2 decomposition into hydroxyl radicals and subsequent oxidation of organic compounds most probably occur over the Fe species. A spillover effect might link these two catalytic systems in order to transfer Pd-chemisorbed H_2O_2 onto the Fe species [53,54].

3.3. Degradation of pentachlorophenol

PCP has proved to be the most difficult chlorophenol to degrade, with regard to both bio- and chemical degradation. Homogeneous systems containing H_2O_2 and metal complexes (iron or manganese) with tetraamidomacrocyclic ligands or phthalocyanines have shown interesting ability for destruction of PCP [55-56]. Although the conventional Fenton reaction is able to oxidize PCP, the achieved mineralization degree is usually unsatisfactory [57]. The heterogeneous system involving magnetite and H_2O_2 (0.8 M) at neutral pH has also shown interesting performance, with complete mineralization of 50 mg/L PCP during a long-term treatment lasting 7 days [58]. In our study, the PCP degradation was carried out using a 26 μM aqueous solution, taking into account the low solubility of undissociated PCP in water (14 mg/L at 20°C [1]). The same three protocols performed for the degradation of DCP were also used for the degradation of PCP. In the case of CRO-He (Figure 7-A), the same behavior as for DCP was observed, i.e. fast disappearance of PCP in less than 5 minutes. At the same time, the corresponding molar amount of Cl^- appeared,

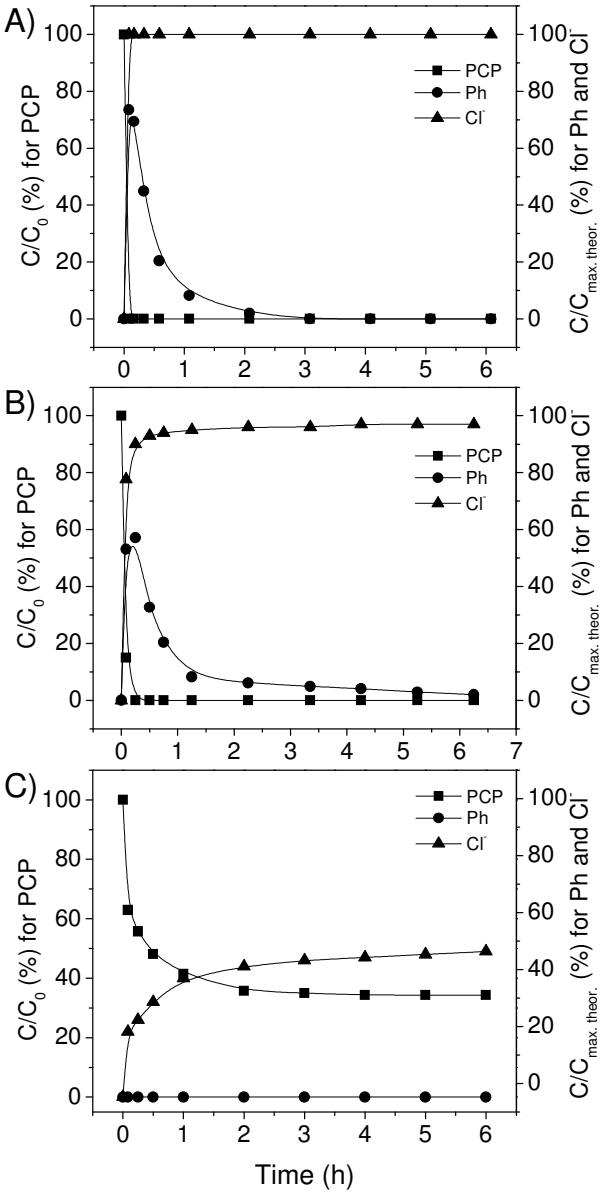

Figure 7. PCP degradation via three protocols. A: CRO-He, B: CRO, C: SRO ($C_{0,PCP}$ = 26 μM, C_{cat} = 1 g/L, $C_{0,FA}$ = 20 mM, O_2 = 20 mL/min). Concentrations of phenol (Ph) and chloride were normalized to the maximum theoretical concentrations according to the reaction stoichiometry (C/C_{max}).

ISBN:/DL:T.1259-2011

which indicates entire dechlorination of PCP. The phenol concentration reached a maximum of 78% of the initial molar PCP concentration. Cyclohexanone was detected as the only side product after 5 minutes. After starting the oxidation stage, degradation of phenol proceeded rapidly, resulting in total destruction of phenol within 3 h. No toxic intermediates, such as 1,4-benzoquinones, were found at the end of the run (6 h).

For the CRO reaction (Figure 7-B), PCP disappeared more slowly than in the CRO-He owing to the interference of the dissolved O_2 in water, as was already observed in the case of DCP. Nevertheless, PCP is completely degraded in less than 20 minutes and the Cl^- concentration detected at the same time is very close to the corresponding total molar content. Furthermore, no other chlorinated organic compounds were detected by GC/MS. The maximum concentration of the phenol produced is 58% of the initial molar PCP concentration. Cyclohexanone was identified as a second by-product of HDC, while no cyclohexanol was detected. In the oxidation stage, phenol degradation started at a significant rate, but diminished clearly after 1 h due to consumption of the bulk formic acid. More than 95% of the formic acid was decomposed within less than 4 h.

In the SRO (Figure 7-C), a fast PCP degradation of up to 65% occurred within the first two hours of the reaction, but afterwards PCP was no longer decomposed. Even by the addition of excess formic acid after three hours, the reaction could not be re-initiated. It seems that the Pd catalyst becomes inactive when catalyzing a fast oxidation of PCP. Zimbron et al. observed that, in the presence of H_2O_2 and Fe^{3+} as catalyst, the H_2O_2 degradation continued after 3 h without significant degradation of PCP, while PCP degradation was possible if Fe^{2+} was used [26]. Commercial H_2O_2 (20 mM) was applied as oxidant (instead of formic acid and oxygen) in order to degrade PCP in the presence of the Fe-Pd catalyst at a pH of 3. In agreement with Zimbron et al., we

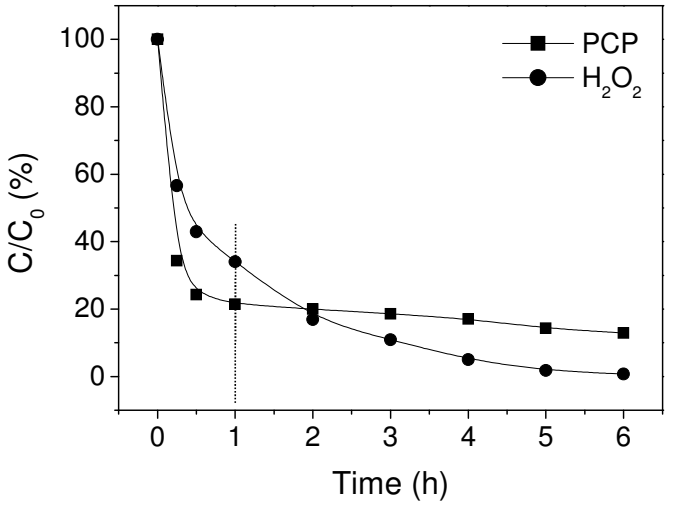

Figure 8. Profiles of PCP and H_2O_2 degradation in the presence of the $FePdAl_2O_3$ catalyst at pH = 3-3.5 ($C_{0,PCP}$ = 26 µM, C_{cat} = 1 g/L, $C_{0,H2O2}$ = 20 mM).

observed inhibition of further PCP degradation after an initial fast reaction period, leading to about 78% PCP conversion within 1 h, while H_2O_2 degradation continued up to 6 h (Figure 8). A possible hypothesis to explain this behavior is the formation of a complex between Fe(III) and a degradation product of PCP which inhibits the Fe(III)/Fe(II) recycling, which in turn is the crucial step in the catalytic Fenton process. As has been characterized, Fe(III) species are in the majority with respect to the other Fe species on the Pd-Fe catalyst. Oxidation of PCP could also start over the minor Fe(0) and Fe(II) species, which are rapidly oxidized to Fe(III), leading to the suppression of the PCP oxidation. Surprisingly, neither phenol nor partially dechlorinated chlorophenols were detected as intermediates of the HDC reaction during the whole reaction period in the SRO protocol. This means that oxidation dominates over HDC during SRO. After a reaction time of 2 h, tetrachlorohydroquinone (THQ) was detected, which had already been

identified as one of the by-products of PCP degradation via the Fenton reaction [57]. THQ disappeared before the end of the run at 6 h. Like the DCP degradation experiments, the pH showed an increasing trend, starting from 2.7 up to around 4.5 at the end of the runs. No metal (Pd or Fe) leaching was detected at the end of each run, proving the remarkable leaching stability of the catalyst.

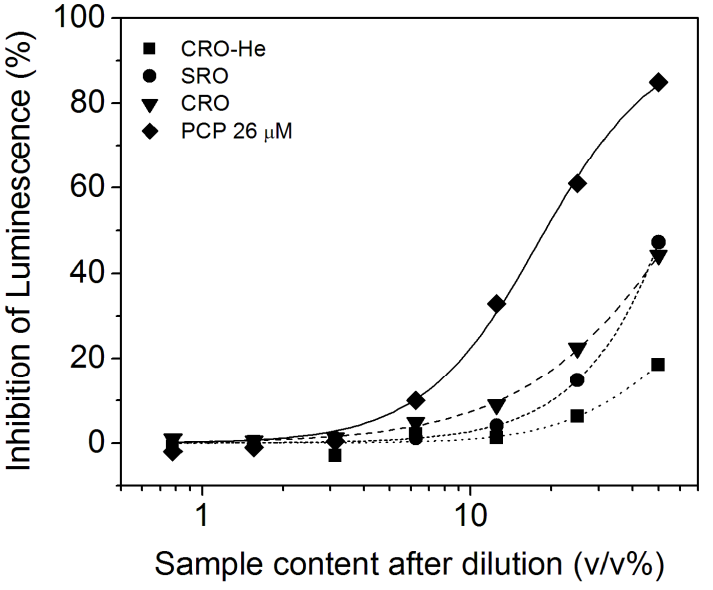

Figure 9. Toxicity measurements of original PCP solution (26 μM) and final solutions from PCP treatment using CRO-He, CRO and SRO protocols ($C_{0,PCP}$ = 26 μM).

TOC analyses showed a decrease in TOC concentrations for all treated solutions of PCP. However, owing to the more than 10% error of TOC analyses for low carbon concentrations (e.g. 2.7 mg/L for the 26 μM PCP solution), these results were not sufficiently reliable to allow a quantitative comparison of the carbon mineralization performance of the three protocols. Therefore, the efficiency of the reactions was only evaluated on the basis of the toxicity measurements for the final solutions. The results graphed in Figure 9 clearly show that the lowest toxicity was achieved by the reaction performed via CRO-

He. The reasons for this are that firstly, the initial HDC step is of advantage since it totally converts PCP (EC_{50} of PCP is 1.4 mg/L) into phenol – a compound with much lower toxicity (EC_{50} 21.1-42 mg/L [49]). Secondly, no significant concentrations of toxic intermediates of phenol oxidation are remaining after a reaction time of 6 h.

4. Conclusions

Chlorophenol degradation was achieved successfully using a combination of HDC (reduction) and heterogeneous Fenton-like (oxidation) reactions involving catalytic *in situ* generation of H_2 and H_2O_2. Formic acid and oxygen are the only reactants which must be added and formic acid was found to be an appropriate source of H_2 for both HDC and H_2O_2 generation. The availability of O_2 is essential for the production of H_2O_2 from formic acid and thus for the oxidation reactions. On the other hand, the occurrence of reductive HDC is favoured under oxygen-free conditions; however, it is also possible in the presence of O_2, i.e. in the CRO and SRO protocols. Which reaction pathway dominates will depend on the reactivity of the substrate for the individual processes. During SRO, reduction and oxidation of DCP occur simultaneously, whereas PCP is only degraded via the oxidation pathway.

For DCP degradation, CRO-He and SRO showed similar efficiencies regarding to the mineralization degrees, while SRO produced superior toxicity reduction results. For PCP degradation, the CRO-He process produced a significantly cleaner medium at the end of the reaction. Conversion of PCP to phenol via HDC followed by catalytic oxidation is preferable to direct oxidation of PCP by catalytic Fenton-like processes, due to the observed self-inhibition effect in the latter reaction. In general, the combination of HDC and AOPs results in a promising performance for the removal of chlorophenols, as well as showing remarkable mineralization and toxicity reduction.

Acknowledgement

Spanish Ministry of Science and Innovation (MICINN) is acknowledged for the funding given through project CTM2008-02453. Marion Hoyer is acknowledged for helpful technical assistance. Iris Christmann & Eberhard Küster, Dept. of Bioanalytical Ecotoxicology, UFZ, are acknowledged for performing the toxicity tests with *V. fischeri*.

References

[1] M. Czaplicka, *Sci. Total Environ.* 322 (2004) 21-39.

[2] M. Pera-Titus, V. García-Molina, M.A. Baños, J. Giménez, S. Esplugas, *Appl. Catal. B: Environ.* 47 (2004) 219-256.

[3] M.A. Keane, *J. Chem. Technol. Biotechnol.* 80 (2005) 1211-1222.

[4] F. Alonso, I.P. Beletskaya, M. Yus, *Chem. Rev.* 102 (2002) 4009-4091.

[5] J.B. Hoke, G.A. Gramiccioni, E.N. Balko, *Appl. Catal. B: Environ.* 1 (1992) 285-296.

[6] H.M. Roy, C.M. Wai, T. Yuan, J.-K. Kim, W.D. Marshall, *Appl. Catal. A: Gen.* 271 (2004) 137-143.

[7] T.T. Bovkun, Y. Sasson, J. Blum, *J. Mol. Catal. A: Chem.* 242 (2005) 68-73.

[8] F.J. Urbano, J.M. Marinas, *J. Mol. Catal. A: Chem.* 173 (2001) 329-345.

[9] Y. Liu, J. Schwartz, C.L. Cavallaro, *Environ. Sci. Technol.* 29 (1995) 836-840.

[10] P.P. Cellier, J.-F. Spindler, M. Taillefer, H.-J. Cristau, *Tetrahedron Lett.* 44 (2003) 7191-7195.

[11] Y. Ukisu, *Appl. Catal. A: Gen.* 349 (2008) 229-232.

[12] J. Wei, X. Xu, Y. Liu, D. Wang, *Water Res.* 40 (2006) 348-354.

[13] B.-W. Zhu, T.-T. Lim, *Environ. Sci. Technol.* 41 (2007) 7523-7529.

[14] F.-D. Kopinke, K. Mackenzie, R. Koehler, A. Georgi, *Appl. Catal. A: Gen.* 271 (2004) 119-128.

[15] C.B. Molina, L. Calvo, M.A. Gilarranz, J.A. Casas, J.J. Rodriguez, *Appl. Clay Sci.* 45 (2009) 206-212.

[16] S. Wang, B. Yang, T. Zhang, G. Yu, S. Deng, J. Huang, *Ind. Eng. Chem. Res.* 49 (2010) 4561-5465.

[17] E.M. Cordi, J.L. Falconer, *J. Catal.* 162 (1996) 104-117.

[18] C.E. Hetrick, J. Lichtenberger, M.D. Amiridis, *Appl. Catal. B: Environ.* 77 (2008) 255-263.

[19] H.-H. Huang, M.-C. Lu, J.-N. Chen, C.-T. Lee, *Chemosphere* 51 (2003) 935-943.

[20] F. Al Momani, C. Sans, S. Esplugas, *J. Hazard. Mater.* B107 (2004) 123-129.

[21] R. Gonzalez-Olmos, U. Roland, H. Taufer, F.-D. Kopinke, A. Georgi, *Appl. Catal. B: Environ.* 89 (2009) 356-364.

[22] M. Hartmann, S. Kullmann, H. Keller, *J. Mater. Chem.* 20 (2010) 9002-9017.

[23] E.G. Garrado-Ramírez, B.K.G. Theng, M.L. Mora, *Appl. Clay Sci.* 47 (2010) 182-192.

[24] A. Hirvonen, M. Trapido, J. Hentunen, J. Tarhanen, *Chemosphere* 41 (2000) 1211-1218.

[25] J. Poerschmann, U. Trommler, T. Górecki, F.-D. Kopinke, *Chemosphere* 75 (2009) 772-780.

[26] J.A. Zimbron, K.F. Reardon, *Water Res.* 39 (2005) 865-869.

[27] M.S. Yalfani, S. Contreras, F. Medina, J. Sueiras, *Appl. Catal. B: Environ.* 89 (2009) 519-526.

[28] M.S. Yalfani, S. Contreras, F. Medina, J. Sueiras, *Chem. Commun.* (2008) 3885-3887.

[29] J.J. Pignatello, E. Oliveros, A. MacKay, Crit. Rev. *Environ. Sci. Technol.* 36 (2006) 1-84.

[30] P. Husek, P. Simek, *Curr. Pharm. Anal.* 2006, 2, 23-43.

[31] F. Pinna, F. Menegazzo, M. Signoretto, P. Canton, G. Fagherazzi and N. Pernicone, *Appl. Catal. A: Gen.* 219 (2001) 195-200.

[32] H. Lieske and J. Völter, *J. Phys. Chem.* 89 (1985) 1841-1842.

[33] F. Pinna, M. Selva, M. Signoretto, G. Strukul, F. Boccuzzi, A. Benedetti, P. Canton, G. Fagherazzi, *J. Catal.* 150 (1994) 356-367.

[34] G. Leitz, M. Nimz, J. Völter, K. Lázár, L. Guczi, *Appl. Catal.* 45 (1988) 71-83.

[35] L.S.F. Feio, C.E. Hori, S. Damyanova, F.B. Noronha, W.H. Cassinelli, C.M.P. Marques, J.M.C. Bueno, *Appl. Catal. A: Gen.* 316 (2007) 107-116.

[36] D. Tessier, A. Rakai, F. Bozon-Verduraz, *J. Chem. Soc. Farad. Trans.* 88 (1992) 741-749.

[37] M. Schwidder, M.S. Kumar, K. Klementiev, M.M. Pohl, A. Brückner, W. Grünert, *J. Catal.* 231 (2005) 314-330.

[38] A.S. Reddy, C.-Y. Chen, C.-C. Chen, S.-H. Chien, C.-J. Lin, K.-H. Lin, C.-L. Chen, S.-C. Chang, *J. Mol. Catal. A: Chem.* 318 (2010) 60-67.

[39] G.D. Pringruber, P.K. Roy and R. Prins, *Phys. Chem. Chem. Phys.* 8 (2006) 3939-3950.

[40] E. Neyens, J. Baeyens, *J. Hazard. Mater.* B98 (2003) 33-50.

[41] L. Calvo, M.A. Gilarranz, J.A. Casas, A.F. Mohedano, J.J. Rodríguez, *J. Hazard. Mater.* 161 (2009) 842-847.

[42] N. Kang, D.S. Lee, J. Yoon, *Chemosphere* 47 (2002) 915-924.

[43] G.H. Rossetti, E.D. Albizzati, O.M. Alfano, *Ind. Eng. Chem. Res.* 41 (2002) 1436-1444.

[44] M.P. Ormad, J.L. Ovelleiro, J. Kiwi, *Appl. Catal. B: Environ.* 32 (2001) 157-166.

[45] A. Detomaso, A. Lopez, G. Lovecchio, G. Mascolo, R. Curci, *Environ. Sci. Pollut. Res.* 10 (2003) 379-384.

[46] *CRC Handbook of Chemistry and Physics*, CRC Press, 91st ed., 2010-2011.

[47] J. Dolfing, B.K. Harrison, *Environ. Sci. Technol.* 26 (1992) 2213-2218.

[48] A. Santos, P. Yustos, A. Quintanilla, F. García-Ochoa, J.A. Casas, J.J. Rodríguez, *Environ. Sci. Technol.* 2004, 38, 133-138.

[49] K.L.E. Kaiser, V.S. Palabrica, *Water. Pollut. Res. J. Can.* 26 (1991) 361-431.

[50] G. Yuan and M.A. Keane, *J. Catal.* 225 (2004) 510-522.

[51] G. Yuan and M.A. Keane, *Ind. Chem. Eng. Res.* 46 (2007) 705-715.

[52] Z. Jin, C. Yu, X. Wang, Y. Wan, D. Li, and G. Lu, *Chem. Commun.* (2009) 4438-4440.

[53] M.S. Yalfani, S. Contreras, J. Llorca, M. Dominguez, J.E. Sueiras, F. Medina, *Phys. Chem. Chem. Phys.* 12 (2010) 14673-14676.

[54] W.C. Conner, J.L. Falconer, *Chem. Rev.* 95 (1995) 759-788.

[55] S.S. Gupta, M. Stadler, C.A. Noser, A. Ghosh, B. Steinhoff, D. Lenoir, C.P. Horwitz, K.-W. Schramm, T.J. Collins, *Science* 296 (2002) 326-328.

[56] A. Sorokin, B. Meunier, *Chem. Eur. J.* 2 (1996) 1308-1317.

[57] J.A. Zimbron, K.F. Reardon, *Water Res.* 43 (2009) 1831-1840.

[58] X. Xue, K. Hanna, M. Abdelmoula, N. Deng, *Appl. Catal. B: Environ.* 89 (2009) 432-440.

UNIVERSITAT ROVIRA I VIRGILI
NEW CATALYTIC ADVANCED OXIDATION PROCESSES FOR WASTEWATER TREATMENT
Mohammad Sadegh Yalfani
ISBN:/DL:T.1259-2011

Chapter 6

Hydrogen substitutes for the *in situ* generation of H_2O_2: an application in the Fenton reaction

This study investigates the ability of formic acid, hydrazine and hydroxylamine to act as H_2 substitutes in conducting phenol degradation by Fenton reaction using in situ generated hydrogen peroxide. The processes were performed with semi-heterogeneous (Pd/Al_2O_3 + soluble Fe^{2+}) and fully heterogeneous ($FePd/Al_2O_3$) catalytic systems under ambient conditions (25 ± 2°C and atmospheric pressure). In contrast to bulk H_2O_2 production conditions, we discovered that hydrazine is able to produce H_2O_2 in situ followed by phenol degradation using Pd/Al_2O_3 + Fe^{2+} at pH 3 without the need for halide ions. However, although phenol degraded quickly, a degree of mineralization exceeding 37% could not be achieved. The significant production of in situ H_2O_2 (evidenced by phenol degradation and the formation of catechol as an oxidation product) at the inherent acidic pH of hydroxylammonium sulfate in the presence of Pd/Al_2O_3 + Fe^{2+} was also found to differ from the bulk production of H_2O_2, in which no H_2O_2 was detected. A remarkable degree of mineralization (ca. 65%) as well as fast phenol degradation during the reaction started at pH 7 over $FePd/Al_2O_3$ may be an advantage of using hydroxylamine. On the other hand, using formic acid, H_2O_2 was produced at a moderate rate, thereby achieving higher efficiency in the degradation and consequently the mineralization of phenol. Most importantly, the catalysts were more stable in the presence of formic acid than hydrazine or hydroxylamine.

ISBN:/DL:T.1259-2011

1. Introduction

The past few decades have seen growing interest in the use of *in situ* generated H_2O_2 for oxidation processes as an alternative to pre-manufactured H_2O_2 [1,2]. In some cases, the application of *in situ* generated H_2O_2 has been found to be potentially safer and more economical than bulk commercial H_2O_2 [3-5]. Few reports have been published on the use of *in situ* generated H_2O_2 for wastewater treatment, specifically for the oxidation of organic pollutants [6,7]. H_2O_2 generation directly from H_2 and O_2 using a metal-supported catalyst has been widely studied [8]. However, this process has several inevitable drawbacks which affect H_2O_2 productivity and selectivity, including (i) the potentially high explosiveness of the O_2/H_2 mixture, requiring researchers to limit their work to less hazardous ratios of the gases; and (ii) the low solubility of O_2 and H_2 in water [9]. The use of alcohols instead of water as a solvent has been suggested by some researchers as a possible method for improving H_2O_2 selectivity [10]. However, if the H_2O_2 generated by means of this process is used *in situ* for the subsequent oxidation reaction, the alcohols themselves may undergo undesired oxidation.

One of the most effective alternatives for overcoming these drawbacks is replacing H_2 with another source. This eradicates the risk of explosion associated with the O_2/H_2 mixture and eliminates one of the low soluble gases. Hydrazine (HZ) and formic acid (FA) have been introduced as H_2 substitutes in the generation of H_2O_2 using alumina-supported Pd catalysts [11,12]. Evans et al. [13] generated H_2O_2 using hydroxylamine (HA) and O_2 catalyzed by Mn complexes. Other authors have shown that alcohols in the presence of homogeneous Pd catalyst and O_2 can produce hydrogen peroxide [14].

HZ and its salts are widely recognized as an H_2 storage material due to their capacity for decomposing to H_2 under mild conditions [15,16]. Choudhary et al. reported that HZ could be used as an H_2 substitute for the production of H_2O_2

over Pd/Al_2O_3 resulting in remarkable H_2O_2 selectivity [11]. In that process, no evidence was found to indicate that H_2 formation occurred through the decomposition of HZ. In other words, H_2O_2 is the product of a direct reaction between HZ and O_2. Pd based catalysts have been found to be inactive for HZ decomposition to H_2 in aqueous solution and under ambient conditions [16]. However, a small amount of H_2 with a short lifetime has been detected in the presence of O_2 [17]. Although HZ is classified as a toxic and possibly carcinogenic compound, no HZ remains at the end of the reaction. The process requires halide ions and mineral acid in order to stabilize the H_2O_2 produced. In the absence of either of these reagents, no H_2O_2 was detected. Recently, the same authors (Choudhary et al.) proposed HA as an H_2 substitute for the *in situ* generation of H_2O_2 using Pd/Al_2O_3 catalyst [18]. The advantage of HA over HZ is its ability to achieve very high H_2O_2 productivity at neutral pH without the need for halide ions. It has been mentioned that without the initial neutralization of the medium, no H_2O_2 was formed. *In situ* generated H_2O_2 from HA and O_2 has been applied in the oxidation of Calmagite dye [7]. We have reported a simple, clean and environmentally-friendly method for the generation of H_2O_2 via FA and O_2 [12]. In this method, FA (as an H_2 substitute) and O_2 react over a Pd/Al_2O_3 catalyst under ambient conditions leading to the generation of hydrogen peroxide. Subsequently, this process was applied in the degradation of phenol in the presence of Fe^{2+} (Fenton´s catalyst) with significant performance compared to the conventional Fenton process [19]. The process was successfully expanded for different categories of organic pollutant such as chlorophenols and pharmaceutical compounds [20].

In this paper, we study the performance of HZ, HA and FA as H_2 substitutes for the *in situ* generation of H_2O_2 in the presence of O_2. The *in situ* generated H_2O_2 is applied in the degradation of phenol (as representative of organic pollutants) through a Fenton-like reaction. The efficiency of the process is

evaluated by means of the phenol conversion, TOC removal results and the evolution of aromatic intermediates (catechol). The effect of the factors enhancing the H_2O_2 formation yield (halide ion and pH) is investigated. The reactions are conducted over a semi-heterogeneous $Pd/Al_2O_3 + Fe^{2+}$ and a fully heterogeneous $Pd\text{-}Fe/Al_2O_3$ catalyst.

2. Experimental

2.1. Catalyst preparation and characterization

Pd/Al_2O_3 (denoted as PdAl) and $Fe\text{-}Pd/Al_2O_3$ (denoted as FePdAl) catalysts were synthesized through conventional impregnation. For PdAl, an acidified solution of $PdCl_2$ was added to a slurry solution of $\gamma\text{-}Al_2O_3$ (prepared by sol-gel). The mixture was aged while stirring for 1 h. Water was removed by rotary vapor at 55°C. The precipitate was dried at 110°C and was then calcined at 400°C for 3 h. Finally, the catalyst was reduced under a flow of H_2 (20 ml/min) at 200°C for 2 h. Pd content on alumina was 5 wt%. To synthesize FePdAl, first γ-alumina was impregnated by an aqueous solution containing a certain amount of $Fe(NO_3)_3.9H_2O$ followed by drying at 110°C and calcining at 400°C for 3 h. Afterwards, the calcined solid was impregnated with Pd followed by drying and calcining through the same procedure as performed for Fe. Finally, the solid was reduced by H_2 at 200°C for 2 h. The Fe and Pd contents were 1 and 5 wt%, respectively.

The catalysts were characterized by XRD, H_2 chemisorption, H_2-TPR, HRTEM and XPS. The details of the characterization techniques and their results have been explained in previous reports [19,20]. In summary, PdAl showed a metallic Pd phase with an average particle size of 20 nm. Characterization of FePdAl demonstrated metallic Pd and Fe^{3+} as the major phases, which were localized in close proximity on alumina so an interaction between the Pd and Fe species would be expected.

ISBN:/DL:T.1259-2011

2.2. Catalytic tests

The phenol degradation reactions were performed under ambient conditions (25°C and atmospheric pressure) in a 100 ml magnetically stirred three-necked glass reactor. The volume of the reaction was 50 ml containing phenol (100 mg/L), Fe^{2+} (if required 10 mg/L), Br^- (if required 1 mM) and the catalyst (0.1 g). Initial concentrations of FA, hydrazine hydrate ($N_2H_4.H_2O$) and hydroxylamine sulfate ($(NH_2OH)_2.H_2SO_4$) were 40 mM, 20 mM and 40 mM respectively. Oxygen was passed through the reaction medium at a flow rate of 20 ml/min. Without exception, all the reactions were performed in darkness to avoid any interfering effect of existing light. The reactions using the FePdAl catalyst were performed under the same conditions as mentioned above, but in the absence of Fe^{2+}. The desired pH of the solution was adjusted using H_2SO_4 or NaOH. Phenol degradation and FA decomposition were monitored by sampling at regular intervals and analyzing by means of high-performance liquid chromatography HPLC (Shimadzu LC-2010 equipped with a SPD-M10A Diode array UV-vis detector). A Varian OmniSpher C18 column and a solution containing Milli-Q H_2O and acetonitrile (60:40) at pH 3.80 adjusted by H_3PO_4 as mobile phase were used to analyze phenol and catechol at a wavelength of 254 nm. An Acclaim OA column and a mobile phase containing 100 mM Na_2SO_4 at pH 2.65 adjusted by methanesulfonic acid as mobile phase were used to analyze FA at a wavelength of 210 nm. H_2O_2 evolution during the reaction was monitored semi-quantitatively by *Quantofix* H_2O_2 indicator strips (MACHERY-NAGEL). HZ was analyzed by titration against KIO_3 in the presence of HCl and chloroform as documented by Penneman et al. [21]. HA was measured by reverse iodometric titration using potassium iodate [22]. Total Organic Carbon (TOC) for each sample was measured using a Shimadzu TOC-5000A analyzer. The reaction solution at the end of each run and after filtration was analyzed by atomic absorption spectroscopy to measure Pd and Fe leaching.

ISBN:/DL:T.1259-2011

3. Results and discussion

3.1. Formic acid

Phenol conversion profiles (Figure 1-A) using H_2O_2 generated *in situ* from FA and O_2 in the presence of PdAl + Fe^{2+} and over FePdAl show similar performances for both processes. A fast decrease of phenol concentration within 1 h (55-65%) followed by a moderate conversion up to 4 h was observed during the reaction periods. Within 4 h, a degree of mineralization of 55% was obtained by means of the semi-heterogeneous (PdAl + Fe^{2+}) system, while better mineralization (66%) was achieved using the fully heterogeneous (FePdAl) catalytic system. Prolonging the reactions up to 6 h resulted in a further decrease of TOC, whereas phenol concentration remained constant. Mineralization occurrence after 4 h can be attributed to the activity of both PdAl and FePdAl catalysts in the degradation of the intermediates in the presence of O_2. The FA decomposition profiles (Figure 1-B) of the above two reactions also demonstrate very similar trends indicating the termination of FA within 4 h. This suggests that Fe does not interfere in FA decomposition over Pd in the reaction over FePdAl.

Halide ions can promote the efficiency of the reaction by poisoning the catalyst, thereby decreasing its hydrogenation activity and the decomposition of H_2O_2 [23]. In the presence of halide ions, H_2O_2 formation using FA and O_2 leaded to H_2O_2 selectivity enhancement after a long reaction period (1 h), while in a short period (5 min) H_2O_2 selectivity did not significantly improve, which is an essential component of the *in situ* application of H_2O_2 [12]. This means that the halide ion effect on H_2O_2 generation is more substantial in the bulk production of H_2O_2. To study the halide ion effect on the *in situ* generation of H_2O_2, we performed phenol degradation using H_2O_2 generated *in situ* over PdAl + Fe^{2+} in the presence of Br^-. The phenol conversion profile of this reaction in Figure 1-A shows a drastically reduced rate in comparison with the same

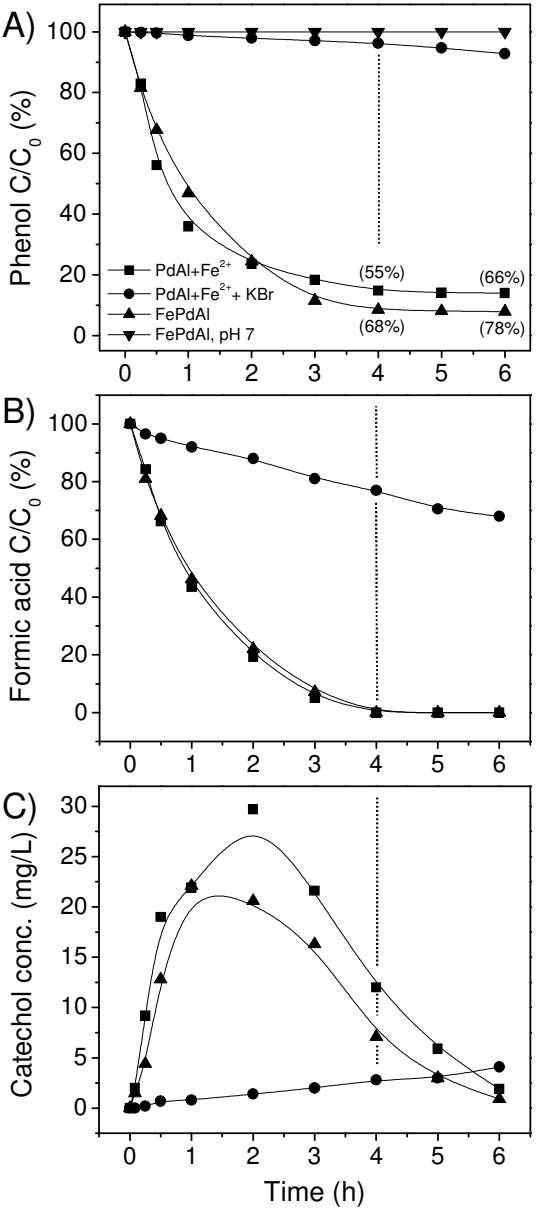

Figure 1. Phenol degradation using *in situ* generated H_2O_2 from FA and O_2 using PdAl + Fe^{2+}, PdAl + Fe^{2+} + KBr, FePdAl and FePdAl (pH 7). (a) Phenol conversion profiles (b) FA conversion profiles. (c) Evolution of catechol.

reaction without Br^-. The FA decomposition profile for this process (Figure 1-B) clearly shows a very slow FA disappearance rate. This behavior can be attributed to Br^-, which deactivates the catalyst for the decomposition of FA. It can be concluded that for the *in situ* generation of H_2O_2, the presence of a poison which deactivates the catalyst leading to the accumulation of H_2O_2 in the medium over a long time is not required; a fast H_2O_2 generation rate for the subsequent oxidation reaction is more important.

In order to test the performance of this catalytic system in a wider pH range, phenol degradation was performed over FePdAl at the initial pH 7 adjusted with NaOH. The phenol concentration profile (Figure 1-A) indicates that no phenol conversion occurred. Other studies have found that under ambient conditions and in aqueous solution, the decomposition rate of the formate ion at pH ≥ 7 is constant and so much slower than FA itself [17]. Consequently, H_2 cannot be produced at an appropriate rate for the formation of H_2O_2.

The formation of intermediates during the process of phenol degradation points to the occurrence of oxidation reactions. Consequently, the existence of an *in situ* generated oxidant is proved. We monitored the evolution of catechol as one of the well-known aromatic intermediates of phenol oxidation (Figure 1-C). For the reactions over PdAl + Fe^{2+} and FePdAl, catechol appears in similar slopes reaching maximums at 2 h and 1 h, respectively. Over FePdAl, catechol disappears a little faster, suggesting a higher capability of the catalyst in the degradation of intermediates, which had already been demonstrated by the degree of mineralization results. In the presence of Br^-, catechol is formed at a very slow rate representing a weak oxidation process. It is worth noting that during the above reactions apparently no H_2O_2 was detected in the reaction medium, suggesting its rapid consumption by the oxidation reaction.

For all the above reactions using PdAl and FePdAl, no Pd and Fe leaching was detected in the final solutions. Single Pd shows high stability when it is

deposited on alumina [19]. Moreover, the coupling of Fe and Pd promotes the resistance of Fe species against corrosion in a moderately acidic medium [20].

3.2. Hydrazine

The reaction of HZ and O_2 over supported-Pd catalyst is supposed to occur based on the following reactions.

(1) $N_2H_4 + 2O_2 \rightarrow 2H_2O_2 + N_2$

(2) $N_2H_4 + O_2 \rightarrow 2H_2O + N_2$

Assuming the optimum circumstance for H_2O_2 formation through the reaction (1), each mol HZ can be oxidized to two mol H_2O_2. Therefore, in order to have a fair comparison between HZ and FA in this study, HZ was used as half of the initial molar concentration of FA, i.e. 20 mM.

H_2O_2 generated *in situ* from HZ and O_2 using a PdAl + Fe^{2+} system at initial pH 3 (Figure 2-A) quickly converted phenol, within 1 h (>50%). HZ disappeared in less than 30 minutes (Figure 2-B), as had been previously observed during H_2O_2 generation [11]. H_2O_2 was detected, reaching a maximum (ca. 20 mg/L) at 30 minutes which vanished after 2 h. The appearance of free H_2O_2 within the solution suggests a higher rate of H_2O_2 formation than H_2O_2 consumption by phenol oxidation. After 2 h, thus, phenol degradation by *in situ* generated H_2O_2 was suppressed. Over FePdAl, similar behavior was also observed for the conversion of phenol and decomposition of HZ (Figure 2-A,B). Most interestingly, while the reaction of HZ and O_2 over Pd/Al_2O_3 in the absence of halide ions and strong mineral acid yielded no H_2O_2 [11], during the oxidation reaction carried out under the same conditions, *in situ* generated H_2O_2 was semi-quantitatively detected.

Phenol degradation using PdAl + Fe^{2+} in the presence of Br^- and started at pH 3 was proceeded at a rate similar to that in the two previous reactions (Figure 2-A), while the conversion of HZ was slightly slower (Figure 2-B).

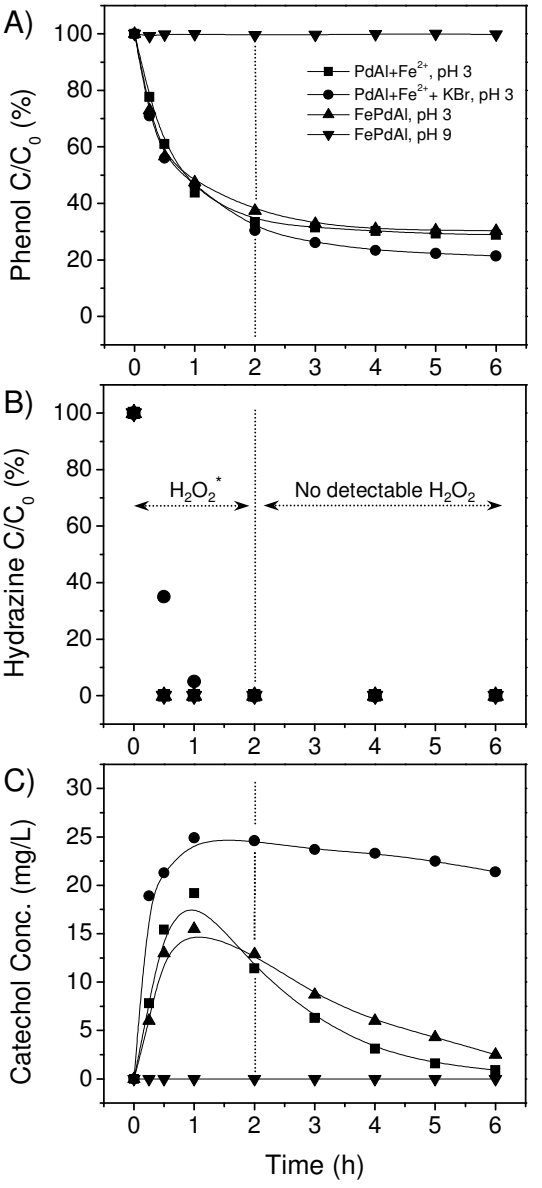

Figure 2. Phenol degradation using *in situ* generated H_2O_2 from HZ and O_2 using PdAl + Fe^{2+} (pH 3), PdAl + Fe^{2+} + KBr (pH 3), FePdAl (pH 3) and FePdAl (pH 9). (a) Phenol conversion profiles (b) HZ conversion profiles. (c) Evolution of catechol.
* No H_2O_2 was detected during the reaction performed using FePdAl (pH 9).

Monitoring of the H_2O_2 produced revealed ca. 40 mg/L H_2O_2 at 30 minutes, which supports the assumption mentioned earlier regarding the higher stability of H_2O_2 formed in the presence of halide ions. After 1 h, H_2O_2 concentration was reduced to less than 5 mg/L. The use of a higher initial concentration of HZ (40 mM) better revealed the influence of Br^- on phenol degradation (Figure 3). HZ conversion clearly decreased in the presence of Br^-, leading to slower conversion of phenol and a weaker degree of mineralization.

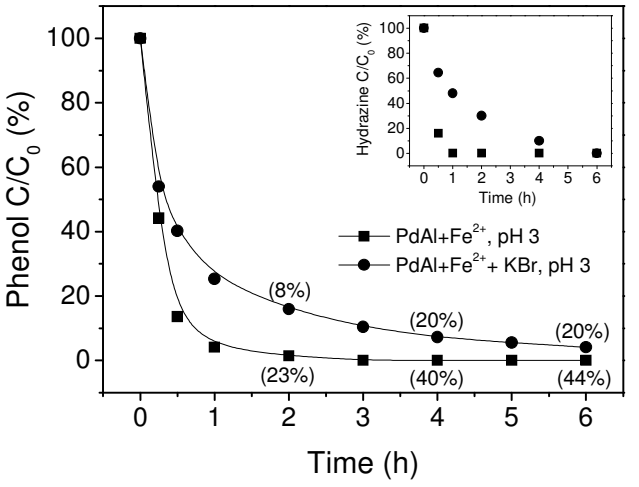

Figure 3. Phenol (100 mg/L) degradation using *in situ* generated H_2O_2 from hydrazine (40 mM) and O_2 (20 ml/min) using PdAl (0.1 g) + Fe^{2+} (10 mg/L) (pH 3), PdAl (0.1 g) + Fe^{2+} (10 mg/L) + KBr (1 mM) (pH 3) (the numbers in the parentheses are the corresponding TOC removal (%)). Inset: hydrazine conversion during the two above reactions.

Phenol degradation was conducted without the addition of acid at inherent basic pH (ca. 9) created by the addition of 20 mM hydrazine hydrate over FePdAl. Surprisingly, no phenol conversion was observed (Figure 2-A), whereas HZ disappeared very quickly (shown in Figure 2-B). Furthermore, no H_2O_2 was detected by the indicator strips during the reaction. It seems that the HZ and O_2 reaction under these conditions was directed mostly toward the formation of H_2O (reaction (2)) [11]. By conversion of HZ in less than 1 h, the pH of the

ISBN:/DL:T.1259-2011

solution drops to 4.6 (the pH of a solution containing phenol and the catalyst) remaining constant until the end of the reaction period (6 h). It can be concluded that the H_2O_2 generation by HZ and O_2 for bulk production and *in situ* purposes essentially needs to be carried out in an acidic pH.

Figure 2-C, shows the evolution profiles of catechol through the phenol degradation reactions. For the reactions involving FePdAl and PdAl + Fe^{2+} started at pH 3, catechol appears at a high rate, reaching a maximum at 1 h, which confirms the occurrence of phenol oxidation. After 1 h, mild degradation continued until the end of the reaction periods. After 2 h, when no H_2O_2 was generated in the reaction medium, catechol oxidation took place in the presence of O_2 and the catalyst [19]. During a reaction using PdAl + Fe^{2+} in the presence of Br^- at pH 3, catechol was produced along with phenol oxidation within 1 h. The catechol concentration even exceeded the maximum concentration obtained in the absence of Br^-, which is consistent with the higher amount of H_2O_2 apparently detected. Nevertheless, after 1 h, the concentration of catechol remained almost constant. These observations indicate that the catalyst was deactivated by Br^-.

For the reactions conducted using PdAl + Fe^{2+} and FePdAl, TOC removal yielded similar profiles (Figure 4). In the presence of Br^-, TOC removal was drastically diminished, which is in agreement with the results of catechol evolution i.e. catalyst deactivation by Br^-. Obviously, no TOC removal was observed for the reaction carried out in the absence of acid (pH 9).

The stability of the catalysts was studied by measuring metal leaching at the end of the reactions. PdAl indicated remarkable stability so that Pd loss was always less than 0.1% compared to the total Pd content of the catalyst. In addition, phenol degradation using the PdAl used (filtered, washed and dried after the first run) + Fe^{2+} yielded results similar to those using fresh catalyst. Pd was also stable on the FePdAl catalyst. However, for this catalyst, Fe indicated

marked leaching (5 mg/L, ca. 20% of the total Fe content of the catalyst) for the reaction started at pH 3. This might be due to a decrease in pH down to 1.6 during the reaction, which is highly corrosive for Fe.

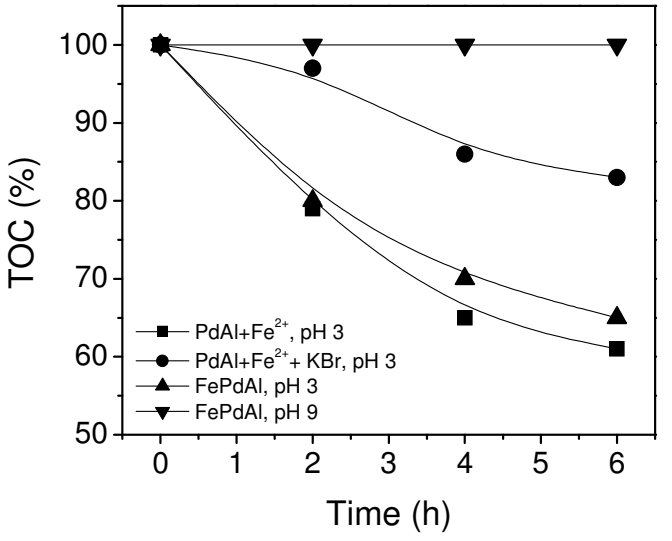

Figure 4. TOC conversions during phenol degradation using *in situ* generated H_2O_2 from HZ and O_2.

3.3. Hydroxylamine

In the presence of O_2, HA conversion can occur as follows:

(3) $2NH_2OH + O_2 \rightarrow H_2O_2 + 2H_2O + N_2$ (ΔH_{298} = -540.1 kJ/mol)

(4) $2NH_2OH + 2º_2 \rightarrow 3H_2O_2 + N_2$ (ΔH_{298} = -329.1 kJ/mol)

Assuming the reaction (3) as the predominant route, i.e. formation of 1 mol H_2O_2 by 2 mol HA, 40 mM hydroxylammonium sulfate was used as initial concentration for all the reactions in order to be comparable with FA and HZ. As a hydroxylammonium sulfate salt, HA has an acidic character; therefore, the Addition of a 40 mM concentration to a solution containing phenol (100 mg/L) and the catalyst (0.1 g) leads to a pH of 3.8. Phenol degradation using PdAl + Fe^{2+} as shown in Figure 5-A, after a relatively fast degradation within 1 h,

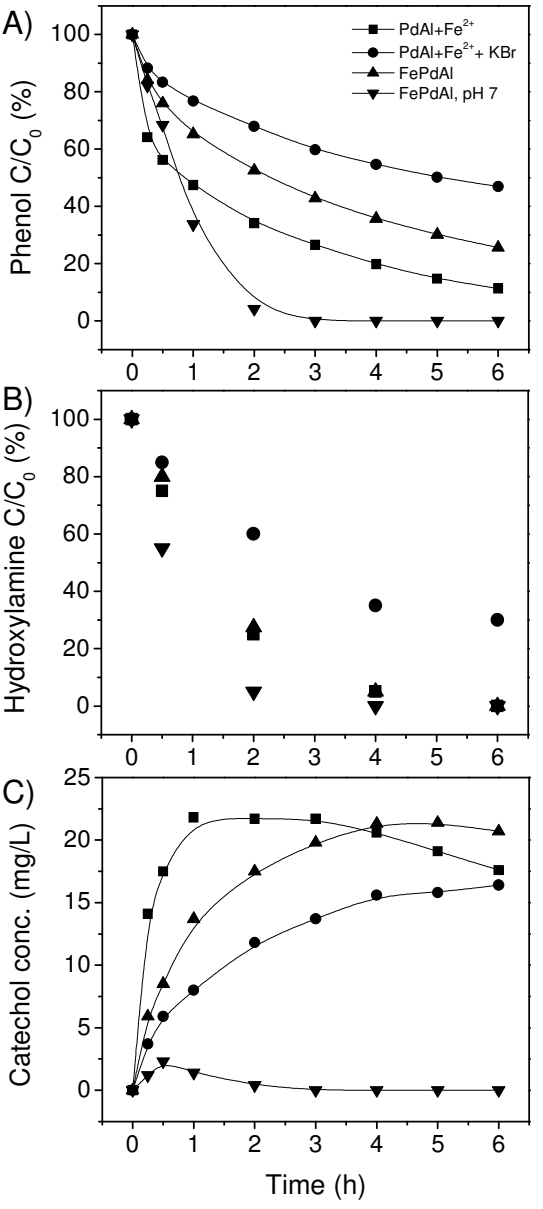

Figure 5. Phenol degradation using *in situ* generated H_2O_2 from HA and O_2 over PdAl + Fe^{2+}, PdAl + Fe^{2+} + KBr, FePdAl and FePdAl (pH 9). (a) Phenol conversion profiles (b) HA conversion profiles. (c) Evolution of catechol.

progresses gradually, reaching 88% conversion after 6 h. The conversion of HA (Figure 5-B) reaches ca. 70% within 2 h followed by its complete disappearance at 6 h. Over FePdAl, phenol conversion took place at a lesser rate than over PdAl (Figure 5-A) whereas the conversion of HA was similar to that over PdAl (Figure 5-B). In the presence of Br^- and using PdAl + Fe^{2+}, the phenol conversion rate was drastically decreased (Figure 5-A), leading to a 47% conversion after 6 h. It is clear that Br^- affects HA conversion. No H_2O_2 was detected during the above reactions, which means that all the H_2O_2 produced was consumed *in situ* by the oxidation reactions. The pH of the medium during the above reactions decreased from 3.8 to 3.2-3.5 at the end of the reaction periods. The oxidation of phenol through the above reactions at such an acidic pH implies H_2O_2 formation. H_2O_2 formation from HA and O_2 had not previously occurred without neutralization [18]. The catalysts showed interesting stability in that no significant metal leaching was detected at the end of each run. Furthermore, a phenol degradation reaction performed using the PdAl used (filtered, washed and dried after the first run) + Fe^{2+} demonstrated results similar to those yielded using fresh catalyst.

Phenol degradation was conducted using HA over FePdAl at the initial pH 7 adjusted by NaOH. Phenol disappeared in less than 3 h as shown in Figure 5-A. Total conversion of HA was achieved in less than 4 h (Figure 5-B) and the formation and the accumulation of a significant amount of H_2O_2 was observed. Within 1 h, a concentration of >150 mg/L H_2O_2 could be detected semi-quantitatively. The H_2O_2 produced showed interesting persistence during the reaction which might be due to the acidic medium created by termination of HA [24]. After 6 h reaction, there still was approximately 15 mg/L H_2O_2 available in the solution. The pH of the solution decreased slowly during the first 30 minutes from 7.0 to 6.4. Then the pH dropped to 3.0 at 1 h resulting in a final pH of 2.8 after 6 h. Maintaining the medium at this pH for 5 h and releasing of

SO_4^{2-} as a result of $(NH_2OH)_2.H_2SO_4$ decomposition might be the cause of 2 mg/L Fe leaching (ca. 8% of total iron content of the catalyst) detected at the end of the run. An experiment showed that such a low concentration of Fe^{2+}, although can slightly proceed the Fenton reaction, is not conclusive for the whole process.

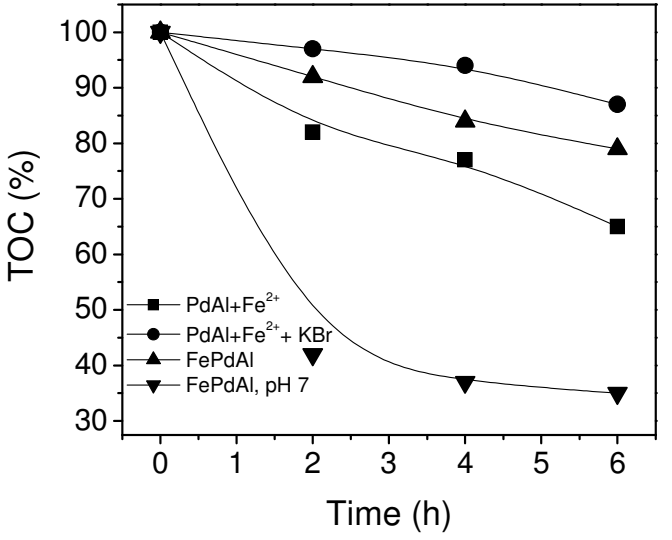

Figure 6. TOC conversions during phenol degradation using *in situ* generated H_2O_2 from HA and O_2.

For the reaction performed using PdAl + Fe^{2+}, catechol concentration rapidly reached a maximum at 1 h followed by moderate decomposition up to 6 h (Figure 5-C). Over FePdAl, the catechol evolution profile shows a continuous increase reaching its maximum at 5 h, suggesting a lesser oxidation activity for this reaction. Using PdAl + Fe^{2+} and in the presence of Br^-, the weaker oxidation activity of the system becomes clear, i.e. the formation of catechol is slower. Interestingly, in the case of the reaction performed over FePdAl at initial pH 7, catechol appears in a small quantity (2 mg/L) at 30 minutes which rapidly

ISBN:/DL:T.1259-2011

degrades in less than 3 h. These results exemplify the remarkable oxidative capability of this system.

The TOC results shown in Figure 6 indicate a degree of mineralization of 35% achieved using PdAl + Fe^{2+} at acidic pH after 6 h. A lesser degree of mineralization was obtained using FePdAl (21% in 6 h), which is in line with lower phenol conversion and catechol appearance. The lowest capacity for mineralization was observed with PdAl + Fe^{2+} in the presence of Br^-. Nevertheless, a degree of mineralization of 65% was achieved by the reaction over FePdAl at pH 7 after 6 h. It should be noted that 95% of such achievement was accomplished within 2 h.

3.4. Comparison of H_2 substitutes

Generally speaking, the bulk production of H_2O_2 over Pd-based catalysts requires the presence of a strong acid and halide ions in order to achieve high selectivity. However, the application of H_2O_2 generated *in situ* for phenol degradation in the presence of halide ions, regardless of the H_2 source, is not very efficient. On the other hand, in contrast to the bulk production in which no H_2O_2 was produced in the absence of halide ions, the oxidation of phenol and its intermediates under such conditions confirmed the formation of H_2O_2. Actually, the H_2O_2 produced is consumed by the oxidation reaction before its decomposition to H_2O and O_2. Therefore, it can be concluded that the presence of halide ions is not in favor of *in situ* generation of H_2O_2.

H_2O_2 formation using FA as an H_2 substitute had previously been shown to be less efficient than HZ and HA. However, FA showed better performance during the *in situ* generation of H_2O_2 employed for the oxidation of organic pollutants (Figure 7). The achievement of higher mineralization and the remarkable stability of the catalyst are advantages of using FA as an H_2 substitute. This behavior of FA suggests a controlled productivity for H_2O_2

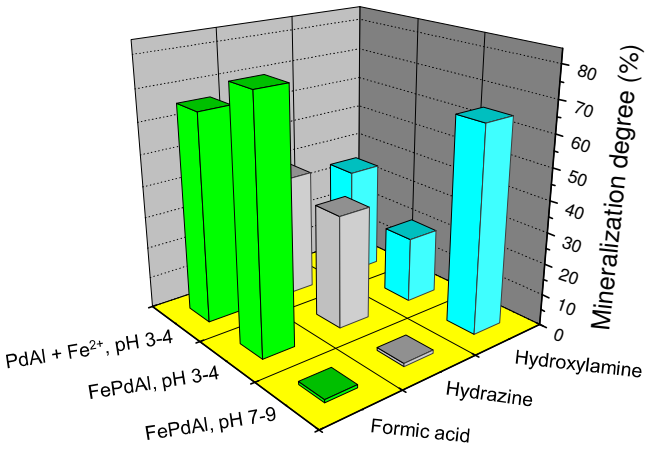

Figure 7. The comparison of the performances of formic acid, hydrazine and hydroxylamine in phenol degradation using *in situ* generation of H_2O_2 under different conditions.

which is suitable for the subsequent oxidation process. HZ cannot compete with FA in the *in situ* generation of H_2O_2 applied in phenol degradation. Firstly, its performance is highly dependent on the presence of strong mineral acid, which can reduce catalyst stability due to metal corrosion. Secondly, its fast decomposition over Pd leads to the production of a large quantity of H_2O_2 which is exposed to dehydration or self-decomposition rather than being consumed as an oxidant. Nevertheless, in the case of HA, the high H_2O_2 productivity obtained at neutral pH may be an advantage when effluents with neutral or nearly basic pH are treated. Phenol degradation by H_2O_2 generated *in situ* from HA was remarkably efficient at neutral pH (Figure 7). It is worth noting that considering this advantage, the initial concentration of HA and the organic compound to be oxidized should be optimized in order to avoid any loss of the H_2O_2 formed.

Acknowledgement

This work was funded by the Spanish Ministry of Science and Innovation (MICINN) project CTM2008-02453 and the Center for Innovation and Business Development (CIDEM) project VALTEC 08-1-0052.

References

[1] M.G. Clerici, P. Ingallina, *Catal. Today*, 41 (1998) 351-364.

[2] S.K. Karmee, L. Greiner, A. Kraynov, T.E. Müller, B.; Niemeijer, W.; Leitner, *Chem. Commun.*, 46 (2010) 6705-6707.

[3] J.E. Remias, T.A. Pavlosky, A. Sen, *J. Mol. Catal. A: Chem.* 203 (2003) 179-192.

[4] B. Chowdhury, J.J. Bravo-Suárez, M. Daté, M. Haruta, *Angew. Chem. Int. Ed.* 45 (2006) 412-415.

[5] Q.; Chen, E.J.; Beckman, *Green Chem.* 10 (2008) 934-938.

[6] Y.–G. Zhang, L.–L. Ma, J.–L. Li, Y. Yu, *Environ. Sci. Technol.*, 41 (2007) 6264-6269.

[7] T.S. Sheriff, S. Cope, M. Ekwegh, *Dalton Trans.* (2007) 5119-5122.

[8] J.K. Edwards, G.J. Hutchings, *Angew. Chem. Int. Ed.*, 47 (2008) 9192-9198.

[9] J.M. Campus-Martin, G. Blanco-Brieva, J.L.G. Fierro, *Angew. Chem. Int. Ed.* 45 (2006) 6962-6984.

[10] Q. Liu, J.H. Lunsford, *Appl. Catal. A : Gen.* 314 (2006) 94-100.

[11] V.R. Choudhary, C. Samanta, P. Jana, *Chem. Commun.* (2005) 5399-5401.

[12] M.S. Yalfani, S. Contreras, F. Medina, J. Sueiras, *Chem. Commun.* (2008) 3885-3887.

[13] D.F. Evans, T.S. Sheriff, *J. Chem. Soc. Chem. Commun.* (1985) 1407-1408.

[14] R. Bortolo, D. Bianchi, R. D' Aloisio, C. Querci, M. Ricci, *J. Mol. Catal. A : Chem.* 153 (2000) 25-29.

[15] S.K. Singh, X.-B. Zhang, Q. Xu, *J. Am. Chem. Soc.*, 131 (2009) 9894-9895.

[16] M. Zheng, R. Cheng, X. Chen, X. Li, L. Li, X. Wang, T. Zhang, *Int. J. Hydrogen Energy* 30 (2005) 1081-1089.

[17] F.-D. Kopinke, K. Mackenzie, R. Koehler, A. Georgi, *Appl. Catal. A: Gen.*, 271 (2004) 119-128.

[18] V.R. Choudhary, P. Jana, *Catal. Commun.*, 8 (2007) 1578-1582.

[19] M.S. Yalfani, S. Contreras, F. Medina, J. Sueiras, *Appl. Catal. B : Environ.,* , 89 (2009) 519-526.

[20] M.S. Yalfani, S. Contreras, J. Llorca, M. Dominguez, J.E. Sueiras, F. Medina, *Phys. Chem. Chem. Phys.* 12 (2010) 14673-14676.

[21] R.A. Penneman, L.F. Audrieth *Anal. Chem.* 20 (1948) 1058-1061.

[22] J. Mendham, R.C. Denney, J.D. Barnes, M.J.K. Thomas, *Vogel´s Textbook of Quantitative Chemical Analysis.* 6th Ed. (2000) 444.

[23] V.R. Choudhary, C. Samanta, *J. Catal.*, 238 (2006) 28-38.

[24] V.R. Choudhary, P. Jana, *Appl. Catal. A : Gen.* 335 (2008) 95-102.

UNIVERSITAT ROVIRA I VIRGILI
NEW CATALYTIC ADVANCED OXIDATION PROCESSES FOR WASTEWATER TREATMENT
Mohammad Sadegh Yalfani
ISBN:/DL:T.1259-2011

Chapter 7

Enhanced Cu activity in catalytic ozonation of clofibric acid by incorporation into ammonium dawsonite

Clofibric acid (CFA) degradation by ozonation in the presence of Cu-dawsonites was studied. Cu-dawsonite materials were synthesized via co-precipitation of $Al(NO_3)_3$ and $Cu(NO_3)_2$ by $(NH_4)_2CO_3$ at pH 7.5-8.0. The as-synthesized and the calcined samples were characterized using XRD, FTIR, N_2-physisorption, TEM and XPS techniques. The CFA degradation was carried out using the as-synthesized and the calcined Cu-dawsonites, dissolved Cu^{2+} and CuO supported on Al_2O_3. The heterogeneous as-synthesized Cu-dawsonite catalysts showed more efficient performance with respect to the other catalysts, despite of significant Cu leaching detected at the end of the reactions. The reactions carried out using the homogeneous dissolved Cu^{2+} (in the concentration range of the leached Cu) indicated low contribution of dissolved Cu^{2+} in the mineralization of CFA and its intermediates; the efficiency was mainly devoted to the activity of Cu incorporated in the dawsonite structure. Characterization of Cu-dawsonites revealed a possibility of Cu localization in the NH_4^+ position which is higher exposed to leaching than that of Al. The reaction performed at initial pH 10 (pH higher than pH_{PZC} of as-synthesized Cu-dawsonite) resulted to the higher TOC and COD reduction after 2 h compared with the reaction at pH 3.7. Also lowest Cu leaching was obtained under these conditions. Enhanced activity of Cu incorporated into the structure of dawsonite in the catalytic ozonation of CFA is probably due to the presence of Cu(I) located in the structure of dawsonite revealed by XPS. Some of the main intermediates have been identified by HPLC-MS suggesting three routes for CFA destruction including C_1-O and C_4-Cl bond breaking and aromatic ring cleavage.

1. Introduction

The residual of pharmaceutical compounds released into the aquatic environment has recently received special attention due to their potential impact on human and environmental health [1]. Some of these compounds such as clofibric acid (CFA, a blood lipid regulator) have shown high persistency when they are introduced in the water [2]. Conventional techniques like sand filtration and coagulation may not operate with an appropriate efficiency to eliminate such compounds, in particular for the drinking water treatment [3]. One way to reduce these contaminants is to decrease their presence in wastewaters by the "on-site" treatment of pharmaceutical plant wastewaters. The wide range of products that are produced in plants, the complexity of the molecules and their resistance to biological degradation, makes necessary the use of advanced oxidation methods. Advanced oxidation processes (AOP) have been found to be effective in the removal of these compounds even in low concentrations [4].

Single ozonation is a powerful oxidation technique, but in many cases is not able to achieve a complete oxidation of organic compounds [5]. It causes the formation of some intermediates e.g. carboxylic acids and aldehydes which do not react with ozone. One of the alternatives in order to have greater mineralization efficiency is to promote the process via the generation of free hydroxyl radicals which are more powerful than molecular ozone. Both homogeneous and heterogeneous catalytic ozonation systems result in the production of radicals so that the process is considered an AOP [6].

The activity of a heterogeneous catalyst in ozonation depends on its ability to adsorb ozone [7]. The adsorption of ozone on the surface is a key factor, because it can be followed by the ozone decomposition to hydroxyl radicals. The decomposition of ozone can take place on different types of active centers. Therefore, basicity and acidity of surface plays an important role in the process.

ISBN:/DL:T.1259-2011

Dispersed solid metal oxides such as TiO_2, Al_2O_3, and MnO_2 have been widely tested as catalyst in ozonation. MnO_2 is the most widely studied metal oxide as a catalyst for ozonation process and is reported to be the most efficient in ozone decomposition in gaseous medium [8]. With Al_2O_3, although is mostly known as support than as catalyst, ozone decomposition can take place on its surface, leading to higher efficiencies of organic pollutants degradation [9].

Among the transition metals, Co, Fe, Ni, Zn and Cu have been widely studied [7]. These metals have been tested in the form of single or supported metal oxide. Cu as CuO was used as a catalyst for ozonation of different types of organic pollutant such as herbicides (e.g. alachlor), chlorophenols, nitrophenols and carboxylic acid (oxalic acid) [10-12]. It has been found that Cu could improve TOC removal by promotion of $^{\bullet}OH$ formation [10]. Shiraga et al. have reported that the incorporation of Cu into the hydrotalcite structure followed by calcinations at 600°C leaded to a catalyst with least metal leaching during catalytic ozonation of phenol and oxalic acid [13]. Enhanced dispersion of Cu atoms through the hydrotalcite matrix can be a reason of such a high activity. Interestingly, as-synthesized Cu-hydrotalcite showed lower Cu leaching compared to the samples calcined at 400, 850 and 1100°C. Also, Co as CoNiAl-hydrotalcite showed higher activity in catalytic ozonation of phenol with respect to CoO, Co_3O_4 and Co supported on CeO_2 and Al_2O_3 [14]. Better performance was obtained by the as-synthesized CoNiAl-hydrotalcite than the calcined one.

Dawsonite is a mineral clay which is naturally found as $NaAl(CO_3)(OH)_2$ [15]. It has a orthorhombic-dipyramidal structure (space group *Imam*) which involves edge-sharing $AlO_2(OH)_4$ and $NaO_4(OH)_2$ octahedral and CO_3^{2-} groups. Replacing Na with NH_4^+, results to ammonium aluminum carbonate hydroxide (AACH) which its structure demonstrates similarity to that of Na-dawsonite, although AACH belongs to the group space of *Cmcm* [16]. Synthesis at pH 10

ISBN:/DL:T.1259-2011

resulted to the formation of a sample with an empirical formula of $NH_4M(CO_3)(OH)_2$ in which M is Al, Cr or Fe [17]. Another procedure performed at pH 7.5-8 reached to a compound with an empirical formula of $(NH_4)Al_6(CO_3)_3(OH)_{14}$ as shown by Vogel et al. [18]. According to the XRD analysis, both formula represent similar crystallographic structures to the mineral dawsonite [17-18]. AACH has shown an interesting ability to incorporate different metal ions within its structure leading to dawsonite-like materials. Dawsonite-like materials have been found as an appropriate precursor for alumina-based catalysts. Calcination of the as-synthesized samples incorporating certain metals (like Mn, Fe) at the temperatures 500-1200 °C results to metal oxide dispersed on alumina [19,20], while specifically, thermal treatment of Ba or La incorporated samples at temperatures up to 1200 °C leads to the formation of hexaaluminate [20,21]. Enhanced dispersion and availability of active species within the dawsonite structure can give rise to an improvement in the catalytic activity of the dawsonite-derived materials. Despite the interesting properties presented by the dawsonite-based materials, they have been scarcely applied in catalytic processes.

In this paper, the performance of Cu incorporated dawsonite in catalytic ozonation of clofibric acid is studied. Cu-dawsonites were synthesized via co-precipitation with different Cu content and were characterized using different techniques. The position and the oxidation state of Cu within the dawsonite structure were discussed. The performance of the as-synthesized and calcined catalysts was compared with a conventional CuO/Al_2O_3 sample. The effect of metal leaching on the ozonation proceeding was studied by performing reactions using different concentration of dissolved Cu^{2+}. Furthermore, the process was experienced at distinct pHs considering the pH of point of zero charge of Cu-dawsonite. The performance of this process was evaluated by the

ISBN:/DL:T.1259-2011

measurement of CFA concentration, chemical oxygen demand (COD) and total organic carbon (TOC).

2. Experimental

2.1. Catalyst preparation

Cu-dawsonites with Cu/Al mass ratios 0 (NH_4DW), 0.02 (Cu2DW) and 0.1 (Cu10DW) were synthesized by co-precipitation at constant pH as explained by Groppi et al. [22]. An aqueous solution (pH ≈ 1 adjusted by HNO_3 if required) of $Al(NO_3)_3.9H_2O$ and $Cu(NO_3)_3.H_2O$ and an aqueous solution of $(NH_4)_2CO_3$ (2M) were drop-wise poured into a beaker under vigorous stirring at 60°C. The pH of the slurry was maintained within the range 7.5-8 during the co-precipitation. Then, the slurry was aged for 3 h at 60°C under stirring to complete the co-precipitation operation. Afterwards, the precipitate was filtered, washed and dried at 110°C for 12 h. A part of Cu10DW was calcined at 500°C for 3 h (denoted as Cu10DW500) and the rest was used as-synthesized. The metal salts and ammonium carbonate were purchased from Sigma-Aldrich and Panreac and used as received. A CuO/Al_2O_3 sample with Cu content of 2 wt% was synthesized via conventional impregnation as reference sample. After impregnation of alumina (prepared by sol-gel method) with the $Cu(NO_3)_2.3H_2O$ aqueous solution followed by water evaporation by rotary vapor at 50°C and drying at 110 °C for 12 h, the sample was calcined at 500°C for 3 h.

2.2. Characterization techniques

Metal content of the Cu-dawsonite samples were measured by ICP-OES (SPECTRO-ARCOS FHS16). XRD measurements were made using a Bruker-AXS D8-Discover diffractometer with parallel incident beam (Göbel mirror) and vertical theta-theta goniometer, XYZ motorized stage mounted on an Eulerian cradle, diffracted-beam Soller slits, a 0.02º receiving slit and a scintillation counter as a detector. The angular 2θ diffraction range was between 5 and 70º.

ISBN:/DL:T.1259-2011

The data were collected with an angular step of 0.05º at 3s per step and sample rotation. Cu_k radiation was obtained from a copper X-ray tube operated at 40 kV and 40 mA (λ=1.541 Å).

N_2 adsorption was performed using a Micromeritics ASAP 2010 apparatus at 77 K. Before analysis, the samples were degasified at 120°C for 12 h. Total surface area was calculated by the BET method.

Fourier transformed infrared analyses (FTIR) were carried out using a JASCO FTIR-680 plus spectrophotometer. The spectra were recorded using the pure solid in powder form within the range 650-4000 cm^{-1} under ambient conditions.

TEM images were acquired using a JEOL JEM-1011 microscope operating at 80 kV. The samples were mounted on a carbon-coated copper grid by placing a few droplets of a suspension of the ground sample in acetone, followed by evaporation under ambient conditions.

X-ray photoelectron spectroscopy (XPS) was performed with a SPECS system equipped with an Al anode XR50 source operating at 150 W and a Phoibos 150 MCD-9 detector. Sample powders were pelleted and fixed mechanically into a special sample holder without glue or tape. Spectra were recorded with pass energy of 25 eV at 0.1 eV steps at a pressure below 5×10^{-9} mbar and binding energies were referred to the C 1s signal. The C 1s peak from the adventitious carbon was used as an internal reference with a binding energy of 284.8 eV. Concerning the oxidation state of copper, the $Cu2p_{3/2}$ core level has been adjusted by using a combination of Gaussian-Lorentzian functions.

2.3. Catalytic ozonation tests

The degradation reactions were performed in a 1L glass reactor containing a 500 mL aqueous solution of CFA (100 mg/L) at ambient conditions (25 ± 2°C and atmospheric pressure). To the CFA solution, 250 mg catalyst was added

ISBN:/DL:T.1259-2011

and the ozone generated by an ozone generator (ANSEROS COM-AD-02) from pure O_2 (40 L/h) was passed through the solution maintaining a constant production of 1.2 g/h of O_3. The samples were taken at regular time intervals. CFA concentrations were measured by high performance liquid chromatography HPLC (Shimadzu LC-2010 equipped with a SPD-M10A Diode array UV-vis detector) at wavelength 254 nm. A Varian OmniSpher C18 column and a solution containing an aqueous buffer (Milli-Q H_2O 1L, methanol 50 mL and H_3PO_4 4mL) and acetonitrile (40:60) were used as mobile phase. The reaction intermediates were identified qualitatively by HPLC (1200 Series) coupled to a 6210 Time of Flight (TOF) mass detector with electrospray ion source (ESI) (Agilent Technologies,S.L.) using the same column as mentioned above. The mobile phase was a mixture of solutions A and B with a flow rate of 0.4 mL/min. A was 0.1% formic acid and 5% Milli-Q water in acetonitrile and B was 0.1% formic acid in water (pH 3.5). The analyses were performed under a linear gradient from 10% A to 100% A at 30 min. remaining steady for further 5 min. Ion source and TOF parameters are as: drying gas temperature 350°C, nebulizer gas flow 10 L/min, nebulizer gas pressure 50 psi, fragmentor voltage 150 V, capillary voltage 4000 V, skimmer voltage 650 V, octapol voltage 250 V and acquisition range 50-1200 m/z. COD was measured by photometry (photometer PC MultiDirect, Tintometer GmbH) using *COD Vario Tube Test* (containing mercury(II) sulfate and sulfuric acid 84%) after digestion of the sample at 150ºC for 2 h. TOC was measured by a Shimadzu 5000-A TOC analyzer. pH of point of zero charge (pH_{pzc}) of Cu-dawsonite was determined by the method reported by Noh and Schwarz [23]. Cu leached at the end of each run was measured by photometry (mentioned above) using *Vario Cu1F10ml* reagent.

3. Results and discussion

3.1. Catalysts characterization

ISBN:/DL:T.1259-2011

Metal content analysis of the samples shown in Table 1, indicates that taking into account the theoretical Cu/Al weight ratio, co-precipitation for the Cu-dawsonite samples has been carried out effectively. Calcination of the Cu10DW sample upto 500°C caused the removal of NH_3, CO_2 and H_2O which resulted in raising the Cu content. Obviously, the Cu/Al ratio remains constant. The textural properties of the samples given in Table 1 show a high surface area for the as-synthesized NH4DW sample. Incorporation of Cu into the dawsonite structure resulted to a decrease in surface area. Pore volume of the Cu-dawsonite samples decreases by increasing the Cu content. All as-synthesized samples have an average pore diameter range of 6-9 nm. After calcination, a decrease of surface area occurs, suggesting a porosity loss as a result of thermal treatment. N_2-physisorption analysis results of Cu10DW500 and CuO/Al_2O_3 (Table 1) are very close to each other indicating similar textural properties. Adsorption-desorption isotherms of the Cu10DW and the Cu10DW500 samples (Figure 1) resemble hysteresis loop type H1. This is the characteristic of a material with a narrow distribution of relatively uniform mesopores [24]. Cu10DW500 shows lower N_2 uptake in particular at lower pressure in comparison with Cu10DW which is in-line with the difference observed in the surface areas of the both samples. TEM images of the as-synthesized and calcined dawsonite samples are shown in Figure 2. The Cu10DW sample (Figure 2-A) displays a bulk and uniform structure containing intra-structural mesoporosity. The Cu10DW500 sample (Figure 2-B) shows small particles forming needles with 30-40 nm length and 2-4 nm diameter. As it is seen in the TEM image, the mesoporosity assigned to the calcined sample comes from inter-particle spaces.

FTIR spectrum of the Cu10DW sample (Figure 3) shows absorption bands of hydroxyl, ammonium and carbonate groups of dawsonite. The details of the band assignments have been reported elsewhere [25]. Briefly, OH^- bands (ν_{OH} at

UNIVERSITAT ROVIRA I VIRGILI
NEW CATALYTIC ADVANCED OXIDATION PROCESSES FOR WASTEWATER TREATMENT
Mohammad Sadegh Yalfani
ISBN:/DL:T.1259-2011

Table 1. Characterization data of the as-synthesized and the calcined samples.

				Cell parameters					
Sample	Cu (wt%)	Cu/Al (theo.)	Cu/Al	*a* (Å)	*b* (Å)	*c* (Å)	S_{BET} (m^2/g)	V_p (cm^3/g)	d_p (nm)
NH_4DW	0	0	0	6.610	12.307	5.667	599	1.17	7.82
Cu2DW	0.35	0.02	0.021	6.625	12.018	5.682	426	0.954	8.95
Cu10DW	1.59	0.1	0.091	6.633	12.285	5.731	338	0.632	7.47
Cu10DW500	3.67	0.1	0.091	-	-	-	297	0.964	12.9
CuO/Al_2O_3	2.0	-	-	-	-	-	299	1.026	13.7

ISBN:/DL:T.1259-2011

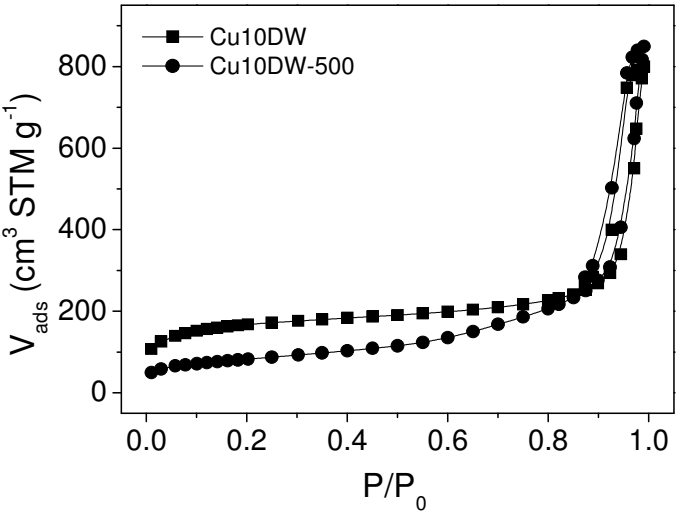

Figure 1. N_2 adsoprtion-desoption isotherms of Cu10DW and Cu10DW-500.

3432 cm^{-1}; δ_{OH} at 980 cm^{-1}), NH_4^+ bands (ν_{NH} at 3174, 3025 and 2840 cm^{-1}; δ_{NH} at 1829 and 1718 cm^{-1}) and CO_3^{2-} bands (ν_3 at 1546, 1447 and 1378 cm^{-1}; ν_1 at 1107 cm^{-1}; ν_2 at 850 cm^{-1} and ν_4 at 757 and 736 cm^{-1}). By calcination at 500°C, the absorption bands of NH_4^+ are totally removed. Hydroxyl bands are transformed to a broad absorption peak representing OH^- group on γ-Al_2O_3. The intensity of the carbonates absorption bands are remarkably reduced, while some stable carbonate species may remain within the structure of the sample, despite of calcinations.

XRD patterns of the as-synthesized and calcined samples are shown in Figure 4. The patterns of the as-synthesized samples are clearly consistent with the characteristic diffractions of ammonium dawsonite ($NH_4Al(CO_3)(OH)_2$, JCPDS 01-076-1923). No other phase is distinguished in the patterns suggesting formation of a single dawsonite-like phase containing Cu and Al through co-precipitation. The cell parameters of as-synthesized dawsonite samples were

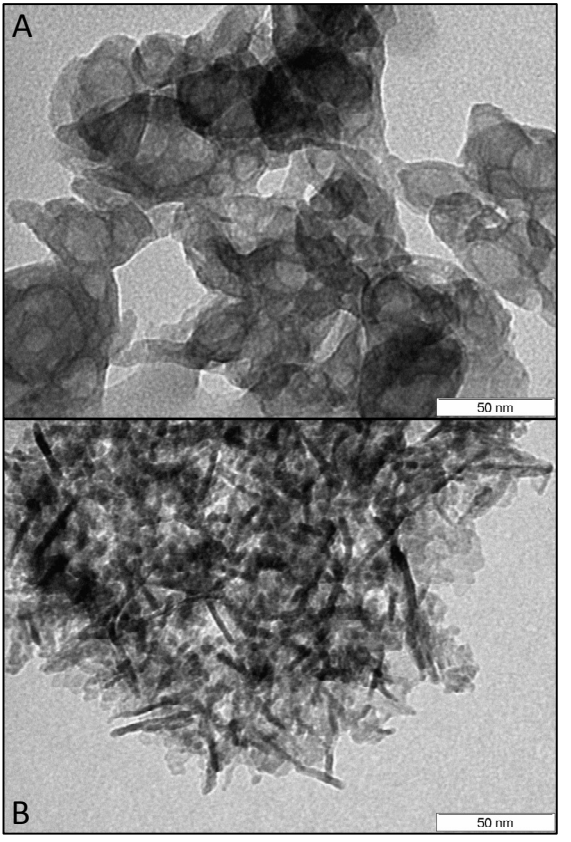

Figure 2. TEM images of: (A) Cu10DW and (B) Cu10DW-500.

calculated taking into account bases-centered orthorhombic as the lattice structure of $NH_4Al(CO_3)(OH)_2$ [26] (Table 1). These data indicate that in the presence of Cu, the dimensions of the unit cell vary. The *a* and *c* parameters grow with increasing the Cu content. These variations of the unit cell dimensions suggest incorporation of Cu within the dawsonite structure. The XRD pattern of the Cu10DW500 sample shows disappearance of the dawsonite peaks resulting in the formation of an amorphous phase. In this pattern, characteristic peaks of γ-Al_2O_3 are sorely detected. The XRD pattern of CuO/Al_2O_3 shows reflections associated to γ-Al_2O_3 with intensities slightly higher than those of Cu10DW500.

ISBN:/DL:T.1259-2011

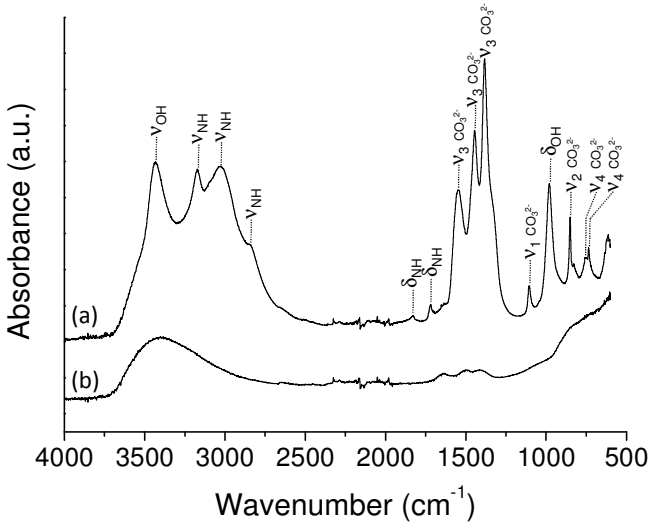

Figure 3. FTIR spectra of: (a) Cu10DW and (b) Cu10DW-500.

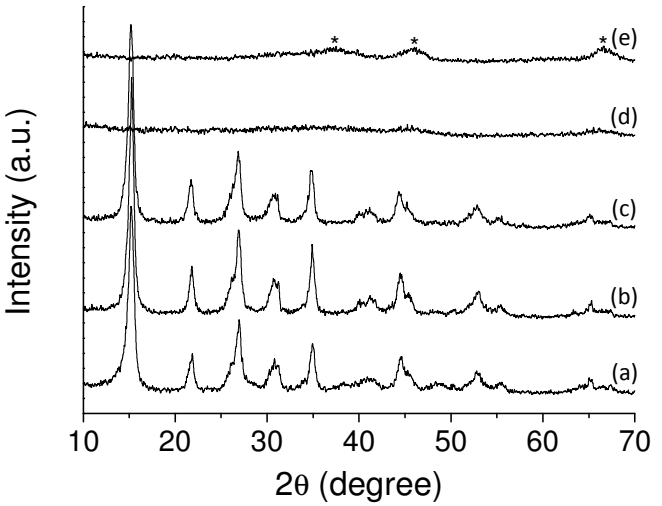

Figure 4. XRD patterns of: (a) NH_4DW, (b) Cu2DW, (c) Cu10DW, (d) Cu10DW-500 and (e) CuO/Al_2O_3; (*) γ-Al_2O_3.

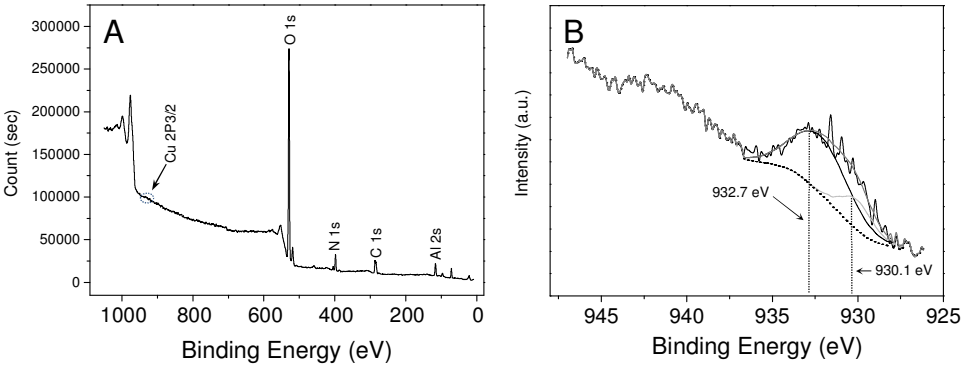

Figure 5. A: XPS wide-scan spectrum of the Cu2DW sample; B: Cu $2p_{3/2}$ core level XPS spectra of the Cu2DW sample.

Oxidation state of Cu in the as-synthesized sample was studied by XPS. Wide-range XPS scan of the Cu2DW sample shown in Figure 5-A, displays characteristic signals related to Al2s, C1s, N1s and O1s. The signals associated to the $Cu2p_{3/2}$ at around 932 eV could be identified under a high resolution. The mass composition of the elements in this sample calculated by peak area attributed to each element revealed a 0.02 mass ratio for Cu/Al. This number is fully in agreement with the theoretical mass ratio of Cu/Al, indicating uniform distribution of Cu and Al on the surface and within the bulk structure of dawsonite. The $Cu2p_{3/2}$ binding energy could be distinguished involving two components at 932.7 and 930.1 eV. $Cu2p_{3/2}$ signals devoted to Cu(II) usually appear at binding energies higher than 933 eV [27]. In addition, since no characteristic satellite shake-up signal at 940-950 eV is observed [28], the existence of isolated Cu(II) species in the sample is not possible. Thus, both signals are attributed to the reduced Cu species. Cu(I) and Cu(0) cannot be distinguished by XPS [29,30]. Owing to not performing any reduction treatment on the sample before XPS analysis, the formation of metallic Cu is also

ISBN:/DL:T.1259-2011

implausible. It means that Cu is accommodated within the structure of dawsonite as Cu(I). It has been previously verified that for CuSiBEA zeolites, no reduction of Cu(II) could occur by X-ray beam even after 6 h being under irradiation [31]. Thus, oxidation state of Cu can be affected by its chemical environment. In a similar case, when Cu(II) was incorporated into the ZSM-5 zeolite via ion exchange at ambient temperature followed by drying at 120°C, it appeared with a reduced oxidation state (Cu(I)) detected by XPS [32]. It was suggested that an electron density transfer from Al atoms to Cu ions was the responsible of this behavior. Furthermore, the synthesis of Cu/zeolite Y by precipitation from Cu(II) acetate at 80°C and then drying at 120°C resulted to the co-existence of Cu(I) and Cu(II) species in the sample [33]. Therefore, for the Cu2DW sample, it can be concluded that occurrence of the Cu species in reduced form is due to their new coordination in the dawsonite structure. Meanwhile, no explanation for the component detected at 930.1 eV could be found.

3.2. Degradation of clofibric acid

The results of CFA degradation by catalytic ozonation using different Cu-based catalysts have been summarized in Table 2. A reaction using single ozone resulted to a fast disappearance of CFA in less than 15 minutes. However the ability of the system in TOC removal was not higher than 28% after 2 h. A final COD elimination of 55% was also obtained. A CFA solution of 100 mg/L has a pH of 3.7. The pH after reaction was 3.2 suggesting the formation of hardly oxidizable acidic intermediates. Degradation of CFA by ozonation in the presence of different catalysts was tested and similar to single ozonation, CFA conversion was completed in less than 15 minutes in all the cases. Using NH_4DW, a clear promotion of the efficiency of the system was observed due to higher TOC (40.6%) and COD (71%) removal results with respect to single

Table 2. CFA degradation results using single O_3 and Cu-based catalysts.

Catalyst	pH final	CFA conv. (%)	TOC removal (%)	COD removal (%)	Cu leached (mg/L) (%)
-	3.2	100	28.1	55.0	-
NH_4DW	4.5	100	40.6	71	-
Cu2DW[a]	3.6	0	0	0	0.23 (12.5)
Cu2DW	4.45	100	55.2	75.3	0.52 (28.2)
Cu10DW	5	100	67.3	82.1	1.29 (15.4)
Cu10DW500	4.8	100	57.9	69.3	3.37 (17.4)
CuO/Al_2O_3	4.6	100	57.8	72.8	2.95 (28.0)
Cu^{2+} (0.5 mg/L)	2.9	100	33.3	61.1	-
Cu^{2+} (2.0 mg/L)	2.9	100	36.7	63	-
Cu^{2+} (3.5 mg/L)	3.0	100	38.3	63.3	-

[a] Reaction in presence of catalyst (Cu2DW) and oxygen

ozonation. Using Cu2DW instead of NH4DW leaded to further improvement of the results in particular for TOC removal (55.2%). These results indicate the role of Cu in degradation of CFA degradation intermediates. In other words, Cu is able to decompose O_3 molecules to hydroxyl radicals which enhance the oxidizing activity of the system [12,34]. It should be noted that no adsorption of CFA on the Cu2DW catalyst was detected in the presence of O_2 flowing without ozone generation. Therefore, the degradation of CFA in the presence of catalyst depends on the oxidizing activity of the system and not to the adsorption of CFA on the catalyst surface [11]. Final pH of the filtered solution shows an increase to 4.5 which can be due to the enhanced ability of the catalytic ozonation process in the degradation of acidic intermediates produced by the oxidation of CFA [12]. In agreement with the above results, the increase of Cu content in the dawsonite structure yields to further improvement of TOC (67.3 %) and COD (82.1 %) removal results. The performance of the CFA degradation in the presence of the calcined catalyst (Cu10DW500) gives rise to a decrease of the efficiency of the process, compared with the non-calcined catalyst. The test

with the CuO/Al_2O_3 catalyst shows results similar to those of Cu10DW500. Although higher dispersion for the dawsonite-derived Cu species was expected, the Cu active species on the Cu10DW500 and CuO/Al_2O_3 catalysts seem to have similar characteristics. It is observed that the Cu incorporated within the dawsonite structure represents a better performance in catalytic ozonation than the CuO supported on alumina.

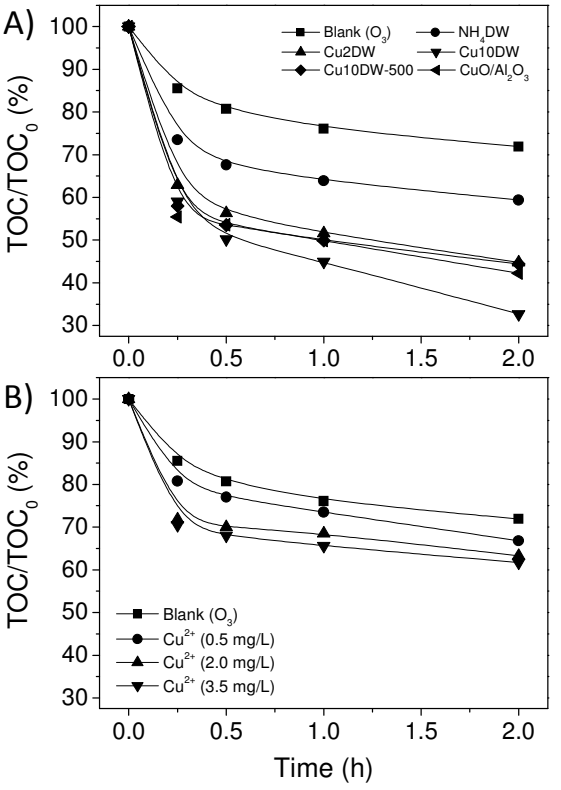

Figure 6. TOC removal (%) during the CFA degradation by catalytic ozonation using: (A) heterogeneous NH_4DW, CuDW and CuO/Al_2O_3 catalysts; (B) homogeneous Cu^{2+} catalyst concentrations 0.5, 2.0 and 3.5 mg/L.

TOC removal profiles of the above reactions graphed in Figure 6-A revealed that the main TOC reduction for each process happened during the first 15

minutes. A similar behavior of rapid TOC reduction in short time has been also observed by other authors [4,35]. This means that the degradation of CFA and readily oxidizable intermediates occur at the same time. The rest of the reaction time was assigned to degradation of hardly oxidizable intermediates. In the case of Cu10DW, TOC removal pursues with a sharper slope with respect to the other catalysts indicating higher activity of this catalyst.

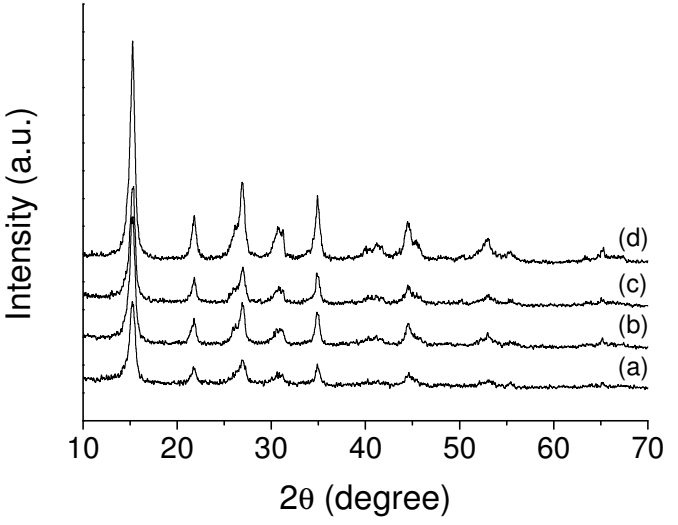

Figure 7. XRD patterns of the fresh (d) and used Cu2DW catalysts after reaction at pH 3.7 (a), pH 7 (b) and pH 10 (c).

CFA degradation was tested in the presence of Cu2DW recovered after a run by filtering, washing and drying. Like the case of fresh catalyst, a total conversion of CFA occurred in less than 15 minutes. The catalyst showed a reduced activity owing to the TOC and COD results. A 42% TOC removal along with 57% COD removal was observed; results that are ca. 23% lower than those for the fresh catalyst. This deactivation of the catalyst can be due to the Cu loss during the first run. However, the catalyst structure did not change during the reaction at acidic pH. As shown in Figure 7, XRD patterns of both fresh and used Cu2DW demonstrate dawsonite structure. In the case of the

ISBN:/DL:T.1259-2011

used catalyst, a reduction in crystalinity is observed regarding to the decreasing of the peaks intensities.

3.2.1. Effect of Cu leaching

The Cu leached during the reactions was measured in the final filtered solutions and the results are shown in Table 2. The blank reaction to test adsorption involving 100 mg/L CFA, Cu2DW and O_2 resulted to 0.23 mg/L Cu leaching. This amount increased to 0.52 mg/L in the presence of O_3. For Cu10DW, although more leaching was detected (1.29 mg/L), the amount of Cu loss was lower with respect to the total Cu content of the sample. In contrary to what was expected, thermal treatment at 500°C did not improve the stability of Cu within the sample matrix. On the other hand, the CuO/Al_2O_3 catalyst showed double Cu loss relative to Cu10DW500. This means that CuO dispersed within the dawsonite matrix is more stable than CuO supported on the alumina surface at acidic pH (3.7-4.8). Further increasing of the calcination temperature of Cu-dawsonite to 700°C did not improve the stability of the material either (not shown). More than 80% of Cu release into the solution occurred during the first 15 minutes of the reactions i.e. when the process underwent highest involvement of oxidation of CFA and consequently formation of acidic intermediates. It could be said that such superficial acidic species caused Cu leaching.

Cu leaching can be rationalized taking a view into the structure of dawsonite and the actual position of Cu within its matrix. The structure of NH_4DW has been described by Watanabe et al. [36]. Based on this structure, incorporation of Cu can be possible in two positions. As a cation, Cu can occupy the position of Al (a trivalent cation) or NH_4^+ (an equivalent cation). Al seems to have strong non-ionic bonds with carbonate oxygens. Thus, assuming Al replacement with Cu, firstly a higher oxidation state for Cu would be expected. Secondly, at such a position, Cu atoms would not be easily dissolved into the solution at pHs ca. 4.

ISBN:/DL:T.1259-2011

Nevertheless, Cu can substitute NH_4^+ keeping its ionic character. The Cu appearance at oxidation state around +1 confirmed by XPS can support the later assumption. In such a case Cu can be subjected to an easier release into the solution as a result of the contact with weak acids or the replacement with a cation like Na^+.

In order to evidence the effect of dissolved Cu^{2+} on the performance of CFA degradation by ozone, a series of homogeneous catalytic ozonation experiments were performed using dissolved Cu^{2+} with a concentration range 0.5-3.5 mg/L (in the range of amounts of leached Cu). The results of these experiments are shown in Table 2 which indicates a small improvement with respect to the single ozonation. In the presence of 0.5 mg/L Cu, TOC and COD increased only between 5-6%. Increasing the Cu amount 7 times higher to 3.5 mg/L did not lead to the improvement of TOC and COD results proportionally. This means that dissolved Cu^{2+} at acidic pH cannot effectively enhance the ozonation process. However, referring to the results obtained using Cu2DW and Cu10DW, it is clearly observed that further enhancements of 20-30% and 15-20% in TOC and COD removals, respectively, achieved with respect to single ozonation, can be therefore attributed to the heterogeneous Cu. It should be noted that the later results were obtained in the presence of 0.5 and 1.29 mg/L Cu^{2+} leached within the reaction media. It seems that Cu in heterogeneous form within the dawsonite structure affords $^{\bullet}OH$ radical generation from O_3 better than the dissolved Cu^{2+}. In other words, considering blank reaction using single ozonation, the contribution of Cu^{2+} as homogeneous catalyst in catalytic ozonation, with respect to the heterogeneous Cu catalyst is not significant. Like the reaction using Cu-dawsonites, in the presence of Cu^{2+} the major TOC removal was carried out within the first 15 minutes and then the mineralization follows with a slow rate (Figure 6-B).

3.2.2. Effect of pH

ISBN:/DL:T.1259-2011

Cu-dawsonite indicated a neutral character according to the pH_{PZC} measurement result for the Cu2DW sample (pH_{PZC} = 6.8). Therefore the reactions in the presence of Cu-dawsonites have been performed at $pH<pH_{PZC}$. In order to study the effect of pH on the performance of CFA degradation by ozonation using Cu-dawsonites, the process was carried out at different initial pH. To do so, the pH of a CFA 100 mg/L solution was adjusted at 7 and 10 by NaOH and then blank tests were performed using single ozonation. Next runs were carried out under the same conditions and in the presence of Cu2DW. Cu2DW was selected for these reactions because of the lower quantity of Cu leached into the solution and to avoid increasing the toxicity of the medium due to the dissolved Cu^{2+}. Single ozonation at pHs 7 and 10 did not yield better performance relative to the reaction at pH 3.7. CFA conversion was completed in 15 minutes and TOC removal profiles are analogous (Figure 8). By starting these reactions, the pH dropped to <4.5 in 5 minutes, likely due to the formation of large amount of acidic intermediates. Therefore, the rest of the processes proceeded at acidic pH and similar performance to the reaction at pH 3.7 has been resulted.

During the reactions in the presence Cu2DW, CFA conversion was completed in less than 15 min, the same as occurred using single ozonation. For the reaction at pH 7, lower efficiency in TOC removal was observed (Figure 8) with respect to the reaction at pH 3.7. COD result also shows lower removal after 2 h (67.3% relative to 75.3% at pH 3.7). Nevertheless, comparing to the single ozonation, it is clear that Cu2DW displays a better performance at initial neutral pH. During this reaction, pH had small reduction from 7 to 5.8 (compared to 4.1 for the single ozonation) which represents higher ability of catalytic ozonation in the degradation of acidic intermediates generated during the process. The reaction at pH 10 using Cu2DW attained remarkable improvements of the TOC (62.2%) and the COD (83.4%) removals with respect

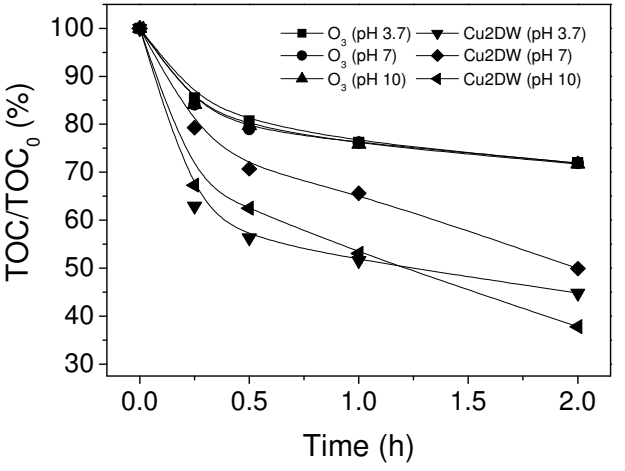

Figure 8. TOC removal (%) during the CFA degradation by single and catalytic ozonation in the presence of Cu2DW at pH 3.7, 7.0 and 10.0.

to the reactions at lower pHs. TOC profile of this reaction in Figure 8, although shows a slower TOC elimination during the first 15 minutes relative to the reaction at pH 3.7, continues with sharper slope up to the end of the reaction period. The pH of the final solution was 6.6, in line with the lower accumulation of acidic intermediates and consequently higher TOC removal at the end of the reaction. These results are consistent with the assumption of radical formation enhancement in the presence of OH^- [37]. In addition, it can be said that the process is more effective when the surface of the catalyst is charged (negatively or positively at acidic or basic pH). Cu leaching was clearly decreased for the reactions started at neutral and basic pHs. The Cu concentrations in the final solutions of these reactions were 0.38 mg/L (pH 7) and 0.36 mg/L (pH 10) which represent a decrease of ca. 30% with respect to the reaction started at acidic pH. Taking into account the K_{sp} of $Cu(OH)_2$ (1.6×10^{-19}) and the final pH of the solutions, the leached Cu species were expected to be totally dissolved.

Meanwhile, Cu2DW kept its dawsonite structure after the reactions at pHs 7 and 10 as shown by their XRD patterns (Figure 7).

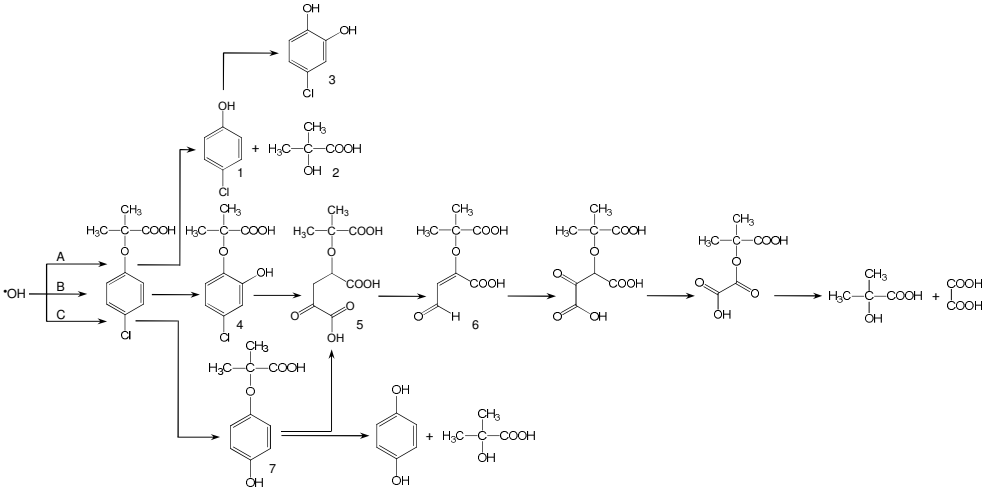

Scheme 1. Different pathways of CFA oxidation by Cu-dawsonite catalyzed ozonation and the molecular structure of the intermediates.

3.2.3. Reaction intermediates

The CFA degradation using ozonation in the presence of Cu-dawsonites passed through the formation of various intermediates. HPLC-MS analysis of the samples taken during the reactions could identify some of them which helped finding the degradation routes of CFA. It should be said that all the intermediates were detected at negative ionization mode. As shown in Scheme 1, $^{\bullet}OH$ can attack on three different points of CFA which are (A) C_1-O bond, (b) aromatic ring and (C) C_4-Cl bond. The 4-chlorophenol (**1**) and 2-hydroxyisobutyric acid (**2**) were identified at m/z 126.99 and m/z 103.03 respectively. The existence of these compounds proves $^{\bullet}OH$ attack on C_1-O bond. Further oxidation of **1** leaded to the formation of 4-chlorocatechol (**3**) detected at m/z 142.99. Hydroxylation of aromatic ring resulted to the formation of **4** with m/z 230.98 which can be 2-(4-chloro-2-hydroxyphenoxy)-2-methylpropionic acid. Subsequent oxidation can cleave the aromatic ring and

produce carboxylic acids **5** and **6**. These later compounds were identified at m/z 245.02 and 201.03, respectively. The oxidation of these acidic intermediates is expected to reach to **2** and oxalic acid as shown by Rosal et al. [35]. $^{\bullet}OH$ is also able to carry out dechlorination via attack on C_4-Cl leading to the formation of 4-hydroxyphenoxy-isobutyric acid (**7**) found at m/z 195.06. This compound may undergo ring cleavage and follow the route B. It may also receive a second $^{\bullet}OH$ attack on the C_1-O bond forming hydroquinone and **2**, although hydroquinone was not detected within the intermediates.

4. Conclusions

The performance of the as-synthesized Cu-dawsonite materials to catalyze the ozonation of CFA showed advantages in comparison to homogeneous dissolved Cu^{2+}, calcined Cu-dawsonite and CuO supported on alumina. These catalysts showed higher efficiency in reduction of TOC and COD of the 100 mg/L CFA aqueous solution, achieving mineralization degrees up to 70%. Characterization of the Cu-dawsonite material revealed that Cu as Cu(I) is incorporated into the matrix of dawsonite. Furthermore, Cu-dawsonite loses partially its activity upon thermal treatment (500°C) with respect to the as-synthesized one. Although Cu-dawsonites showed low stability due to significant Cu leaching during the reaction, the contribution of homogeneous dissolved Cu in ozonation was found not to be conclusive. The experiments proved that the efficiency of the process is mainly attained by the heterogeneous Cu-dawsonite catalyst. The high amount of Cu leaching was discussed based on the position of Cu in the dawsonite structure. Considering NH_4-dawsonite as original matrix, it was suggested that the Cu is positioned in place of NH_4^+ and thus is more readily exposed to be released into the solution. The Cu-dawsonite catalyst demonstrated interesting structure stability, so that the recovered catalyst after the reactions analyzed by XRD showed a similar crystallographic structure as the fresh sample. The reaction carried out at

initial pH 10 (pH higher than the pH_{PZC} of Cu2DW) resulted to an improved performance and lowest Cu leaching. The identification of the reaction intermediates by HPLC-MS suggested three routes for the destruction of CFA involving C_1-O and C_4-Cl bond breaking and aromatic ring cleavage. This study indicated that the dawsonite-incorporated Cu species present higher activity in catalytic ozonation than dissolved Cu^{2+} and CuO supported on alumina. Nevertheless, further investigations are required in order to reach higher stability for these materials.

Acknowledgement

This work was funded by the Spanish Ministry of Science and Innovation (MICINN) project CTM2008-02453. Rosa Ras is appreciated for the technical assistance in HPLC-MS analyses.

References

[1] C. Tixier, H.P. Singer, S. Oellers, S.R. Müller, *Environ. Sci. Technol.* 37 (2003) 1061-1068.

[2] H.R. Buser, M.D. Muller, N. Theobald, *Environ. Sci. Technol.* 32 (1998) 188-192.

[3] T.A. Ternes, M. Meisenheimer, D. McDowel, F. Sacher, H.-J. Brauch, B. Haist-Gulde, G. Preuss, U. Wilme, N. Zulei-Siebert, *Environ. Sci. Technol.* 26 (2002) 3855-3863.

[4] R. Andreozzi, V. Caprio, R. Marotta, A. Radovnikovic, *J. Hazard. Mater.* B103 (2003) 233-246.

[5] B. Kasprzyk-Hordern, M. Ziólek, J. Nawrocki, *Appl. Catal. B: Environ.* 46 (2003) 639-669.

[6] C. Gottschalk, J.A. Libra, A. Saupe, *Ozonation of water and waste water. A practical guide to understanding ozone and its applications.* 2nd Ed. 2010 WILEY-VCH.

[7] J. Nawrocki, B. Kasprzyk-Hordern, *Appl. Catal. B: Environ.* 99 (2010) 27-42.

[8] S. T. Oyama, *Catal. Rev. –Sci. Eng.* 42 (2000) 279-322.

[9] C. Cooper, R. Burch, *Water Res.* 33 (1999) 3695-3700.

[10] J. Qu, H. Li, H. Li, H. He, *Catal. Today* 90 (2004) 291-296.

[11] I. Udrea, C. Bradu, *Ozone Sci. Technol.* 25 (2003) 335-343.

[12] Y. Pi, M. Ernst, J.-C. Schrotter, *Ozone Sci. Technol.* 25 (2003) 393-397.

[13] M. Shiraga, T. Kawabata, D. Li, T. Shishido, K. Komaguchi, T. Sano, K. Takehira, *Appl. Clay Sci.* 33 (2006) 247-259.

[14] M. Gruttadauria, L.F. Liotta, G. Di Carlo, G. Pantaleo, G. Deganello, P. Lo Meo, C. Aprile, R. Noto, *Appl. Catal. B: Environ.* 75 (2007) 281-289.

[15] A.J. Frueh, J.P. Golightly, *Can. Mineral.* 9 (1967) 51-56.

[16] T. Iga, S. Kato, *J. Ceram. Soc. Jpn.* 86 (1978) 509-513.

[17] A.A. Ali, M.A. Hasan, M.I. Zaki, *Chem. Mater.* 17 (2005) 6797-6804.

[18] R.F. Vogel, G. Marcelin, W.L. Kehl, *Appl. Catal.* 12 (1984) 237-248.

[19] I. Pitsch, W. Goβner, Brückner, M. Mehner, S. Möhmel, D.-C. Uecker, M.-M. Pohl, *J. Mater. Chem.* 11 (2001) 2498-2503.

[20] M.S. Yalfani, M. Santiago, J. Pérez-Ramírez, *J. Mater. Chem.* 17 (2007) 1222-1229.

[21] G. Groppi, M. Bellotto, C. Cristiam, P. Forzatti, P.L. Villa, *Appl. Catal. A*, 104 (1993) 101-108.

[22] G. Groppi, C. Cristiani, P. Forzatti, M. Bellotto, *J. Mater. Sci.* 29 (1994) 3441-3450.

[23] J.S. Noh, J.A. Schwarz, *Carbon* 28 (1990) 675-682.

[24] G. Ertl. H. Knözinger, J. Weitkamp, *Handbook of Heterogeneous Catalysis*, Eds.; 1997, Wiley-VCH: Weinheim.

[25] C.J. Serna, J.V. Garcia-Ramos, M.J. Peña, *Spectrochim. Acta, Part A*, 41 (1985) 697-702.

[26] T. Iga, S. Kato, *ISIS Annual Report,* 86 (1978) 509.

[27] B. Xie, C.C. Finstad, A.J. Muscat, *Chem. Mater.* 17 (2005) 1753-1764.

[28] S. Li, H.Z. Wang, W.W. Xu, H.L. Si, X.J. Tao, S. Lou, Z. Du, L.S. Li, *J. Colloid Interface Sci.* 330 (2009) 483-487.

[29] J.P. Tobin, W, Hirschwald, J. Cunningham, *Appl. Surf. Sci.* 16 (1983) 441-452.

[30] B.R. Strohmeier, D.E. Leyden, R.S. Field, D.M. Hercules, *J. Catal.* 94 (1985) 514-530.

[31] J. Janas, J. Gurgul, R. P. Socha, S. Dzwigaj, *Appl. Catal. B: Environ.* 91 (2009) 217-224.

[32] H.Y. Chen, L. Chen, J. Lin, K.L. Tan, *Inorg. Chem.* 36 (1997) 1417-11423.

[33] M. Richter, M.J.G. Fait, R. Eckelt, M. Schneider, J. Radnik, D. Heidemann, R. Fricke, *J. Catal.* 245 (2007) 11-24.

[34] L. Zhao, Z. Sun, J. Ma, H. Liu, *Environ. Sci. Technol*. 43 (2009) 2047-2053.

[35] R. Rosal, M. Gonzalo, K. Boltes, P. Letón, J.J. Vaquero, E. Garcia-Calvo, *J. Hazard. Mater.* 172 (2009) 1061-1068.

[36] T. Watanabe, T. Masuda, Y. Miki, Y. Miyahara, H.-J. Jeon, S. Hosokawa, H. Kanai, H. Deguchi, M. Inoue, *J. Am. Ceram. Soc.* 93 (2010) 3908-3915.

[37] K. Ikehata, M.G. El-Din, *Ozone Sci. Technol.* 26 (2004) 327-343.

UNIVERSITAT ROVIRA I VIRGILI
NEW CATALYTIC ADVANCED OXIDATION PROCESSES FOR WASTEWATER TREATMENT
Mohammad Sadegh Yalfani
ISBN:/DL:T.1259-2011

General Conclusions

ISBN:/DL:T.1259-2011

1. Formic acid is introduced as a promising substitute for H_2 in the generation of H_2O_2 process in the presence of O_2 under ambient conditions. Pd/ Al_2O_3 was found as an appropriate catalyst for the above process. Other supports such as TiO_2 and carbon could not compete with Al_2O_3.

2. The H_2O_2 generated from formic acid and O_2 over Pd/Al_2O_3 is suitable for subsequent in situ application in aqueous solutions. Fenton reaction using H_2O_2 generated in situ from the above process showed higher capacity in the mineralization of phenol solution with respect to conventional Fenton process.

3. A fully heterogeneous catalytic system consisting Pd-Fe catalyst synthesized via consecutive impregnation (first Fe then Pd) to proceed simultaneously the in situ generation of H_2O_2 and the Fenton process has been developed. The catalyst showed very high stability (considering metal leaching results during the reactions). Interaction between Pd and Fe species indicating a close vicinity between metallic Pd and Fe_2O_3 particles was in favor of this process.

4. The above heterogeneous Fenton system (oxidation process) was applied successfully for the degradation of chlorophenols as a combination with hydrodechlorinaton reaction (reduction process) within a simple one-pot reaction. For low chlorinated chlorophenol (2,4-dichlorophenol) simultaneous reduction-oxidation protocol performed more efficiently regarding to TOC and toxicity measurement results, while consecutive reduction-oxidation reached to lower toxicity for high chlorinated chlorophenol (pentachlorophenol).

5. The efficiency of this new catalytic system has been successfully tested for the degradation of clofibric acid as representative of pharmaceutical compounds.

6. In situ generation of H_2O_2 using formic acid, hydrazine and hydroxylamine (as H_2 substitutes) utilized for phenol degradation via Fenton process, showed that firstly, the reaction conditions for bulk production and in situ generation of H_2O_2 such as the presence of halide ion and the pH of the solution could not be

similar. For example the presence of halide ion is not in favor of the in situ generation of H_2O_2. Secondly, formic acid produces in situ generated H_2O_2 with a more controlled rate in acidic pH with respect to hydrazine and hydroxylamine. On the other hand, for wastewaters with neutral pH, Fenton process using in situ generated H_2O_2 can be taken place by hydroxylamine with high efficiency.

7. Cu species incorporated into the dawsonite structure showed higher activity in catalytic ozonation of clofibric acid compared with dissolved Cu^{2+}, calcined Cu-dawsonite and CuO supported on alumina. Cu species was found as a reduced phase within the matrix of dawsonite. The Cu-dawsonite samples experienced Cu leaching during the reaction, while keeping the dawsonite crystalline structure. However, the effect of homogeneous dissolved Cu^{2+} was found to not be conclusive with respect to the heterogeneous Cu catalyst. By means of this catalytic process the efficiency in mineralization compared to single ozonation is greatly enhanced.

ISBN:/DL:T.1259-2011

List of publications

1. M.S. Yalfani, S. Contreras, F. Medina, J. Sueiras, Direct generation of hydrogen peroxide from formic acid and O_2 using heterogeneous Pd/γ-Al_2O_3 catalysts, *Chem. Commun.* **2008**, 3885-3887.

2. M.S. Yalfani, S. Contreras, F. Medina, J. Sueiras, Phenol degradation by Fenton's process using catalytic *in situ* generated hydrogen peroxide, *Appl. Catal. B: Environ.* **2009**, 89, 519-526.

3. M.S. Yalfani, S. Contreras, J. Llorca, M. Dominguez, J. Sueiras, F. Medina, Simultaneous *in situ* generation of hydrogen peroxide and Fenton reaction over Pd-Fe Catalysts, *Phys. Chem. Chem. Phys.* **2010**, 12, 14673-14676.

4. S. Contreras, M.S. Yalfani, F. Medina, J. Sueiras, Effect of support and second metal in catalytic *in situ* generation of hydrogen peroxide by Pd-supported catalysts: Application in the removal of organic pollutants by means of the Fenton process, *Water Sci. Technol.* **2011**, *in press.*

5. M.S. Yalfani, A. Georgi, S. Contreras, F. Medina, F.-D. Kopinke, Chlorophenol degradation using a one-pot reduction-oxidation process, *Appl. Catal. B: Environ.* **2011**, DOI: 10.1016/j.apcatb.2011.02.017, *in press.*

6. M.S. Yalfani, S. Contreras, F. Medina, J. Sueiras, Hydrogen substitutes for the *in situ* generation of H_2O_2: an application in the Fenton reaction, s*ubmitted to J. Hazard. Mater.*

7. M.S. Yalfani, S. Contreras, J. Llorca, F. Medina, Enhanced Cu activity in catalytic ozonation of clofibric acid by incorporation into ammonium dawsonite, *submitted to Appl. Catal. B: Environ.*